Novel mechanisms of regulation of the Cdc42 GTPase-activating protein CdGAP/ARHGAP31, a protein involved in cell migration and adhesion

Martin Primeau

Department of Anatomy and Cell Biology
McGill University, Montreal, Québec, Canada

Submitted in August, 2010

A thesis submitted to McGill University in partial fulfillment
of the requirements of the degree of

Doctor of Philosophy

Acknowledgements

I would first like to thank Dr. Nathalie Lamarche-Vane for allowing me to perform research in her laboratory. After a master in Biochemistry, I deeply wanted to work on Rho GTPases and Dr. Lamarche accepted to let me join her team. The guidance and support she provided during this work allowed me to learn far more than I expected when joining her laboratory. I would like also to thank the members of my PhD committee, Dr. Craig Mandato and Dr. Peter McPherson, for their precious inputs. I need as well to point out how the collaboration of multiple research groups at McGill has made this experience enriching. I also owe many thanks to the Department of Anatomy and Cell Biology, and all of its faculty members, staff members, and students.

I would like to acknowledge the Canadian Institutes for Health Research (CIHR) and the McGill Faculty of Medicine which awarded me respectively a Canada Graduate Scholarship and an Internal Scholarship Award. I thank everyone in the Lamarche-Vane laboratory, both present and past members, especially Dr. Josée-France Villemure, Jonathan Degeer, Vilayphone Luangrath, Judith Antoine-Bertrand, Fereshteh Karimzadeh and Yi He. I would like to add to this list the names of Dr. Julien Chevalier and Driss Mountassif. Your help and advices over the years are very much appreciated.

Finally, it is impossible to end this section without underlying how precious the support of my family and friends has been. To all of you who have supported me when I was down, thank you.

Douce, Catherine, Papa et Maman, je ne vous serai jamais assez reconnaissant. Merci.

Abstract

The Rho GTPases form a family of enzymes that control numerous cellular processes including cell migration and proliferation through effects on the cytoskeleton, membrane trafficking and cell adhesion. The activity of these molecular switches is modulated by GTPase-activating proteins (GAPs), a group of negative-regulators which includes Cdc42-GTPase-Activating Protein (CdGAP). This protein specifically negatively-regulates the Rho GTPases Cdc42 and Rac1. In this study, we show that CdGAP is regulated by lipid-, protein- and intramolecular-interactions. First, we demonstrate that a polybasic region (PBR) of CdGAP preceding the GAP domain and found in numerous Rho family GAPs is required for CdGAP specific association with phosphatidilinositol-3,4,5-trisphosphate ($PI(3,4,5)P_3$). We show that the binding of $PI(3,4,5)P_3$ is required for CdGAP-mediated GAP activity *in vitro*, and that an intact PBR is required for its CdGAP-mediated GAP activity *in vivo*. Second, we characterize the binding site for the negative-regulator of CdGAP Intersectin-1 located in the Basic-Rich (BR) domain of CdGAP. We present evidence that this interaction mediated by the SH3D domain of Intersectin requires one to three lysine residues located in the Basic-Rich (BR) domain of CdGAP. Thirdly, we show that CdGAP is negatively-regulated by its C-terminal domain. This observation is part of a study that links two human CdGAP gene mutations to a syndrome which presents a combination of aplasia cutis congenita (ACC) and terminal transverse limb defects (TTLD). In this syndrome, the deletion-mutant gene products which lack the residual amino-acid of CdGAP at its C-terminus have an increased activity compared to wild-type proteins. We show that this C-terminus can bind to the GAP domain of CdGAP, providing a model to explain how the absence of the C-terminus induces this syndrome. In summary, this work provides novel insight into understanding the mechanisms of regulation of CdGAP, a protein involved in cell migration and adhesion with unexpected roles related to human diseases.

Résumé

Les Rho GTPases forment une famille d'enzymes qui contrôlent de nombreux processus cellulaires, tels que la migration cellulaire et la prolifération, grâce à leurs effets sur le cytosquelette, le trafic membranaire et l'adhésion cellulaire. L'activité de ces interrupteurs moléculaires est modulée par les protéines activatrices de GTPases (GAPs), un groupe de régulateurs négatifs qui inclu CdGAP (Cdc42-GTPase activating protein). Cette protéine régule négativement les Rho GTPases Cdc42 et Rac1 de façon spécifique. Dans la présente étude, nous montrons que CdGAP est régulée par des interactions lipidiques, protéiques et intramoléculaire. Premièrement, nous démontrons qu'une région polybasique (PBR), précédant le domaine GAP et retrouvée dans plusieurs GAP de la famille Rho, est requise pour l'association spécifique de CdGAP avec le phosphatidilinositol-3,4,5-trisphosphate ($PI(3,4,5)P_3$). Nos résultats suggèrent que l'activation des GAP requiert la liaison du $PI(3,4,5)P_3$ à CdGAP dans un contexte *in vitro* et un PBR intact pour que CdGAP provoque ses effets GAP-dépendants dans un contexte *in vivo*. Deuxièmement, nous caractérisons le site de liaison du régulateur négatif de CdGAP Intersectin-1. Ce site est localisé dans le domaine riche en résidus basiques (BR) de CdGAP. Nous suggérons que cette interaction, médiée par le domaine SH3D d'Intersectin, requiert de un à trois résidus lysine dans le domaine BR de CdGAP. Troisièmement, nous montrons que CdGAP est régulé de manière négative par son propre domaine C-terminal. Cette observation fait partie d'une étude qui associe deux mutations humaines du gène *CdGAP* à un syndrôme présentant une combinaison d'aplasie cutis congenita (ACC) et de malformation des doigts et des orteils (TTLD). Les gènes mutants produisent des protéines tronquées qui ont une activité GAP supérieure à la protéine de type sauvage. Nous montrons que ce C-terminal peut lier le domaine GAP de CdGAP, supportant un modèle expliquant comment l'absence du C-terminal

induit ce syndrome. En bref, ce travail présente un nouvel aperçu des mécanismes de régulation de CdGAP, une protéine impliquée dans la migration cellulaire et dans l'adhésion des cellules en plus d'être directement impliquée dans une maladie humaine.

Table of Contents

List of Tables

List of Figures

Abbreviations

Abr	Active BCR-related
Abi1/2	Arabidopsis Protein 1/2
Abl	Abelson tyrosine kinase
ACC	Aplasia cutis congenita
Amot	Angiomotin
AP1	Activator protein 1
ARAP	ArfGAP, RhoGAP, Ankyrin repeat, Ras-associating (RA), and five PH domains
Arf	ADP-ribosylation factor
ARHGAP	Rho GTPase activating protein
Arl	Arf-like protein
Arp2/3	Actin-related protein 2 and 3 complexes
ATP	Adenosine 5'-triphosphate
β-Pix	PAK-interacting exchange factor
BAR	Bin–Amphiphysin–Rvs
Bcr	Breakpoint cluster region
Bmx	BMX non-receptor tyrosine kinase
BR	Basic-rich
BSA	Bovine serum albumin
BTB	Broad-Complex / Tramtrack / Bric-à-Brac

C1	Phorbol esters / diacylglycerol binding domain
C2	Ca^{2+}-binding motif
Cdc42	Cell division cycle 42
CdGAP	Cdc42 GTPase-activating protein
CdGAPr	Drosophila CdGAP homolog
Cdk	Cyclin-dependant kinase
cDNA	Complementary DNA
Chp	Cdc42 homolog protein
CHN1	Chimerin-1 gene
CIP	Cdc42-interacting protein
COP	Coat protein
COS-7 cells	*C. aethiops* (green monkey) origin-defective SV-40 fibroblast cells
Crk	v-crk sarcoma virus CT10 oncogene homolog
CRM1	Chromosome maintenance region 1 (exportin 1)
DAPI	4',6-diamidino-2-phenylindole
DBC2	Deleted in breast cancer 2
Dbl	proto-oncogene in Diffuse B-cell Lymphoma cells
DEP	Density-enhanced phosphatase
DH	Dbl Homology
DHR1	Dock180 homology region 1
DHR2	Dock180 homology region 2

Dia	Diaphanous
DLC-1	Deleted in Liver Cancer 1
DMEM	Dulbecco's Modified Eagle Medium
DNA	Desoxyribonucleic acid
Dock	Dedicator of cytokinesis
DTT	Dithiothreitol
DRF	Diaphanous-related formin homology
ECL	Enhanced chemiluminescence
ECM	Extracellular matrix
Ect2	Epithelial Cell Transforming Sequence 2
EDTA	Ethylenediaminetetraacetic acid
EGF	Epidermal growth factor
eiF4E	Eukaryotic translation initiation factor 4E
ELMO	Engulfment and cell motility protein
ER	Endoplasmic reticulum
ERK	Extracellular-signal regulated kinases
ERM	Ezrin, Radixin, Moesin
Exo70, Exo84	Exocyst complex components
FAK	Focal Adhesion Kinase
FBS	Fetal Bovine Serum
FCH	FER / CIP4-homology

FF	Phenyalanine-phenylalanine
FilGAP	Filamin A-associated RhoGAP
Fyn	Fyn proto-oncogene
GABARAP	Gamma-aminobutyric acid receptor-associated protein
GAP	GTPase-activating proteins
GEF	Guanine Nucleotide Exchange Factor
GC-GAP	GAB associating Cdc42 GAP
GDI	Guanine Nucleotide Dissociation Inhibitor
GDP	Guanosine diphosphate
GGA	Golgi-localized γ-ear-containing Arf-binding protein
GLUT4	Glucose transporter-4
GMIP	Gem interacting protein
GPCR	G protein-coupled receptor
GRAF	GTPase regulator associated with FAK
GRIT	GTPase regulator interacting with TrkA
GSK3	Glycogen Synthase Kinase 3
GST	Glutathione S-transferase
GTP	Guanosine triphosphate
HCl	Hydrogen Chloride
HEPES	4-(2-hydroxyethyl)-1-piperazineethanesulfonic acid
HRP	Horseradish peroxidase

Ig	Immunoglobulin
ILK	Integrin-linked kinase
IPTG	Isopropyl β-D-1-thiogalactopyranoside
JNK	c-jun N-terminal kinase
kDa	Kilodalton
LARG	Leukemia Associated RhoGEF
Lbc	Proto-oncogene Lbc
LiCl	Lithium Chloride
LIMK	LIM domain kinase
LUVs	Large-unilamellar vesicules
MAPK	Microtubule associated protein-2 kinases
MAPKK	MAPK kinase
MAPKKK	MAPKK kinase
MDCK cells	Madin-Dardy canine kidney epithelial cells
MEF	Murine embryonic fibroblasts
$MgCl_2$	Magnesium chloride
MgcRacGAP	Male Germ Cell RacGAP
MLL	Mixed lineage leukemia
MLVs	Multilamellar Vesicles
mRNA	Messenger ribonucleic acid
MTOC	Microtubule-organizing center

mTOR	Mammalian target of rapamycin
Myo9	Class IX myosin-RhoGAP 9
NaCl	Sodium Chloride
NaF	Sodium Fluoride
Na_3VO_4	Sodium Orthovanadate
Nap1	Nef associated protein 1
NES	Nuclear export signal
Net1	Neuroepithelial cell transforming gene 1 protein
NF-κB	Nuclear factor-kappa B
NGF	Nerve growth factor
N1E-115 cells	Neuroblastoma cells
NKIRAS	NFκB Inhibitor-interacting RAS-like
NLS	Nuclear localization signal
NP40	Nonyl phenoxypolyethoxylethanol
PAK	P21-activated kinase
PAR	partitioning defective protein
PBR	Polybasic region
PBS	Phosphate-buffered saline
PC	Phosphatidylcholine
PC12 cells	Cell line derived from a pheochromocytoma of the rat adrenal medulla
PCR	Polymerase chain reaction

PDGF	Platelet-derived growth factor
PDZ	Domain present in PSD-95, Dlg and ZO-1/2
PEI	Polyethylenimine
PFA	Paraformaldehyde
PH	Pleckstrin Homology
PI	Phosphatidylinositol
PI3K	Phosphatidylinositol 3-kinase
PI(4,5)P_2	Phosphatidilinositol-4,5-disphosphate
PI(3,4,5)P_3	Phosphatidilinositol-3,4,5-trisphosphate
PKC	Protein Kinase C
PMSF	Phenylmethylsulfonyl fluoride
PPC	Bacterial pre-peptidase C-terminal domain
PRD	Proline-rich domain
PX	Phox domain
Rab	Ras in brain
Rac	Ras-related-C3 botulinum toxin substrate
Ral	Ras-like
Ran	Ras-related nuclear protein
Rap	Ras-proximal
Ras	Rat sarcoma
RasD	Ras Induced by Dexamethasone

REBG	Ras-related and Estrogen-Regulated Growth inhibitor
REM	Rad and Gem-related
RheB	Ras homolog enriched in brain
Rho	Ras homologous
RICH1	RhoGAP interacting with CIP4 homologs protein 1
RICS	RhoGAP involved in the b-catenin-N-cadherin and NMDA receptor signaling
Rif	Rho in filopodia
RING	Really Interesting New Gene
Rnd	Resistance-nodulation-cell division
ROBO	Homolog of drosophila roundabout
ROCK	Rho-associated coiled-coil-containing protein kinase
RSK	p90 Ribosomal S6 Kinase
SAM	Sterile alpha motif
Sar	Secretion-associated and RAS-related
Sra-1	Steroid receptor RNA activator 1
Sec5, Sec14	Exocyst complex subunits 5 and 14
SH2	Src homology 2
SH3	Src homology 3
SHP2	Src homology region 2-containing protein tyrosine phosphatase-2
siRNA	Small interfering RNA
Slit	Homolog of drosophila slit

Sos	Son of Sevenless
SRGAP	SLIT/ROBO Rho GTPase-activating protein
START	StAR-related lipid-transfer domain
SUVs	Small-unilamellar vesicules
TB	Terrific Broth
TBS	Tris-buffered saline
TC10	10th protein cloned from a human teratocarcinoma cell line
TCGAP	TC10/Cdc42 GTPase activating protein
TCL	TC10-like
Tiam1	T-cell lymphoma invasion and metastasis 1
TJ	Tight junction
Tris	Tris(hydroxymethyl)aminomethane
TTLD	Terminal transverse limb defects
TTF	Translocation three four
Trio	Triple functional domain protein
TrkA	Tyrosine kinase receptor A
TSC2	Tuberous sclerosis complex 2
U2OS cells	Human osteosarcoma cells
VCA	Verprolin-cofilin-acidic domain
WASP	Wiscott-Aldrich syndrome protein
WAVE	WASP family Verprolin-homologous protein

WRCH	Wnt-responsive Cdc42 homolog
WW	Tryptophan-Tryptophan
ZAP70	ζ-chain-associated protein kinase of 70kDa

Contributions of Authors to Manuscripts

This thesis is formed in a manuscript-based structure. In accordance with faculty regulations, manuscripts co-authored by others must be accompanied by an explicit statement regarding who contributed to the work. Copyright waivers from the co-authors can be found in the appendix.

Chapter 2:

My contribution to the manuscript entitled “A stretch of polybasic residues in CdGAP binds to Phosphatidylinositol-3,4,5-Trisphosphate and regulates its GAP activity“ included designing and performing all experiments shown, except for figures 2.5 and 2.7B which where performed in collaboration with F.K. Nathalie Lamarche-Vane and I each contributed to the writing of the paper.

Chapter 3:

My contribution to the manuscript titled “The SH3D domain of Intersectin binds to CdGAP through a novel basic-rich motif” involved designing and performing all experiments shown. Nathalie Lamarche-Vane and I each contributed to the writing of the paper.

Chapter 4:

My contributions to the manuscript entitled “Mutations in ARHGAP31, a regulator of Cdc42 and Rac1 GTPases, cause scalp and transverse limb birth defects” involved designing and performing experiments shown in figures 3C, 3D and supplementary figure 3. It also involved the production and purification of specific antibodies used in figure 4C. Nathalie Lamarche-Vane and I both contributed to the writing of the paper with Drs. Richard Trembath and Rajiv Machado.

Submitted Manuscripts

This thesis includes the following manuscripts submitted:

Chapter 2:

A stretch of polybasic residues in CdGAP binds to Phosphatidylinositol-3,4,5-Trisphosphate and regulates its GAP activity (2010). Martin Primeau, Fereshteh Karimzadeh, Driss Mountassif, Isabelle Rouiller and Nathalie Lamarche-Vane. Submitted to Molecular Biology of the Cell.

Chapter 3:

The SH3D domain of Intersectin binds to CdGAP through a novel basic-rich motif (2010). Martin Primeau and Nathalie Lamarche-Vane, Submitted to FEBS Letters.

Dedicated to André Primeau, a man that contributed with his 5th grade degree to build a society in which his grand-son had the opportunity to study for years.

Merci grand-papa!

Chapter 1 - Introduction and Literature Review

1.0 Historical perspective

Unicellular microorganisms were the first form of life to develop on Earth, approximately 4 billion years ago [1]. Over the next 3 billion years, succeeding generations of these energy converting entities have led to the development of more complicated cells, all built according to one law : creating and keeping order from disorder [2]. With the aim of successfully replicating themselves, these cells had to take into consideration their environment. Therefore, to introduce molecules into, and to clear waste from the cell, tools that helped the cells to sense their environment were generated. In some cases, these tools allowed unicellular oraganisms to live in symbiosis, and to cooperate instead of acting independently [3]. Eventually, true cell “communism” appeared when a single germ cell managed to generate multiple cells, all specialized and cooperating in order for the whole community to be able to replicate itself.

In order to live in symbiosis efficiently, the cells of multicellular organisms had to specialize to distinct roles, and develop efficient communication tools. To achieve these tasks, living entities generated ways of performing complex biological processes at low energetic costs. Conservation of the GTPase module in prokaryotic and eukaryotic cells is a nice example of this prerequisite. GTPases are conserved molecular switches that are built according to a common structural design, which is efficient in accomplishing work at a low energy cost. Throughout the course of evolution, the GTPase module was successfully adapted to different tasks, in accordance to the function of the cells. Currently, it is found in almost every living organism on Earth, and, is therefore one of the best examples of Evolution’s ability to create functional diversity from a conserved structure and mechanism.

1.1 The Ras Superfamily of Small GTPases

The story of small monomeric GTPases associated with the Ras family of proteins began in 1964 and 1968, with two studies of rat retroviruses generating solid tumours in mice: the Moloney's leukaemogenic virus [4] and an erythroblastosis virus [5, 6]. Both viruses bore a similar sequence [7, 8] and encoded two uncommon proteins of 21 kDa and 60 kDa [9], the latter found to be homologous to the *src* gene [10]. The genes encoding the 21 kDa protein were given the names of *Harvey-ras* (*H-ras*) and *Kirsten-ras* (*K-ras*), after the authors who discovered the retroviral strains, and an acronym derived from the words rat sarcoma [11, 12]. In 1981, activated human *ras* genes were discovered in human cancer cells [13-15].

Because of its link with human cancer progression, the *ras* gene has been the subject of intense research since the beginning of the 1980's. Its protein product was found to be associated with the plasma membrane [16], able to bind GTP [17, 18] and it could convert GTP to GDP [19, 20]. In this way it was discovered that Ras can act as a molecular switch that is "on" when bound to GTP, and "off" when bound to GDP. Because of these findings, and based on protein sequence homology between the G protein-coupled receptor (GPCR)-associated G-proteins and Ras, the latter was thought to participate in signal transduction across the cellular membrane [21]. Regulators of this GTP/GDP cycle were later discovered [22-25]. Guanine nucleotide exchange factors (GEFs) activate a GTPase by catalyzing the exchange of GDP for GTP, whereas GTPase-activating proteins (GAPs) enhance the intrinsic GTPase activity of these proteins, thereby leading to their rapid conversion to the inactive GDP-bound form.

Over the years, and to a higher degree with the human genome being sequenced, the number of *ras* homolog genes has increased from its two founding members to 159 [26-28]. Based on protein primary sequence analysis, these members of the Ras superfamily of small monomeric G-proteins have been divided into five families (Arf, Rab, Ran, Ras and Rho), each having its own specialization in the cell (Table 1.1).

Despite some exceptions, each monomeric GTPase from the Ras family is expressed as a unique globular domain termed the G domain (Figure 1.1), which contains a pocket that can either bind GTP or GDP. Depending on its nature, the nucleotide transforms the tertiary structure of the GTPase it binds to. The presence of the GTP in the pocket restricts the mobility of the two regions flanking the nucleotide binding site [29]. These regions, called switch-1 and -2, are implicated in the binding of most GTPase interacting partners, such as effectors, Guanine nucleotide Dissociation Inhibitors (GDIs), activators like GEFs or inhibitors like GAPs [30].

In order to act efficiently as intermediates of signal transduction, most Ras family GTPases are modified by the addition of a lipid which anchors them to membranes (Figure 1.1). Depending on the nature of the protein, this lipid modification can be either called N-myristoylation, prenylation (farnesylation or geranylgeranylation) or palmitoylation [31]. N-myristoylation consists of the covalent linkage of a 14-carbon fatty acid to a glycine found precisely after the initial methionine at the N-terminus. Prenylation is either the addition of a 15-carbon farnesyl group or a 20-carbon geranylgeranyl isoprenoid moiety to the first cysteine found in what is called the C-terminal CAAX box. Finally, S-palmitoylation represents the reversible covalent linkage of a 16-carbon fatty acid on a cysteine residue. In GTPases, these modifications occur on free cysteines found in the C-terminal tail independently of the presence of a CAAX box [33].

Table 1.1. Members of the Ras superfamily of GTPases

Subfamily	Members number	Predominant lipid modification	Function
Arf	30	Myristoylation (N-terminus)	Vesicle formation and trafficking
Rab	70	Geranylgeranylation (1x or 2x) (C-terminus)	Vesicle trafficking
Ran	1		Nuclear shuttling
Ras	35	Farnesylation, Geranylgeranylation and/or Palmitoylation (C-terminus)	Cell differentiation and proliferation
Rho	20	Farnesylation, Geranylgeranylation and/or Palmitoylation (C-terminus)	Cell cytoskeleton control and cell proliferation

Figure 1.1 – The tridimensional structure of GTPases (Cdc42)

GTPases from the Ras superfamily share the same structural backbone which is slightly different from subfamily to subfamily. Here, the structure of Cdc42 reveals the main characteristics of Ras superfamily GTPases and the particularities of Rho GTPases. Positioning of both switch-1 and switch-2 (green) on Ras GTPases depends on the nature of the nucleotide (red) sitting in their binding pocket. Therefore, association with GDP or GTP stabilizes the switches in different positions, generating distinct binding interfaces on the protein. With the exception of RhoBTB-1 and -2, the G domain of Rho GTPases contains a lipid modification at its C-terminus (magenta). GTPases from the Ras and Rab subfamilies also contain a C-terminal lipid modification, whereas the Arf proteins are modified by the addition of a lipid group at their N-terminus. In several cases, notably in RhoGTPases, the site of lipid addition is preceded by a cluster of basic residues (blue). The RhoGTPase family members have a unique insert region (cyan) which is recognized by some effectors and by GAPs. Here, Cdc42 is associated with GDP and is in the conformation it adopts when it forms a complex with RhoGDI (Protein Data Bank 1DOA) [32]. Image generated with UCSF Chimera.

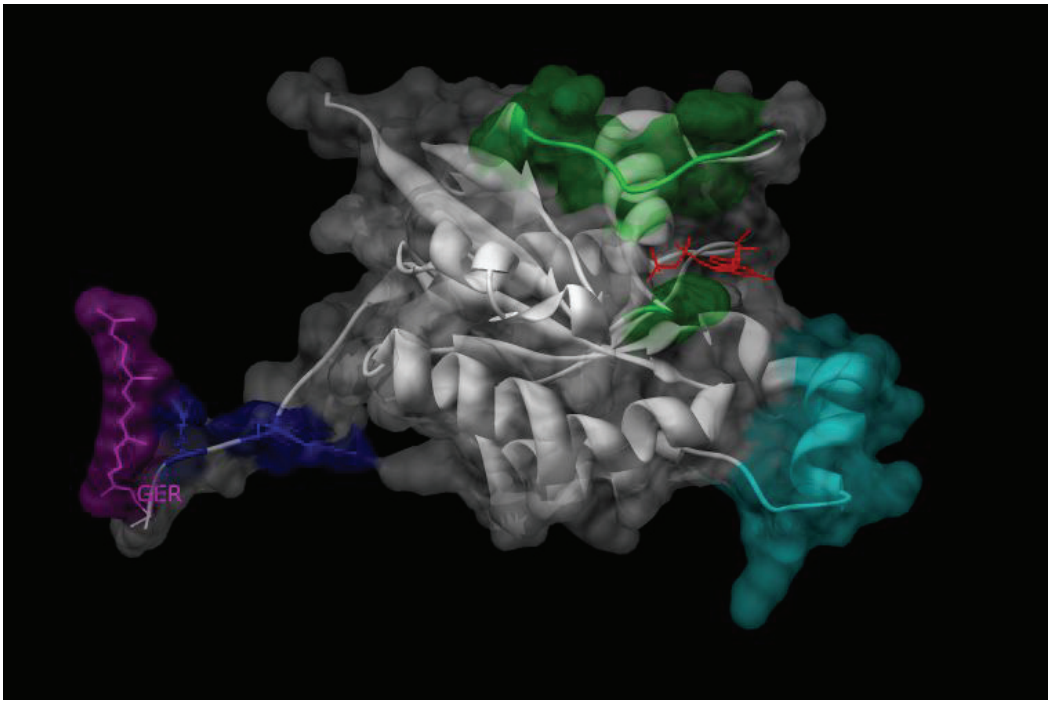
GER

1.1.1 The Ras subfamily

The subfamily of Ras GTPases, including H-Ras and K-Ras, contains 33 other members based on protein sequence homology [28]. Despite sharing a similar primary sequence, proteins of this family have different functions, from cell proliferation and differentiation to cell adhesion [28]. Most proteins of this group are modified by the addition of a geranylgeranyl group at their C-terminus, although it is possible, based on primary sequence analysis, that some members are myristoylated and/or palmitoylated.

As its name suggests, the Ras oncoprotein branch, which involves H-Ras, K-Ras and N-Ras, is a group of proteins that can transform a cell when ectopically expressed [34]. This capacity is inherent to their involvement in cell differentiation and organ development [28]. Under their GTP-bound activated form, these proteins bind and activate effector proteins like the serine/threonine protein kinase RAF (MAPKKK), or the lipid phosphatidylinositol-3-kinases (PI3Ks), two groups of effectors involved in the transmission of mitogenic signals through the activation of Erk1/2 and PKB/AKT, respectively [28].

The Rap (Ras-proximal) branch proteins function as regulators of integrin-mediated cell adhesion, cell junction formation, cell secretion and cell polarity [35]. While they share the same group of effectors with the Ras proteins, their regulators, GEFs and GAPs, are different [36].

Another well characterized branch of the Ras Superfamily is the Ral (Ras-like) group. These proteins do not bind to the same effectors as Ras and Rap and instead participate in the proper assembly of the exocyst complex by interacting directly with two of its components, Sec5 and Exo84 [37]. For this reason, Ral is implicated in the targeting of Golgi-derived vesicles to the basolateral membrane of polarized epithelial cells and to the growth cone of differentiating PC12 cells [38, 39].

RheB (Ras homolog enriched in brain) is a very important component of a pathway that links signal transduction to cell metabolism through its action on mTOR. RheB is a direct target of the GAP TSC2 [40]. Once activated, the PKB/AKT kinase phosphorylates and inactivates TSC2 [41], indirectly promoting the activation of RheB, which then binds and activates the serine/threonine kinase mammalian target of rapamycin (mTOR). Active mTOR indirectly participates in the release of the eiF4E translation initiation factor, and therefore promotes mRNA translation and protein synthesis [42].

These four subgroups encompass the best characterized proteins of the Ras subfamily. Little is known on the cellular function of the most recently identified proteins RasD (Ras Induced by Dexamethasone), NKIRAS (NFκB Inhibitor-interacting RAS-like), REM (Rad and Gem-related) and REBG (Ras-related and Estrogen-Regulated Growth inhibitor) [28].

1.1.2 The Rab subfamily

The first four members of the Rab (*ras* genes from rat brain) family were discovered in 1987 using a rat brain cDNA library screen for the identification of novel homolog proteins to Ras [43]. They were named Rab1, -2, -3 and -4. This was only the beginning of the Rab subfamily of GTPases, since the human genome database now predicts 70 genes encoding for Rab-related proteins [28].

Over 70% of the Rab GTPases are characterized by the double addition of a geranylgeranyl group to the two reactive cysteines located at their C-termini [28]. Eight members contain only one geranylgeranyl group while six are not prenylated at all. Despite these last members, lipid modification of the Rab proteins is central to their role as internal membrane traffic conductors. Rab GTPases also participate in the budding, uncoating and fusion of new vesicles and their movement in the cell. These tasks require a tight control of Rab

functions by RabGDI, RabGEFs, and as many as 38 different RabGAPs have been the focus of recent literature reviews [28, 44, 45].

1.1.3 The Ran subfamily

The Ran protein is very similar in protein sequence to the Rab proteins [28], although its striking role in the cell is sufficient to consider it as a subfamily itself. Ran is the most abundant GTPase in a cell [46] and is a regulator of nuclear import and export [47], a function tightly linked to the nature of the nucleotide it binds. The nucleotide status of Ran is not seen as an active or inactive state, since Ran-GDP and Ran-GTP each have their own effectors. Ran-GTP is mostly found in the nucleus, where Ran is loaded with GTP by its GEF RCC1. In the cytoplasm, the presence of different GAPs contribute to the induction of its GDP-binding status [48].

Ran controls the assembly and disassembly of complexes that form between transported cargos and effectors involved in entering or exiting the nucleus through the nuclear pore. Once a complex between a nuclear localization signal (NLS) containing protein and importin enters the nucleus, Ran-GTP causes the dissociation of the complex by binding to importin. Conversely, Ran-GTP promotes the formation of complexes between nuclear export signal (NES) containing proteins and binds to the exportin CRM1. Once the complex leaves the nucleus, RanGAPs will convert Ran-GTP into Ran-GDP. The latter will re-enter the nucleus through passive transport across the nuclear pore in order to start the cycle again [48].

Ran is also a major player in the assembly of the mitotic spindle during mitosis and consequently in the timing of cell-cycle transitions [48]. Considering its different roles, the absence of any lipid modification on this protein is not

surprising. Four other GTPases are close homologs of Ran but they are commonly associated with the Rab family [28].

1.1.4 The Arf Subfamily

The first Arf (ADP-ribosylation factor) protein was discovered as a cellular cofactor required for cholera toxin to ADP-ribosylate adenylate cyclase and to exert its toxic effect [49]. Four years later, the gene encoding for this protein was cloned and associated to the Ras subfamily of proteins, based on protein sequence homology [50]. In contrast to other GTPases of the Ras superfamily, the ARF subfamily members do not contain a lipid anchor at their C-terminus. Instead, a myristoyl group is added at their N-terminus but does not guarantee by itself their anchorage to lipid membranes in the cell [28]. In fact, amino acids at their N-terminal extremity form an amphipathic helix. Upon GTP-binding, this helix is moved from the protein, and hides the hydrophobic residues within the lipid monolayer of a membrane [51]. This amphipathic helix is thought to induce membrane curvature [52, 53]. Therefore, the nucleotide binding state of an Arf GTPase is tightly coupled to its association with membranes.

Arf proteins are principally associated with the budding and transport of vesicles, Golgi apparatus maintenance, endocytosis, endosome recycling and phagocytosis: all functions requiring a tight control of membrane trafficity. The six best characterized proteins of this group are Arf-1 to -6. Arf-1 to -5 facilitate cargo formation by recruiting effectors to the Golgi apparatus, including coat protein COPI, the clathrin adaptor protein 1 (AP1) and the Golgi-localized γ-ear-containing Arf-binding proteins (GGAs) [54]. Arf6 localizes to the plasma membrane and the endocytic system, where it is implicated in the endosomal-membrane traffic [55].

Other members of this family include the Sar and Arl proteins. Sar1 is localized to the endoplasmic reticulum (ER) and is required for ER-to-Golgi transport by promoting vesicle formation through its interaction with COPII components [56]. Arl proteins are less well characterized, and would also be involved in membrane movements within the cells [57].

1.1.5 The Rho Subfamily (briefly)

The Rho (Ras homologous) subfamily represents, beside Ran, the smallest group of Ras-related GTPases with 20 members [58]. They were shown to be key regulators of cytoskeletal dynamics and are therefore involved in several cellular processes, including cell polarity, migration, vesicle trafficking and cytokinesis, but also in gene expression [59]. A comprehensive review of the members of this family will be presented in the next section (1.2) of this chapter.

The analysis of the Ras superfamily of small GTPases reveals a large spectrum of cellular functions covered by these proteins. Cell proliferation, cell motility and polarity, nuclear shuttling, and endocytic trafficking are all controlled by this family of molecular switches that have been adapted throughout the course of evolution. These findings make the GTPases prime examples of evolution's wonderful ability to create functional diversity from an efficient molecular tool.

1.2 The Rho Subfamily

While they share with Ras proteins the same topology, members of the Rho subfamily have a 9-12 amino acid insert region between the 5th β-strand and the 4th α-helix of the GTPase domain. This insert region is involved in the interaction with GAPs and some effectors (Figure 1.1) [30, 60-63]. Similar to other members of the Ras superfamily, amino acid substitution of specific residues influences the nucleotide binding state of a GTPase. For instance, the substitution G12V or Q61L in Cdc42 produces GAP-insensitive protein mutants, although they can still bind these proteins. Alternatively, the substitution T17N in Cdc42 produces a GTPase unable to bind GTP, and so, stays in a GDP-bound state. It is thought that overexpressed GTPase^{T17N} in cells acts as a dominant-negative protein because it has high affinity binding to GEFs [64].

Most Rho GTPases are anchored to membranes through a lipid modification (prenylation and/or palmitoylation) at their C-terminus. This lipid modification requires the presence of basic residues before the lipid modification site (Table 1.2) [65-67]. These residues serve to induce binding of Rho GTPases to specific types of cellular membranes but they can also be important for protein binding and act as a NLS [68].

For years, the focus on Rho GTPases has been put on three members: Cdc42, Rac1 and RhoA. However, the first link between Rho GTPases and the actin cytoskeleton was established in a study revealing that *Clostridium botulinum* exoenzyme C3 was mediating disappearance of actin filaments by its action on RhoC [69]. Then, additional studies showed that the closely related GTPases RhoA and Rac1 could induce the formation of actin stress fibres and the generation of lamellipodia, respectively [70, 71]. Finally, microinjection

Table 1.2. The C-terminus sequence of Rho GTPases and their associated lipid modification

GTPases	C-terminus sequence	Prenyl.	Palmitoyl.
Cdc42a	-PPEP**KK**S**RR**C̲VLL[1]	GG[2]	
Cdc42b	-PPETQP**KRK**C̲CIF	GG?	yes
TC10	-P**KK**HTV**KKR**IGS**R***C*IN*C*C̲LIT	F?[3]	yes
TCL	-P**KKKKKR***C*SEGHS*C*C̲SII	F?	yes?
Wrch-1	-YSDTQQQP**KK**S**K**S**R**TPD**K**M**K**NLS**K**SWW**KK**YC*C*FV	No	yes
Wrch-2	-H**K**A**R**LE**KK**LNA**K**GV**R**TLS**R**C**R**W**KK**FF*C*FV	No	yes
Rac1[4]	-PPPV**KKRKRK**C̲LLL	GG	
Rac2	-PQPT**R**QQ**KR**AC̲SLL	GG	
Rac3	-PPPV**KK**PG**KK**C̲TVF	GG	
RhoG	-PTPI**KR**G**R**SC̲ILL	GG	
RhoA	-A**RR**G**KKK**SGC̲LVL	GG	
RhoB	-**KR**YGSQNG*C*IN*C*C̲KVL	GG/F	yes
RhoC	-V**RK**N**KRRR**GC̲PIL	GG	
Rnd1	-PSPLPQ**K**SPV**R**SLS**KR**LLHLPS**R**SELISSTF**KK**E**K**A**K**SC̲SIM	F	
Rnd2	-L**RR**TDS**RR**GMQ**R**SAQLSG**R**PD**R**GNEGEIH**K**D**R**A**K**SC̲NLM	F	
Rnd3	-VK**R**N**K**SQ**R**AT**KR**ISHMPS**R**PELSAVATDL**RK**D**K**A**K**SC̲TVM	F	
RhoD	-S**R**G**R**NFW**RR**ITQGFC̲VVT	F?	
Rif	-AL**KK**AQ**R**Q**KKRR**LC̲LLL	GG?	
RhoBTB1	-**RR**HLQFW**K**SHL**KK**VQ**K**PLLQAPFLPP**K**APPPVI**K**VP-[5]	No	
RhoBTB2	-**RR**HLQFW**K**SHL**KK**VQ**K**PLLQAPF**R**NSEPPPIIVVPD-[5]	No	
RhoH	-QA**RRR**N**RRR**LFSINEC̲KIF	GG	

[1] Basic amino acids (bold); Prenylated cysteines (underlined); palmitoylated cysteines (italic);

[2] GG, geranylgeranyl; F, farnesyl, P, palmitoyl

[3] Question marks underlines a sequence prediction that was not demonstrated;

[4] Both Rac1 isoforms are identical at their C-terminus.

[5] The residues sown are found at the C-terminus of the GTPase domain.

studies performed in mammalian cells showed that activated forms of Cdc42 could trigger the formation of filopodia [64]. Taken together, these results suggested a simple picture in which these GTPases were solely affecting the actin cytoskeleton. However, it is now evident that the cellular functions of Rho GTPases are not limited to their participation in the control of actin filaments organization.

The Rho family of GTPases is divided in eight branches based on primary sequence homology: RhoA, Rac1, Cdc42 and their related GTPases, but also the groups of Wrch, Rnd, RhoBTB, RhoH and finally RhoD/RIF (Figure 1.2).

1.2.1 RhoA, RhoB and RhoC

RhoA was first cloned from a cDNA library from Aplysia in 1985 [72]. Having 35% of homology with the human protein Ras, this protein was hypothesized to be part of another subfamily of GTPases, and history has proven them right. The first studies on Rho GTPases started with two of its yeast homologs, Rho1 and Rho2 [73]. Rho1, but not Rho2, was shown to be an essential gene, and viability of yeast cells could not be rescued by Ras, suggesting two different roles for these proteins inside the cell [73].

In humans, the Rho group consists of three proteins (RhoA, RhoB and RhoC) whose primary sequence is highly related (Figure 1.2) [76, 77]. The functions of Rho in cellular responses have been investigated extensively using the clostridium botulinum toxin C3 transferase which ADP-rybosylates Rho proteins and renders them inactive [78, 79]. Inhibition of RhoA prevents this enzyme from inducing cell rounding and stress fibre formation when microinjected into fibroblasts [80, 81].

Figure 1.2 – Phylogenetic tree of the Rho family of small GTPases

Twenty distinct genes encode for a total number of 21 Rho-associated GTPases in *Homo sapiens* forming eight different subgroups. The RhoA related GTPases (RhoA, RhoB and RhoC), the Rac1 related GTPases (Rac1, Rac2, Rac3 and RhoG), the Cdc42 related GTPases groups (Cdc42a, Cdc42b, TC10 and TCL) which are also related to the Wrch members (Wrch-1 and Wrch-2), the Rnd GTPases (Rnd1, Rnd2 and Rnd3), the RhoD and Rif group, the RhoBTB1 and RhoBTB2 group and the unique RhoH group. Protein sequences of the 21 human Rho family members were aligned using Clustal W and these data were inserted in treeview [74] to generate the phylogenetic tree. This figure was modified from Primeau and Lamarche-Vane [75].

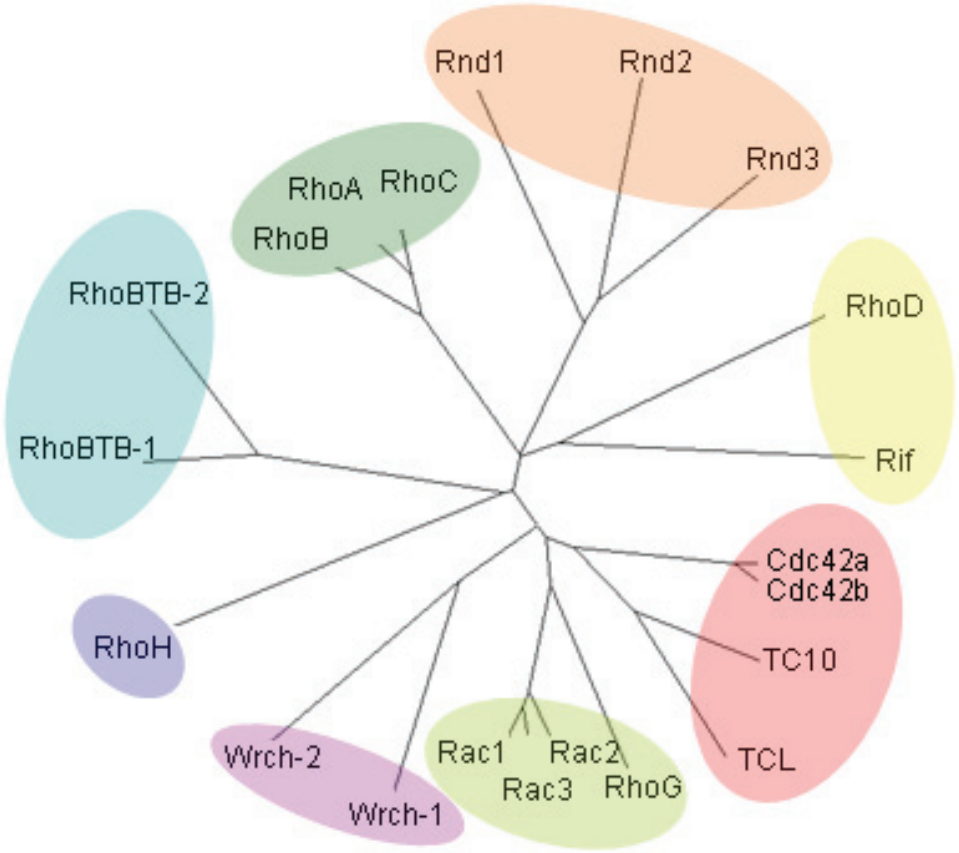
Rnd1
Rnd2
Rnd3
RhoA
RhoC
RhoB
RhoBTB-2
RhoBTB-1
RhoD
Rif
Cdc42a
Cdc42b
TC10
TCL
RhoH
Wrch-2
Wrch-1
Rac1
Rac2
Rac3
RhoG

RhoA and RhoC are both geranylgeranylated [81], while RhoB can be prenylated by either a farnesyl or a geranylgeranyl group [82]. RhoB is also palmitoylated on other cysteine residues at its C-terminus (Table 1.2) [83]. Those differences account partly for the different localizations of Rho proteins in the cell. RhoA and RhoC are found at the plasma membrane whereas RhoB is located mostly on endosomes [84].

Differences in function between these proteins are also observed during cancer development. An increase in RhoA or RhoC expression and/or activity correlates with the onset of human cancers [85, 86], while RhoB is found to be downregulated in some cases [86, 87]. RhoB-null mice are viable, but have increased susceptibility to carcinogen-induced skin tumours [88], suggesting that RhoB indeed acts as a tumor suppressor protein. However, it is not known yet how RhoB carries out this role [89, 90].

Implication of RhoA in cancer is thought to be partly mediated by its effect on actin reorganization through ROCK (Rho-associated protein Kinase). ROCK stimulates actomyosin-based contractility leading to cell migration via blebbing at the cell front, as well as tail retraction [91, 92]. It also reduces F-actin severing, initiated by cofilin, by indirectly inhibiting the latter by its action through LIMK [93]. RhoA also activates mDia, a protein that nucleates *de novo* actin filaments [94, 95]. Interestingly, activation of ROCK and mDia by RhoA is mediated by the removal of an autoinhibitory domain following RhoA interaction [96, 97]. Through these pathways, RhoA participates in the maturation of focal adhesions when activated by integrins upon attachment to the extracellular matrix (ECM) [98, 99]. RhoA is also specifically activated at the tight junctions of epithelial cells through GEF-H1 [100]. Tight junctions function as dynamic barriers to selectively regulate the diffusion of water, ions, and other small molecules through the paracellular space between neighbouring cells. By stimulating actomyosin contractility, RhoA increases paracellular permeability by

destabilizing tight junctions [101]. The participation of RhoA in cancer development is not limited to its involvement in the control of cell migration and adhesion. RhoA is also known for its role in the regulation of the progression of the G1 phase to S phase of the cell cycle. Under its GTP-binding form, it prevents the activation of p21Waf1/Cip1 by Ras, therefore stimulating passage from the G1 phase to the S phase [102, 103].

1.2.2 Rac1, Rac2, Rac3 and RhoG

The Rac subfamily contains four members, with the highly related Rac1, Rac2 and Rac3 that share at least 92% of homology, and the more distant homolog, RhoG, that shares 72% homology with Rac1 (Figure 1.2). In 1992, the publication of a key paper brought attention to Rac1. It was shown for the first time that microinjection of constitutively active Rac1 into fibroblasts led to the formation of lamellipodia and membrane ruffles [70]. This observation revealed how Rac1 could rearrange the actin cytoskeleton and change cell morphology. Its key role in tissue homeostasis and embryonic development was later shown by generation of a Rac1-null mouse that turned out to be embryonic lethal due to defects in the formation of the three germ cells layers during gastrulation [104].

The Rac1 gene encodes for two different isoforms, Rac1a and Rac1b, the latter being an alternative splice variant first discovered in colon cancer cells [105]. This isoform contains an additional 19 amino acids sequence after the second switch of the GTPase, which generates a near constitutively active GTPase because of its incapacity to be restrained by RhoGDI [106, 107]. Rac1a is also mutated in various tumours and is thought to be involved in malignant cell transformation [86, 108]. Like Rac1, Rac2 is overexpressed in some tumours [85], whereas hyperactive Rac3 promotes proliferation of breast cancer cells [109].

Rac1, Rac2 and Rac3 have different expression patterns. Rac1 and Rac3 are expressed ubiquitously, but Rac3 is enriched in the brain. The expression of Rac2 is restricted only to haematopoietic cells where it participates to their development and maturation. The latter is supported by Rac2-null mouse shown to be unable to develop a correct haematopoietic system [110].

The major effects of activated Rac proteins on the cell are mediated through a protein complex containing WAVE (WASP family VErprolin homologous protein), Sra-1, Nap1 and Abi1/2 [111-113]. By binding to Sra-1, Rac1 participates in the release of an autoinhibition domain of WAVE that allows its interaction with monomeric actin and the Arp2/3 complex, through its verprolin-cofilin-acidic VCA domain [113]. Together, they induce actin polymerization and branching at the cell surface to promote membrane protrusion. Rac1 also achieves this function by stimulating the dissociation of gelsolin from actin. Gelsolin severs actin filaments, and stays associated with the fast-growing end of actin filaments (barbed-end), preventing polymerization [114].

Rac proteins also activate the serine/threonine protein kinases PAK-1 to -3 from the PAK (p21-activated kinase) family [115-117]. While the implication of these kinases in cell motility is debatable [118-121], they would provide a link between Rac proteins and gene transcription regulation since Pak kinases have been shown to activate JNK, MAPK and NF-κB pathways [116]. Nevertheless, several reports suggest that PAK is required for lamellipodia formation [122-124]. First of all, PAK phosphorylates filamin and allows this protein to crosslink actin filaments to organize them as a mesh precisely where PAK is activated [123]. And second, PAK can also phosphorylate and inhibit myosin light chain kinase and act against the activity of RhoA to decrease acto-myosin contractility [122]. Finally, PAK promotes formation of the Arp2/3 complex by phosphorylating one of its components, p41-Arc [124].

Similar to other RhoGTPases, the C-terminal sequences of Rac GTPases contain a prenylation site (Table 1.2), which renders all proteins from this subfamily geranylgeranylated. This modification in the basic-rich C-terminal sequences distinguishes Rac1, Rac2 and Rac3 from each other (Table 1.2). This difference in modification changes the ability of Rac GTPases to bind effector proteins. For instance, Rac1 has a higher affinity for PAK1 than Rac2 although this affinity is reversed when chimeric Rac1 and Rac2 proteins swap C-terminal extensions [125]. Similarly, Rac3, but not Rac1, binds to CIB (Calmodulin- and integrin-binding protein) through its C-terminus sequence although they differ by only 3 amino acids [126]. The basic-rich C-terminal region also accounts for striking differences observed when Rac1 or Rac3 are expressed in N1E-115 neuroblastoma cells. Rac1 localizes at the cell membrane and induces cell spreading, whereas Rac3 induces cell rounding and localizes around the nucleus [127]. Depletion of Rac1 was shown to promote cell rounding and impaired cell-matrix adhesion, whereas depletion of Rac3 induces neurite-like protrusions as if the activities of both proteins were opposing each other [127]. This requirement of an intact C-terminal region for proper localization had previously been shown for Rac1 and Rac2 [128, 129].

Several functions have been associated with RhoG, including neurite outgrowth [130], neural progenitor cell proliferation [131], macropinocytosis [132] and phagocytosis [132, 133]. Under its activated form, RhoG binds and activates the RacGEF Dock180, which then activates Rac1 [134]. At least two types of bacteria take advantage of this pathway; during infection of endothelial cells, Salmonella and Yersinia stimulate integrin signaling at the cell surface and trigger successive activation of RhoG and Rac1 to stimulate phagocytosis [135, 136].

1.2.3 Cdc42 and its related GTPases TC10 and TCL

Cdc42 (Cell division cycle 42) takes its name from the genetic screen that allowed its identification back in 1973 [137]. Out of 148 genes, the 42nd was shown to be essential for *Saccharomyces cerevisiae* survival and division. Seventeen years later, the gene was cloned and sequenced during a phenotype-rescue experiment [138]. For the first time, Cdc42 was associated with cell polarity since its overexpression perturbed bud formation in *Saccharomices cerevisiae* [138, 139]. A year later, its human homolog was cloned under the name of G25K (25kDa GTP-binding protein) [140], and shown to complement the *cdc42-1* mutation in yeast [141].

Attention was drawn on Cdc42 when it was found to be activated by the GEF Dbl [142]. Dbl had previously been isolated from a primary human diffuse B-cell lymphoma in a screen using NIH3T3 cells to assess cell transformation [143-145]. Considering that Dbl was a potent oncogene, these results suggested that Cdc42 could be the physiological mediator of Dbl-induced transformation, and indeed this was the case. Years later, it was shown that the activated form Cdc42^{F28L} was able to induce foci formation in NIH3T3 fibroblast cells [146].

During the same time, the group of Alan Hall discovered the effects of constitutively active Cdc42 on the cell shape of fibroblasts [64]. The microinjection of purified active Cdc42^{V12} into serum-starved Swiss 3T3 cells induces filopodia and focal complex formation at the plasma membrane. Moreover, the use of dominant negative and constitutively active forms of RhoA, Rac1 and Cdc42 suggested that Cdc42-induced filopodia occurred prior to Rac1-induced lamellipodia and RhoA-induced stress fibres, suggesting a hierarchical relationship among Cdc42, Rac1 and RhoA.

Cdc42 is expressed as two different splice variants in humans, Cdc42a and Cdc42b, which differ in only 10 C-terminal amino acids (Table 1.2) [147, 148]. While Cdc42a is expressed ubiquitously, the expression of Cdc42b is restricted to the brain. The most striking consequence of the change in sequence identity resides in the secondary modification of both proteins. While Cdc42a is prenylated [147, 149], Cdc42b is reversibly palmitoylated [147, 148]. Dual prenylation and palmitoylation of Cdc42b has not been tested yet although its sequence predicts it is [150]. In neurons, Cdc42b concentrates in dentritic spines where it is thought to have a specific role in inducing post-synaptic structures [148]. Stimulation of neurons with glutamate induces rapid depalmitoylation on several proteins, including Cdc42b, which causes it to disperse from the dentritic spines. Since depalmitoylation correlates with morphological changes at the synapse, it is proposed that Cdc42b may participate in the activity-driven changes that shape synapse structure and function [148].

TC10 and TCL (TC10-like), the two closest homologs of Cdc42, also have distinct C-terminal sequences [151]. TC10 and TCL are predicted to be palmitoylated like Cdc42b, and farnesylated based on the amino acid identity of their terminal CAAX boxes [67]. This CAAX contributes to the distinct roles for these two GTPases in the cell. TCL localizes to the plasma membrane and the early endosomes, where it is involved in membrane receptor recycling by being required for the transition of endocytic vesicles to early endosomes [152]. Interestingly, chimeric Cdc42a or TC10 proteins ending with the C-terminal amino acids of TCL behave as wild type TCL, suggesting that the GTPase module itself is interchangeable and that function identity of TCL is contained within its C-terminal residues [152].

TC10 is required for promoting expansion and axonal specification in developing neurons by triggering the translocation to the plasma membrane of

the exocyst component exo70 in the distal axon and growth cone, thus promoting the addition of new membrane [153]. Similarly, TC10 is involved in vesicle trafficking, by regulating the translocation of glucose transporter type 4 (GLUT4) to the cell surface of adipocytes [154]. Upon insulin stimulation, TC10 is activated and promotes exocytosis of GLUT4 containing vesicles by helping the assembly of membrane docking regulating proteins [155]. This activation is partly mediated by kinase Cdk5 which phosphorylates a threonine residue located within the C-terminal basic-rich region of TC10 to facilitate its localization to lipid rafts [156]. Similar to Cdc42, TC10 is also implicated in axonal regeneration. Peripheral nerve or spinal cord injury in rats induces expression of TC10 in regenerating neurons at the site of the injury [157, 158].

Similarly to other RhoGTPases, Cdc42 is able to remodel actin structures when activated. This ability is most often mediated by activation of effectors of the Wiskott-Aldrich syndrome protein (WASP) group [159-161]. WASP is a protein expressed solely in haematopoietic cells and its gene, located on chromosome X, was found to be mutated in a genetic disease named Wiskott-Aldrich syndrome (WAS) [162]. Males with WAS fail to make an immune response to antigens because of defective T-cell/B-cell interactions [163] and fail to produce mature lymphocytes and platelets [164]. WASP has one homolog expressed ubiquitously in human tissues, but at higher levels in the brain, termed N-WASP (neuronal-WASP) [165]. N-WASP is the protein required by Cdc42 to induce filopodia in fibroblasts [166]. Upon interaction with Cdc42-GTP, N-WASP releases its VCA domain and, as for WAVE, interacts with monomeric actin and the Arp2/3 complex to nucleate new actin filaments and to crosslink them in an actin meshwork [167]. Both TCL and TC10 bind to WASP and N-WASP, although the affinity of TC10 for WASP is nearly 1000-fold weaker than that of Cdc42 [168].

Cdc42 also binds and activates selected members of the DRF group (Dia1, Dia2 and Dia3) [169]. DRF proteins stimulate the nucleation and extension of non-branching actin filaments. They dimerize to form a barrel that surrounds the barbed end (fast-growing end) of actin filaments, not only preventing the binding of capping proteins, but also inducing polymerization [170, 171]. This translates in the cell in filopodia-like structures.

As for Cdc42 and Rac1, TC10 and TCL both bind and activate Pak1, Pak2 and Pak3 kinases. As discussed previously, activation of these kinases affects actin-filament organization, but is also required for the activation of various signaling pathways that contribute to cell cycle progression and proliferation, such as the JNK and MAPK pathways [117, 172]. Notably, PAK1 is required for the ability of Cdc42, Rac1 and Rac3 to induce cell transformation [109, 146, 173].

The most important contribution of Cdc42 and its related members remains its implication in the establishment of cell polarity. Cell polarization is at the base of many cellular processes including migration, differentiation and morphogenesis. It was originally demonstrated that overexpression of Cdc42 perturbs bud formation in *S. cerevisiae* while its mutation prevents budding [138, 139]. This role for Cdc42 in polarization is conserved from yeast to humans. Cdc42 functions primarily through the PAR polarity protein complex composed of partitioning-defective-6 (PAR6), PAR3 and atypical protein kinase C zeta (PKCζ) to induce cell polarity [174, 175]. In migrating cells, activated Cdc42 recruits the complex to the leading edge of the cell which then captures and stabilizes microtubules at the migrating front, reorienting the Golgi apparatus and the microtubule-organizing center (MTOC) [176, 177]. Epithelial cells also have a polarized morphology that is defined by an asymmetrical distribution of proteins to form distinct apical and basal regions. Cdc42 and the PAR complex are required for this polarization and will localize to the apical region in a Cdc42-

dependant manner [178]. Both constitutively active and dominant negative mutants of Cdc42 affect tight junction formation and the polarized trafficking of proteins to the apical and basal regions [175, 179]. Polarity maintenance promoted by Cdc42 and the Par complex is thought to be mediated by endocytic trafficking through targeting of recycling endosomes to specific intracellular sites [180]. TC10 has also been shown to associate with Par3/6 and PKCζ [181], which may explain how it contributes to endocytic trafficking [155].

1.2.4 Wrch-1 and Wrch-2

Wrch-1 and Wrch-2 are distantly related to Cdc42. Wrch-1 was discovered in a study looking for genes whose expression was increased upon stimulation of Frizzled by the growth factor Wnt-1 [182]. Activation of this signaling pathway is central to embryonic development, but also contributes to tumour formation. In fact, overexpression of Wrch-1 or a constitutively active form of Wrch-1 in mammary epithelial cells mimics Wnt-1 stimulation, and induces cell transformation [182]. Wrch-2/Chp is also able to induce fibroblast cell transformation when overexpressed [183]. Both Wrch-1 and -2 bear a particular N-terminal extension of around 50 amino acids that is enriched in proline residues. For Wrch-1, it serves as a binding site for the scaffold protein Grb2, which promotes the activation of Wrch-1 [184]. While Wrch-1 has, like other Rho GTPases a CAAX box at its C-terminus, this protein is not prenylated [185]. However, Wrch-2/Chp is palmitoylated [183, 185], which accounts for its special intracellular localization. In osteoclasts, Wrch-1 localizes mostly to podosomes while it is found enriched at focal adhesions in Hela cells and fibroblasts [186]. In MDCK epithelial cells, Wrch-1 localizes along the apical and basolateral membranes, and negatively regulates tight junction assembly during epithelial cell polarization by activating the Par polarization complex Par6/Par3/PKCζ [187]. Interestingly, Wrch-1 is specifically phosphorylated by

Src within its C-terminus, which relocalizes Wrch-1 from the plasma membrane to endosomal vesicles [188].

1.2.5 Rnd1, Rnd2 and Rnd3

The Rnd proteins are close protein homologs to the Rho protein, but substitutions of few residues in their primary sequence completely change the nature of these proteins [189, 190]. First, they differ from regular GTPases by their inability to hydrolyse GTP and are consequently kept in a constitutively active form. Secondly, their C-terminus ends with a CAAX box, which associates with farnesyl-transferase instead of geranylgeranyl-transferase, therefore changing the nature of the lipid added to these proteins in comparison to Rho proteins [189]. The farnesyl group allows Rnd proteins to escape from RhoGDI sequestration in the cytoplasm and to stay attached to membranes at all times [189, 190].

These properties allow the Rnd proteins to antagonize the functions of Rho GTPases. For instance, overexpression of Rnd1 and Rnd3 in fibroblasts promotes focal adhesion disassembly and cell rounding [190], a phenotype that is opposite to the one observed when RhoA is expressed. Rnd3 will achieve this by competing with RhoA for one of its effectors, the serine/threonine protein kinase ROCK [191]. An other model suggests that Rnd1 and Rnd3 bind and activate p190RhoGAP, which in turn inactivates RhoA [192].

While the expression of Rnd3 is ubiquitous, Rnd2 is restricted to testis and Rnd1 is principally found in the brain [190]. In neurons, Rnd1 promotes growth cone retraction of axons expressing the repulsive receptor plexin-B1. Upon interaction with its substrate Sema-4D, plexin-B1 recruits Rnd1 and stimulates the RasGAP activity of Plexin-B1, which induces a loss of adhesion and retraction of the growth cone [193].

1.2.6 RhoD and Rif

RhoD and RhoF/RIF form a distinct class of Rho GTPases that share a unique small 15 amino acid extension at their N-terminus for which no function has yet been associated. Both genes originate from a common ancestor gene they share with Rho and Rnd proteins (Figure 1.2) [194]. While Rif first appeared in chordates, as most of the non-classical GTPases, RhoD is unique to mammals, making this last protein the youngest of the RhoGTPases in humans [194].

When expressed as constitutively activated forms, both proteins induce the formation of filopodia [195, 196], although they are much longer and thinner then those induced by Cdc42 [197]. While Cdc42 induces actin filament elongation by activating Arp2/3 or proteins from the formin family, RhoD and Rif promote actin filaments elongation by recruiting and activating, respectively, hDia2C and mDia2 [198, 199], two proteins of the formin family which nucleate actin filaments.

RhoD and Rif are both associated with endosomes through their geranylgeranyl group and polybasic C-terminus residues. Active RhoD recruits hDia2C to early endosomes, promoting the activation of c-Src at the early endosome membranes, which in turn causes a stronger association of the endosomes to the actin fibres [197]. Therefore, it is proposed that the overall role of RhoD and Rif is to act on transportation of early endosomes and mediate their fusion in late endosomes [197].

1.2.7 RhoBTB

Genes from the RhoBTB family were originally identified in a genetic screen for Rho homologs in *Dictyostelium discoideum* [200]. In humans, both members of this group lack a prenylation signal and have a unique tertiary structure, with a GTPase domain followed by two BTB (Broad-Complex/Tramtrack/Bric-à-Brac) domains. These domains are usually found in transcription factors. Both RhoBTB1 and RhoBTB2/DBC2 associate, through their first BTB domain, to Cullin3 and to the RING domain protein Roc1 to form a functional E3 ubiquitin ligase complex [201, 202]. While specific targets for this E3 ligase remain to be found, the contribution of RhoBTB proteins to this activity seems to be of key importance. Breast tumour biopsies have revealed that RhoBTB2 expression is reduced in breast tumours, and absent in 3.5% of the cases [203]. Two missense mutations were also identified in breast cancer specimens, and one of them, located in the first BTB domain, prevents formation of the E3 ligase complex [203]. This finding led to the hypothesis that RhoBTB2 functions as a tumour suppressor gene. RhoBTB1 could have the same role, since loss of function of RhoBTB1 is associated with head and neck cancer [204].

A third member, RhoBTB3, was never accepted as a Rho GTPase because of its incapacity to bind GTP. In fact, a recent study now suggests it binds and hydrolyse ATP, and may function through its interaction with Rab9 in protein transport from endosomes to the trans Golgi network [205].

1.2.8 RhoH/TTF

RhoH/TTF (translocation three four) was originally discovered in a chimaeric transcript generated by the recombination of chromosomes 3 and 4 in a patient suffering from non-Hodgkin's lymphoma [114]. Its expression is limited to haematopoietic cells, and as for the Rnd proteins, will constitutively bind to GTP to antagonize the function of other Rho proteins [206]. In addition to its competitor role, RhoH has been implicated in TCR signaling, as identified by gene-targeting studies in the mouse [207]. Its absence prevents proper recruitment of the kinase ZAP70 to the T-cell synapse, which impairs the positive selection, maturation and proliferation of thymocytes, resulting in T-cell deficiency [208].

As it is the case between the different subgroups of GTPases found in the Ras superfamily, the Rho GTPase family itself represents a fascinating example of how a simple module can be adapted to different usages in an organism. However, there is still a long road to walk before we understand the discrete differences between members of each subfamily. It is noteworthy that small differences in the nature of the amino acids located at the C-terminus of these proteins can have a dramatic impact on their location in a cell, and on the identity of the protein they are associated with.

1.3 Regulators of GTPases

Functional GTPase switches go through the same cycle (Figure 1.3), transiting between three conformational states: GDP-bound, “empty”, and GTP-bound. The “empty” state is an intermediate step that occurs between the time GDP is replaced by GTP in the guanine nucleotide binding site of the GTPase. The GTP-bound and GDP-bound states represent two different conformational states of a GTPase, named respectively “active” and “inactive” states because the former activates effector enzymes whereas the latter does not.

For most GTPases, the proportion of molecules in the “active” position depends on the relative rates of two reactions: the dissociation between a GTPase and bound GDP, and the hydrolysis of bound GTP. These rates are respectively termed by two fractional rate constants: k_{diss}·GDP and k_{cat}·GTP. The ratio between GTP-bound and GDP-bound forms can therefore be defined by the following equation in a system at equilibrium where the empty state of a GTPase i snot considered [209]:

$$\frac{\text{GTPase}\cdot\text{GTP}}{\text{GTPase}\cdot\text{GDP}} = \frac{k_{diss}\cdot\text{GDP}}{k_{cat}\cdot\text{GTP}}$$

Therefore,the relative proportion of protein in the active GTP-bound state can rise by increasing k_{diss}·GDP or decrease by reducing k_{cat}·GTP. For GTPases, specific proteins are in charge of changing these rate constants. The proteins increasing k_{diss}·GDP are termed Guanine-nucleotide Exchange Factors (GEFs), whereas GTPase-Activating Proteins (GAPs) increase the k_{cat}·GTP. With these events taking place at the cell membrane,

Figure 1.3 – RhoGTPases cycle

RhoGTPases are molecular switches that cycle between an inactive and an active state when binding to GDP or GTP, respectively. Cycling between GDP and GTP occurs strictly at the membrane and is assisted by two different families of proteins. The Guanine-nucleotide Exchange Factors (GEFs), including the Dbl and DOCK families, stabilizes the transition state of the GTPase, opening its nucleotide-binding pocket and allowing a new nucleotide, usually a GTP due to its abundance, to take the place of the former one. Under this activated state, GTPases are able to associate with their effector proteins to induce a signaling pathway. GTPases Activating Proteins (GAPs) also associate with the GTP-binding form of GTPases and help the latter to hydrolyse the GTP to GDP, switching the GTPase from its active to its inactive state. Membrane targeting of RhoGTPases is also under the control of another group of proteins called the RhoGDIs. These have the ability to sequester lipid-modified GTPases in the cytoplasm.

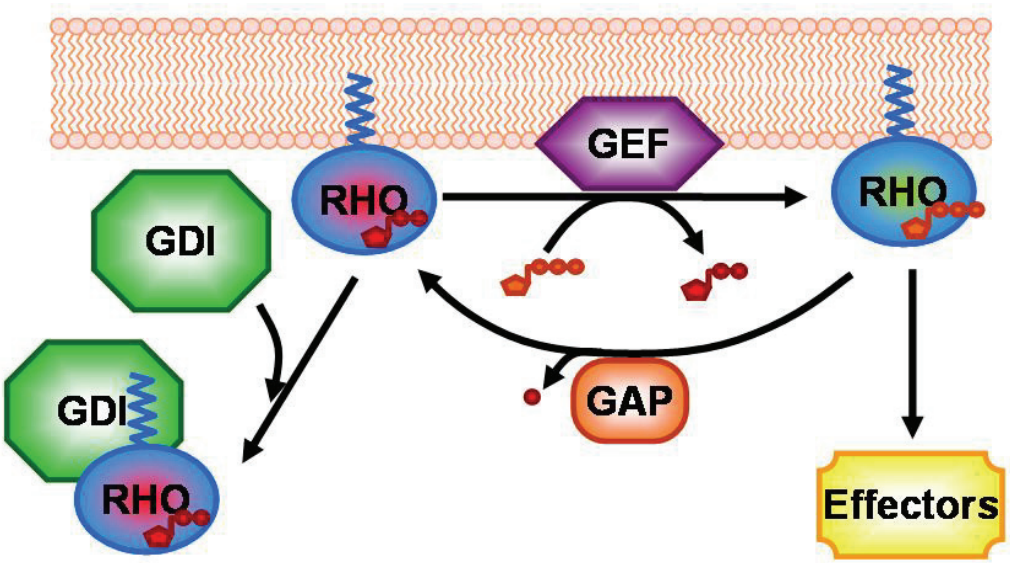

Legend

= GTP

= GDP

= inorganic phosphate

localization is required and controlled by two main events. GTPases first need to be modified following by the addition of a lipid moiety and require detachment from RhoGDI, a protein that sequesters lipid modified GTPases in the cytoplasm.

1.3.1 The Dbl Homology Domain Containing Factors (GEFs)

The first Rho specific GEF, Dbl, was identified in a genetic screen used to find genes inducing the transformation of NIH 3T3 cells [143, 144]. Further work showed that this chimaeric protein turns out to be a constitutively active GEF for Cdc42 and RhoA [142, 210], owing to the absence at its N-terminus of an auto-inhibitory sequence [211].

The ability to transform cells was then found in various proteins, including Vav, Tiam1, Ect2, Net1, p115RhoGEF and Lbc, which all share a protein module comprising two domains: a DH (Dbl homology) domain followed by a PH (Pleckstrin homology) domain [212-217]. The DH domain is responsible for the GEF activity since it stabilizes GTPases in a conformation that allows its separation from the nucleotide. The GTP concentration being approximately ten fold higher than the GDP concentration [209], GTP rapidly replaces the leaving GDP, generating an “active” GTPase. The PH domain was originally hypothesized to recruit the GEF at the plasma membrane, however, PH domains of the Dbl-family members bind phospholipids with a low affinity and with little specificity, which implies that these interactions are insufficient for membrane localisation [218]. The crystal structure of the DH-PH module of the GEF Dbs active towards Cdc42 has revealed direct contacts between the PH domain and the GTPase, suggesting that the PH domain could assist the DH domain in its task [219]. This could explain why both domains are required to induce transformation [220, 221].

Since the discovery of Dbl, proteins containing the DH-PH module reached the number of 69 distinct homologs, activating Rho GTPases within particular spatio-temporal contexts and with different specificities [222]. Most GEFs have a broad expression profile. Vav2, Sos, Trio, Abr, Bcr are a few examples of proteins which are found in every adult tissue. However, some are limited to specific tissues. Vav1 and Lsc are both restricted to haematopoietic cells [213, 214], while the GEF Intersectin-L is found only in the brain [215, 216]. Several GEFs, including Intersectin-L, TRIO and Kalirin, are also expressed as multiple splice variant isoforms during development [223-226]. Most GEFs have been shown to be specific to one or two GTPases, the most notable being β-Pix (Cdc42, Rac1), Fgd-1 to -4 (Cdc42), Intersectin-1 and -2 (Cdc42), Sos-1 and -2 (Rac1), Tiam1 (Rac proteins), Tuba (Cdc42) and Trio (Rac1/RhoG for its N-terminus module; RhoA for its C-terminal module) [212, 217]. This information is still relatively preliminary, as in most cases, only RhoA, Rac1 and Cdc42 have been tested so far. Moreover, specificity was addressed mainly in *in vitro* studies using deletion mutants of the GEFs and without considering membrane insertion of the GTPases. Therefore the context is relatively distant from the one where both proteins interact together *in vivo* [222, 227].

Part of the specificity of these proteins in a cellular context arises from regions found outside of the DH-PH module. GEFs of the Dbl family are often multi-domain containing proteins [222, 227], which are in part responsible for localization and for recruiting different proteins to a particular area in the cell. One good example is Intersectin-1L, a GEF for Cdc42 that recruits through its SH3 domains N-WASP, and therefore brings activated Cdc42 and its specific effector in the same environment [228]. Another example is Vav1, which uses its SH2 domain to be recruited right where it gets activated at the T-cell receptor (TCR), providing a local GEF activity that participates in the formation of immunological synapses upon TCR activation [229, 230].

A large number of GEFs from the Dbl family contain autoinhibitory domains that allow the GEFs to stay in a dormant phase until they get activated by the correct signaling molecule. In several cases, that stimulus comes from a kinase, as for the Vav proteins. The DH domain of Vav is kept inhibited by a small alpha helix that sits on its GTPase-binding interface. Phosphorylation by Src-family kinases of a particular tyrosine in that helix unfolds it, and allows the GEF to activate GTPases [231, 232]. In other situations, the autoinhibitory domain is removed by direct interaction with proteins, like β-Pix, which requires an interaction with Pak or Cbl to be active [223].

Various mutations in Dbl-family members are responsible for human diseases [222]. One such example is a result of bad replication of the Bcr gene and the Abl kinase gene coding sequences. This mutation, known as the Philadelphia chromosome, generates a chimaeric protein in which the autoinhibitory domain of Abl is replaced by Bcr. This protein is a constitutively-active kinase that leads to acute lymphocytic leukemia independently of the Bcr GEF activity [233]. Gene alterations involved in the expression of truncated mutants have also been linked to development defects. Mutations in the gene encoding the Rac GEF Alsin induce the generation of truncated proteins lacking the DH-PH module [225]. Patients with this mutation suffer juvenile onset amyotrophic lateral sclerosis (ALS2) [234, 235]. The Cdc42 specific GEF Faciogenital dysplasia 1 (Fgd1) is also not expressed correctly in a syndrome that is, like its name suggests, a developmental disorder characterized by the malformation of specific skeletal structures [236, 237]. Although the discovery of several GEFs originates from NIH3T3 transformation assays, it turns out that this technique does not always correlate *in vivo* with oncogenic abilities. Consequently, most GEFs identified as constitutively-activated mutants are not associated with human cancers [222]. However, Tiam1 mutations were associated with renal, hepatic and prostate cancer [238-242] and a number of Tim splice variants were associated with breast tumor formation [243].

Additionally, rearrangement between the genes encoding the Rho GEF LARG and MLL causes the expression of a chimaeric protein that has been associated with acute myelogenous leukemia, and involves its RhoGEF activity [244].

1.3.2 The Dock family of GEFs

Around the turn of the century, a new group of GEFs was uncovered with the discovery that Dock180 is able to induce Rac1 activation [230, 231] by itself, without the involvement of a Dbl-family GEF [232]. Dock180 was originally identified as a binding protein for the SH3 domain of c-Crk [233] and ELMO, with which it forms a complex required for phagocytosis and cell migration in *C. elegans* [245, 246]. From that point, the Dock family expanded to 11 members in mammalian cells [247], with Dock1/Dock180, Dock2, Dock3 and Dock7 being Rac1-specific GEFs [232, 233], Dock9 being a Cdc42-specific GEF [238] and Dock6 being specific to both [248]. No Dock GEF has been reported to activate RhoA.

Similarly to the Dbl family of GEFs, Dock GEFs contain a conserved domain responsible for GTPase binding and nucleotide exchange (DHR2), found at the C-terminus of most Dock proteins, and a lipid binding domain (DHR1) located N-terminally to the DHR2 domain [249]. In the case of Dock1/Dock180, Dock2 and Dock7, this domain binds phosphatidylinositol-(3,4,5)-trisphosphate ($PI(3,4,5)P_3$), which recruits these proteins to the cell membrane [235, 236]. RhoG has also been shown to be required for localizing Dock proteins [134]. Following cell adhesion to fibronectin, RhoG is activated and interacts with the Dock/ELMO/Crk complex via ELMO. This forces the recruitment of the complex at the plasma membrane where Rac1 is activated.

In mammals, the functions of Dock proteins are becoming increasingly better understood. Dock2, whose expression is restricted to haematopoietic

cells, is required for lymphocyte migration, as cells from Dock2 null mouse failed to migrate towards chemokines *in vitro* [250]. Dock7, whose expression is high in developing rat brains and in hippocampal neurons is thought to be involved in the axonal determination of these cells [251, 252].

1.3.3 The Guanine Nucleotide Dissociation Inhibitors (GDIs)

Guanine nucleotide dissociation inhibitors (GDIs) are GTPase chaperones that allow GTPases to be “soluble” in the cytoplasm. They perform this task by hiding the hydrophobic geranylgeranyl moiety that normally allows GTPases to be anchored to lipid membranes. Therefore, they can either function by transporting a GTPase to a membrane, or extracting a GTPase from a lipid bilayer, independently of their nucleotide-binding state [253].

Through their action on Rho GTPases, RhoGDIs are involved in a multitude of phenotypes including cell division, morphology, migration, vesicular trafficking and gene expression. Three different RhoGDI (RhoGDI1, RhoGDI2 and RhoGDI3) proteins have been identified in humans. RhoGDI1 binds to all Rho GTPases tested to date with similar affinity, but will not, as RhoGDI2 and RhoGDI3, bind the GTPases that are either farnesylated (Rnds), palmitoylated (Cdc42b, RhoB, TC10, TCL, Wrch1 and Wrch2), or lacking a prenyl moiety (RhoBTB1 and RhoBTB2) (Table 1.2) [254]. RhoGDI2 also seems to have a broad specificity, although it has less affinity for Cdc42 [247]. RhoGDI3 is the most divergent of the three and is associated with the Golgi apparatus and vesicular membranes [255, 256]. To date, RhoGDI3 has only been shown to interact with RhoG [255, 257].

Several studies have attempted to show how the affinity of RhoGDIs for GTPases could be modulated in order to control the ratio of GDI-bound GTPases to GDI-unbound GTPases. Protein interaction, lipid interaction and

phosphorylation are possible mechanisms. For instance, RhoGDI was found to be constitutively phosphorylated in resting neutrophils [258]. Interestingly, dephosphorylation of RhoGDI produced a protein with lower affinity for RhoA. Several different kinases are thought to phosphorylate RhoGDI1 based on a two-dimensional gel analysis [247, 251]. PAK1 is one of them. It phosphorylates RhoGDI1 on two sites and contributes by this way to reduce the affinity of RhoGDI for Rac1, but not for RhoA [252]. The phosphorylation event that seems to have the greatest impact on RhoGDI function is mediated by Src on a tyrosine located at the GDI-GTPase interface. When phosphorylated at this site, RhoGDI1 and RhoGDI2 are not able to associate with GTPases [253, 254].

Several *in vitro* studies have suggested that long carbon chain lipids could induce separation of the GTPase from the GDI [255, 256]. However, the facts that RhoGDI binds principally to the geranylgeranyl group of GTPases and that lipids are being anchored in membranes *in vivo* suggest that this mechanism might not be applied *in vivo*. Alternatively, it has been suggested that protein interaction could promote dissociation of GTPases from RhoGDI proteins: the ERM (Ezrin, Radixin, Moesin) family of proteins, the tyrosine kinase Bmx, and the p75 neurotropin receptor have been described to achieve this task [259-261].

1.3.4 The GTPase-Activating proteins (GAPs)

According to the Human Genome Project, the Rho specific GTPase-Activating Proteins (RhoGAPs) family represents the 38th largest family of proteins expressed by human cells with 77 members [26]. This is about four times the number of Rho GTPases, which suggests different specificities, but also different implications in time and space for those GAPs.

Similar to other Ras superfamily members, Rho GTPases are very ineffective enzymes given their slow GTP-hydrolysis rate. Therefore, to switch from an “active” GTP-binding to an “inactive” GDP-binding conformation, they need the assistance of GAPs. This protein accelerates the hydrolysis step by several orders of magnitude. First, it stabilizes a glutamine residue of the GTPase in a position allowing a water molecule in the pocket for an in-line nucleophilic attack to the gamma-phosphate. Secondly, the GAP domain completes the phosphate-binding site with an additional arginine residue, the arginine finger, which stabilizes the transition state by neutralizing negative charges at the gamma-phosphase [262, 263].

Like GEF proteins, GAP domain-containing proteins may include as many as 8 domains involved mostly in protein-protein interactions (BAR, C1, C2, DEP, FCH, FF, GEF, PDZ, PH, PPC, SAM, SEC14, SH2, SH3, START, WW) and/or lipid-binding interactions (C1, C2, BAR, DEP, Sec14, PH, PDZ, START) [264, 265]. These domains are hypothesized to play an important role in the tight control of RhoGAPs activities, just as posttranslational modifications and/or binding of second messengers. These interactions and modifications will affect the GAP by changing its localization or by releasing it from its autoinhibitory state. Here, these regulation modes and diseases associated to these GAPs will be approached as we overview some members of this large family.

ARHGAP1 / Cdc42GAP / p50RhoGAP

The first identified RhoGAP was ARHGAP1 / Cdc42GAP / p50RhoGAP, a ubiquitously expressed protein found to increase GTPase activity of all the Rho proteins tested to date (RhoA, Rac1, Cdc42, TC10) with a marked specificity for Cdc42 [266]. ARHGAP1 contains a C-terminal GAP domain and an N-terminal Sec14 domain thought to bind lipids. Interestingly, both domains interact in a yeast two-hybrid experiment, and it is suggested that prenylated-GTPase binds Sec14 to open the protein and allow the GAP to activate the GTPase [267]. Given that these results are not based on *in vivo* experiments, and while the results could be interpreted differently, this model would require additional experiments to be validated. The precise biological function of this gene has not been established yet. However, a Cdc42GAP-null mouse was generated showing increasing levels of Cdc42-GTP in tissues, resulting in a delayed and shortened reproductive period for females, a reduced cell size, anaemia and premature aging [268, 269]. The latter was confirmed by experiments showing a premature accumulation of genomic abnormalities and induction of cellular senescence. Given that ARHGAP1 is a negative regulator of Cdc42 and that Cdc42-GTP levels are increased in ARHGAP1-null mouse tissues, it is hypothesized that ARHGAP1 has implications in genome stability. A noticeable phenotype associated with the ARHGAP1-null mouse is also a reduction in bone mineral density [269]. This observation correlates with the results of a large-scale meta-analysis of genome-wide association studies that identified ARHGAP1 among 20 genes that could be involved in osteoporosis [270].

p190RhoGAP-A / ARHGAP35 and p190RhoGAP-B / ARHGAP5

Although ARHGAP1 was the first GAP to be identified, no GAP has been more studied at this point than p190RhoGAP-A, also known as ARHGAP35. Its close relative, ARHGAP5 (p190RhoGAP-B) has also been the focus of several studies [271, 272]. These GAPs are ubiquitously expressed multidomain

proteins that consist of an N-terminal GTP-binding domain, followed by four FF domains thought to promote protein interactions, and a C-terminal GAP domain [267]. p190RhoGAP-A plays a crucial role in regulating actin cytoskeletal rearrangements in axonal pathfinding and stability [273, 274] and in response to integrin functional engagement and growth factor stimulation [273, 275, 276]. These roles are thought to rely on the ability of this GAP to activate GTP-hydrolysis of RhoA [272]. Studies on ARHGAP5- and p190RhoGAP-A-deficient mice have revealed that each protein is essential for normal embryonic development given a variety of defects in tissue morphogenesis [273, 277-280]. p190RhoGAP-A null mice exhibit defects in axon guidance and fasciculation, neural tube closure, and eye development and die soon after birth [273, 277, 278] while ARHGAP5-null mouse have growth problems, and therefore present with stunted growth. The latter phenotype would be due to the alteration of signaling pathways induced by insulin [259, 260]. In contrast to ARHGAP1-null mouse showing elevated levels of Cdc42-GTP, these mice do not show a general increase in Rho-GTP levels, which suggests a context-dependent regulation of Rho proteins.

Phosphorylation events mediated by Src [253, 256, 261, 262] and GSK3-β [281] have been shown to regulate p190RhoGAP-A. Phosphorylation by Src causes a change in p190RhoGAP-A localization, moving from the perinuclear region to the cell periphery. This event correlates with dissolution of stress fibres and disruption of the actin cytoskeleton [282]. Inversely, GSK3-β phosphorylation at the C-terminus of p190RhoGAP-A inhibits its GAP-activity both *in vivo* and *in vitro*. Interestingly, p190RhoGAP-A-null fibroblasts were shown to be defective for polarized cell migration. This problem could only be rescued by reintroduction in these cells of wild-type p190RhoGAP-A. Mutants lacking the specific serine and threonine residues targeted by GSK3-β were unable to do so, therefore linking p190RhoGAP-A with polarized cell migration [281].

p190RhoGAP-A is also regulated by lipids. As for other regulators of GTPases, GAPs need to be localized at a membrane to exert their activity on GTPases. Therefore, it is not surprising to find lipid-binding domains within these proteins. However, in the case of p190RhoGAP-A, lipid binding seems to change the specificity of the GAP. A small region enriched in basic residues located at the N-terminus of the GAP domain is responsible for phosphatidylserine interactions [283, 284]. In the presence of phosphatidylserine, p190RhoGAP-A loses its ability to act on RhoA, and becomes a potent activator of Rac1 [283]. However, these experiments were conducted *in vitro*, using prenylated GTPases in the absence of membranes which makes it difficult to reconcile with an *in vivo* environment.

Protein-protein interactions also regulate the GAP activity of these proteins. p190RhoGAP-A is at the center of a crosstalk between two different Rho GTPases: Rnd3 and RhoA. The Rnd proteins, as discussed previously, constitutively bind to GTP, and can compete with RhoA for effector binding. Alternatively, Rnd3 promotes the inactivation of RhoA by binding to p190RhoGAP-A at its center, thereby increasing its GAP activity and reducing the levels of Rho-GTP [192].

α-chimaerin / ARHGAP2 and β-chimaerin / ARHGAP3

The regulation of α-chimaerin / ARHGAP2 and β-chimaerin / ARHGAP3 by lipids is well characterized and has been the subject of numerous publications [285-289] . Chimaerins are Rac specific GAPs [288, 289] that both exist as splice variants known as α1- and α2-chimaerin and β1- and β2-chimaerin, respectively [285, 290]. All isoforms share a C-terminal GAP domain preceded by a C1 domain, with an additional N-terminal extension containing an SH2 domain in α2- and β2-chimaerin [285]. In its resting state, chimaerin has its GAP and C1 domains associated in a way that sterically blocks the GTPase-binding interface of the GAP domain [291]. Like in PKC proteins, the C1 domain

of chimaerins associates at the plasma membrane with diacylglycerol. By doing so, it not only promotes recruitment of the protein at the membrane, but also partitioning of the C1 and GAP domains, allowing the latter to bind GTPases [290]. Interestingly, β2-chimarerin seems to be retroactively inhibited by diacylglycerol, as it activates PKCδ, which in turns negatively regulates β2-chimarerin by phosphorylation of a serine residue between its SH2 and C1 domains. This regulatory mechanism is limited to β2-chimarerin as the PKC phosphorylation site is not conserved in either β1- or α-chimaerin isoforms [292].

Chimaerin isoforms have different expression patterns. α1-, α2- and β2-chimaerin are mostly found in the brain, whereas β1-chimaerin seems to be expressed exclusively in testis and in germ cells [293-295]. The expression of α-chimaerins at early development stages in the brain suggests a possible role in neuron development [296]. Indeed, α2-chimaerin is a primary component of the machinery inducing growth-cone collapse induced by semaphorin-3A/neuropilins and mediates, like β2-chimaerin, ephrin/EphA4 signaling [286-289]. Recently, α2-chimaerin was linked to Duane's Retraction Syndrome [297], a congenital eye movement disorder characterized by the inability of the eye to move in some specific orientations. Heterozygous mutations in *CHN1*, the gene coding for both α1- and α2-chimaerin, were found conserved in patient families and were shown to generate hyperactive GAP proteins that could escape their autoinhibited state by the C1 domain. This increase in Rac-specific GAP activity in oculomotor neurons is thought to prevent the correct innervation of their target extraocular muscles, preventing them from being fully functional. Impaired semaphorin or ephrin signaling in this context remains to be evaluated.

SRGAP1 / ARHGAP13, SRGAP2 / ARHGAP34, SRGAP3 / ARHGAP14 and SRGAP4 / ARHGAP4

Chimaerins are not the only GAPs involved in chemorepellent signaling. The four SRGAP proteins (SRGAP1/ARHGAP13, SRGAP2/ARHGAP34,

SRGAP3/ARHGAP14 and SRGAP4/ARHGAP4) have been extensively linked to the Slit/Robo pathway [298, 299]. Slit proteins are secreted by the floor plate, and prevent crossing of axons through the midline of the brain and spinal cord by interacting with their Robo receptor on growth cones [298]. When activated, Robo recruits the Cdc42 specific SRGAP1 through a proline-rich sequence recognized by an SH3 domain contained in SRGAP proteins [298, 300], and will therefore indirectly induce a change in the growth cone migration by locally inactivating Cdc42. However, this mechanism might show some variations with regard to the specificity of SRGAPs for GTPases. SRGAP1 associates with Cdc42, SRGAP2 and SRGAP3 are specific to Rac1 [298, 300] and SRGAP4 targets all three GTPases *in vitro* [301, 302]. GAPs of this family all have a BAR lipid-binding domain at their N-terminus. This domain has the property to recognize bent membranes and/or to induce bending of the membrane [303]. Studies in SRGAP2 revealed that the BAR domain itself could affect neuron progenitor cell migration, and generation of filopodia-like extensions [299].

ARHGAP17 / RICH1 / Nadrin

ARHGAP17/RICH1/Nadrin is another BAR-containing GAP that is a key molecule involved in organizing apical polarity in MDCK epithelial cells by maintaining the integrity of tight junctions (TJs) [304]. To perform this task, it is targeted to TJs where it is kept inactive by its association with a complex of proteins centered by the scaffolding protein angiomotin (Amot) [304]. The activation mechanism of ARHGAP17 remains to be identified, but by acting through Cdc42, this GAP is a key component of a new sorting mechanism implicated in TJ maintenance. When ARHGAP17 is inactivated, Cdc42-GTP recycles the endosomes containing the TJ transmembrane proteins back to the plasma membrane. Conversely, when ARHGAP17 is activated, Cdc42-GDP will target the endosomes to degradation via lysosome association. The whole process would maintain TJ proteins within one area of an epithelial cell [304]. As

for SRGAP proteins, oligophrenin and GRAF GAPs, ARHGAP17 associates with membrane through its BAR domain [305].

Oligophrenin

Oligophrenin also associates with membranes through a BAR domain and a PH domain, both located N-terminally to the GAP domain. This protein, which is equally specific towards RhoA, Rac1 and Cdc42, is highly expressed in the brain, and is present in both the axons and dendrites of neurons [306]. Mutations in its gene have been associated with X-linked mental retardation [306-309], cerebellar hypoplasia and lateral ventricle enlargement [310]. All mutations identified to date have been shown, or are predicted, to be loss-of-function mutations [310]. This idea was confirmed by oligophrenin-null mouse which show behavioural, social and cognitive impairments [311]. Oligophrenin has been shown to be required for dentritic spine morphogenesis [306], synapse maturation and plasticity [312]. In addition to these roles, Oligophrenin has also been shown to control synaptic vesicle endocytosis [313], a process that is mediated by associating its proline-rich sequence at its C-terminus with the SH3 domain of endophilin A1 [313].

ARHGAP26 / GRAF and ARHGAP10 / GRAF2

Oligophrenin shares homology with two other GAPs: ARHGAP26 / GRAF and ARHGAP10 / GRAF2. They all have the same domain organization except for an SH3 domain found at the C-terminus of the last two proteins. ARHGAP26 has recently been shown to be regulated by an intramolecular interaction between its BAR and GAP domains [314]. Results taken from one oligophrenin study were pointing in the same direction, suggesting a possible conserved regulatory mode for all three members of this family [315]. ARHGAP26 is activated after binding to membranes through its BAR and PH domains. It acts locally on RhoA and associates with dynamin with its SH3 domain to participate

in clathrin-independent endocytosis [316]. ARHGAP10 works in the organization of the Golgi apparatus where it is recruited by Arf1-GTP [317]. By acting locally on Cdc42, it would participate in the dynamic Golgi organization as depletion of ARHGAP10 in Hela cells induces a shortening of the Golgi stacks [317].

ARAPs (ARAP1, ARAP2 and ARAP3)

ARAPs members (ARAP1, ARAP2 and ARAP3) also mediate crosstalk between the Arf and Rho GTPases. These multi-domain proteins are both ARFGAPS and RhoGAPs, which associate via their PH domains to $PI(3,4)P_2$ and $PI(3,4,5)P_3$ [318, 319]. ARAP1 and ARAP3 have GAP activity for RhoA, while ARAP2 can bind RhoA, but is unable to increase its GTPase activity [320]. ARAP1 is thought to be involved in Golgi maintenance as it localizes to these membranes with its associated GTPase Arf1 [318]. When overexpressed in NIH3T3 cells, it induces the redistribution of Golgi markers, a loss of stress fibres and cell rounding in a RhoGAP-dependant way. ARAP3, which associates with Arf6, is found on endosomes and at the plasma membrane after stimulation of the cells by EGF or PDGF [319].

DLC1 / ARHGAP7, DLC2 / ARHGAP37 and DLC3 / ARHGAP38

DLC1/ARHGAP7, DLC2/ARHGAP37 and DLC3/ARHGAP38 (Deleted in Liver Cancer proteins) have been the focus of numerous studies once DLC1 was shown to be downregulated in hepatocellular carcinoma [321]. They are now all associated with different cancers and are expressed ubiquitously [322]. DLC-1 tumour-suppressor properties rely on its focal adhesion targeting region at its N-terminus, a RhoGAP domain specific for RhoA and a C-terminus START domain [322]. The mechanism by which it prevents cancer growth still remains to be established with precision, but initial data suggests it maybe implicated in cell adhesion. DLC-1 null-mouse embryos die before day 10.5 with defects in the neural tube, brain, heart and placenta [323]. However, murine embryonic

fibroblasts (MEFs) derived from these embryos showed disrupted actin filaments and fewer focal adhesions, suggesting that DLC-1 is required for strong cell adhesion [323]. DLC1 was recently shown to bind specifically to phosphatidylinositol-4,5-P_2 (PI(4,5)P_2) through a small basic-rich stretch of amino acids at the N-terminus of its GAP domain [324]. This interaction is hypothesized to position the GAP domain right below the membrane so that it can act on RhoA. Interestingly, DLC1 has been demonstrated to activate PLCδ1 PI(4,5)P_2 hydrolysis activity locally through protein-protein interactions [325], suggesting a retro-inhibition mechanism.

MgcRacGAP

While GAPs are generally cytosolic, MgcRacGAP is localized to the nucleus at interphase and is implicated in cytokinesis [326, 327]. Its mRNA is regulated by the cell cycle, increases during the S phase and peaks at the G2 phase [326]. During metaphase, it accumulates at the mitotic spindle and then at the midbody during cytokinesis. MgcRacGAP is found *in vivo* to be specific to RhoA after it gets phosphorylated by Aurora B [327]. It associates with the RhoA specific GEF Ect2, which together regulate the fast cycling of RhoA proteins throughout cytokinesis [328-330]. MgcRacGAP GAP activity is required early during cytokinesis for the formation and maintenance of a region where RhoA-GTP is restricted, called the Rho activity zone. This mechanism limits the activation of effectors to this zone, and promotes the local formation of the actomyosin contractile ring which eventually completes cytokinesis. [330].

Myo9a and Myo9b

Myo9a and Myo9b are two other original GAPs: they are single-headed plus-end-directed motor proteins that contain a RhoA specific RhoGAP domain at their C-terminus [331]. Myo9a is expressed in the brain and in testis, and seems to be required for brain development since Myo9a-null mouse develop

severe hydrocephalus [332]. Myo9b is expressed principally in haematopoietic cells. Mutations in this gene have been linked with the occurrence of celiac disease [333], although a molecular explanation for this link remains to be established.

ARHGAP24 / FilGAP

ARHGAP24/FilGAP is a Rac-specific GAP that binds filamin A at its C-terminus [334]. Filamins are important cytoskeleton organisation proteins as they crosslink actin filaments in the cell. Several mutations in filamin A are associated with congenital disorders [335]. In a few cases, these mutations perturb the interaction between filamin A and FilGAP [335] and could perturb lamellipodia formation since FilGAP and filamin colocalize to lamellipodia upon EGF stimulation of HEK 293 cells. Interestingly, the activity of FilGAP is increased after phosphorylation by ROCK, suggesting a scenario where active RhoA decreases the levels of Rac1-GTP. FilGAP would therefore act as a mediator of the antagonism between RhoA and Rac1 to suppress protrusion and promote cell retraction [334].

1.3.5 The GTPase-Activating proteins (GAPs) of the CdGAP family

From the group of 77 RhoGAPs can be extracted a subfamily of four homolog genes in humans called the CdGAP/ARHGAP31 family. This group of proteins is present solely in vertebrates, although CdGAPr, an ortholog gene found in arthropods (drosophila, bee, wasp, etc.), suggests that the founding member appeared before coelomate diversification (Figure 1.4).

CdGAPr has been the focus of two studies in *Drosophila melanogaster* [336, 337]. The first one provided information regarding the expression of CdGAPr mRNA. The latter was found to accumulate at the blastoderm posterior

pole after cellularisation. During gastrulation, CdGAPr mRNA localizes to groups of epidermal cells, but also to neuro-ectoderm prior to neuroblast delamination [336]. CdGAPr mutants have not been reported to present development defects at these stages. However, during the development of the visual system, photoreceptor cells send their axons from the eye disc to their targets in the optic lobe of the brain through a structure called the optic stalk, and CdGAPr mutants are unable to develop that structure properly [337].

The expression of CdGAPr is restricted to bipolar surface glial cells which form a sheath around neurons of the optic stalk and force them to form a bundle. Disruption of CdGAPr, or of the FAK homolog Fak56D, prevents normal fasciculation of the neurons because surface glial cells fail to be organized into a tubular structure. Interestingly, these genes interact genetically as shown by trans-heterozygous mutants which exhibit a stronger phenotype. Taken together, these data suggest that CdGAPr could be involved in cell adhesion [337]. Studies related to the mammalian homologs of CdGAPr suggest they could be involved in other areas.

CdGAP / ARHGAP31

CdGAP / ARHGAP31 is the closest homolog of ARHGAP30 and is also composed of a single GAP domain (Figure 1.4). This GAP was originally identified in a yeast two-hybrid screen looking for interacting partners for $Cdc42^{Q61LY40C}$ an effector mutant of Cdc42 that lacks binding to PAK1 but retains the ability to induce filopodia formation [338].

Analysis of the primary sequence of CdGAP and of its protein homologs suggests that in addition to the GAP domain, other regions of this protein could be of primary importance based on sequence amino acid conservation (Figure 1.4). First, each member of this family has a stretch of basic residues after the

Figure 1.4 – CdGAP subfamily of RhoGAPs

CdGAP, ARHGAP30, RICS and NOMA-GAP form a discrete subfamily of RhoGAPs which all have in common a polybasic cluster (+, magenta) at the N-terminus of their GAP domain (green) followed by a basic region (BR, blue) enriched in positively charged amino acids. Proteins of this family also share a C-terminal tail enriched in serine and proline residues which generates potential SH3 domain binding sites (PxxP motifs) (orange marks). One of these potential binding sites is highly conserved between CdGAP and ARHGAP30 and is linked here by a dashed line. RICS long isoform and NOMA-GAP have an extended N-terminal sequence containing PX and SH3 domains. The same domains are present in the distant homolog CdGAPr in *Drosophilia melanogaster* but absent of their closer *Caenorhabditis elegans* homolog rrc-1. Identity % and Similarity % were measured using the BLOSUM62 matrix of Bioedit.

CdGAP / ARHGAP31 / KIAA1204 (1425 aa)

ARHGAP30 (1093 aa)

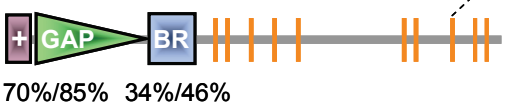

RICS / ARHGAP32 / Grit / KIAA0712 (1740 aa and 2012 aa)

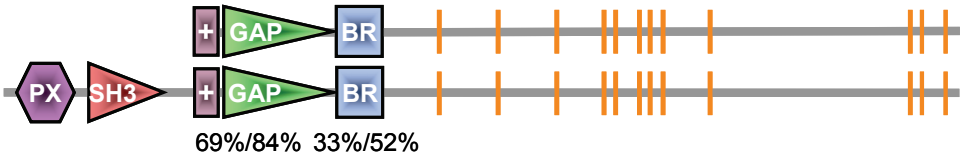

NOMA-GAP / ARHGAP33 / TCGAP / Snx26 (1305aa)

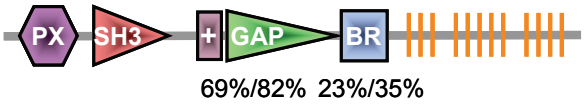

***D.melanogaster* CdGAPr** (1840aa)

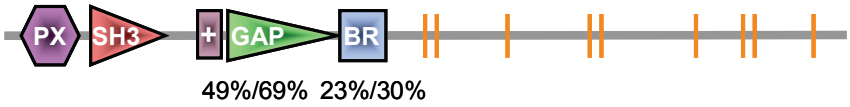

***C.elegans* rrc-1** (759aa)

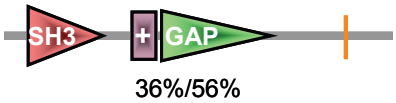

Identity % / Similarity %

N-terminus of the GAP domain, which is highly conserved within the different homologs. Secondly, each member of this family shares a 100 amino acids basic-rich (BR) region after the GAP domain. Beside protein-protein interactions, no function has yet been associated to this region which might have conserved its role within each member of this family. Thirdly, at the C-terminus of the BR domain, members of this family share a long stretch of low identity conservation enriched in proline and serine residues. Therefore, this sequence contains several PxxP motifs which are potential SH3 domain binding motifs [74, 339] and/or could act as a PEST motif which is associated with a lack of ordered secondary structure and rapid turnover of the protein *in vivo* [340]. Interestingly, ARHGAP30 and CdGAP share at their C-terminus a stretch of 15 amino acids composed principally of hydrophobic and proline residues (Figure 1.4). This sequence is homologous to the motif of Eps15 that is associated with Crk SH3 domain and could therefore serve as a docking site for Crk [341].

CdGAP is ubiquitously expressed, with the highest expression found in heart, lung and brain tissues of mouse [338, 342] and in the heart and muscle tissues of human foetus [343]. This GAP is specific both *in vivo* and *in vitro* to Cdc42 and Rac1 [338, 342, 343]. Interestingly, a study using fluorescence resonance energy transfer-based Cdc42 and Rac1 probes showed that upon EGF stimulation of COS cells, Rac activation mediated by CdGAP is inhibited while it does not change the ability of CdGAP to activate the GTPase activity of Cdc42. This suggests that a secondary modification changes the *in vivo* specificity of CdGAP [344, 345]. CdGAP expression in cells leads to cell rounding as a result of a disruption of cortical actin and a loss of focal adhesions, followed by the formation of pseudopodial protrusions, or blebs [343, 346].

CdGAP associates with Intersectin, a scaffold protein involved in endocytic and exocytic events in the cell [347]. Intersectin also exists as a longer

isoform in the brain which contains at its C-terminus extra DH, PH and C2 domains that transform this protein into a RhoGEF specific to Cdc42 [228]. The interaction involves 3 of the 5 SH3 domains of Intersectin, which associates with CdGAP by a region located outside of the proline-rich region, and which will be the focus of the fourth chapter of this thesis. Additional experiments suggested that the interaction was mostly mediated by the SH3D domain of Intersectin, a domain for which no binding partner was known at the time. While expression of CdGAP in Swiss 3T3 cells prevents PDGF-induced lamellipodia formation, co-expression of CdGAP and Intersectin in Swiss 3T3 fibroblasts prevents CdGAP from inducing the same phenotype [347]. *In vitro* GAP assays confirmed that the SH3D domain of Intersectin inhibits the GAP activity of CdGAP [347]. Interestingly, the presence of part of the PRD is required for that inhibition of CdGAP by the SH3 domain, even if the PRD does not bind the SH3 domain itself [347].

In U2OS osteoblast-like cells, CdGAP localizes to focal adhesion sites [346]. Interestingly, stimulation of integrins in an experiment where cells were plated on collagen-coated plates increased the Rac specific GAP activity of CdGAP [346]. As was previously observed in other cell types, overexpression of CdGAP in U2OS cells leads to a reduction in cell spreading and in lamellipodia occurrence [343, 346, 347]. Expression of CdGAP also prevents U2OS cells from being polarized and inhibits their random motility [346]. Localization of CdGAP to focal adhesion is partly mediated by actopaxin, which associates with the GAP and BR domains of CdGAP [346]. Actopaxin is a well known component of focal adhesions and it associates with the kinase ILK, paxillin and the Rac1/Cdc42-specific GEF PIX. This interaction does not affect the GAP activity of CdGAP, but the interaction is required for CdGAP-induced inhibition of lamellipodia formation [346]. Besides this role in cell adhesion, more recent work has shown that CdGAP expression could be linked to changes in the migratory properties of a cell. Indeed, downregulation of CdGAP by siRNA in mammary

tumour cells reduces TGF-β-induced migration and invasion properties of these cells [348].

CdGAP has also been shown to be phosphorylated on numerous serine and threonine residues in response to serum and PDGF stimulation [342, 343]. These events require CdGAP associations with Erk1/2 and RSK1/2 which both phosphorylate CdGAP *in vitro* on multiple sites. Interestingly, T776 substitution to alanine residues in CdGAP seems to increase the GAP activity of these mutants compared to wild-type CdGAP [342]. It is hypothesized that phosphorylation of these residues will negatively regulate the GAP activity of CdGAP [342]. T776 is also targeted by the serine/threonine kinase GSK3α and GSK3β [349]. It is therefore suggested that GSK3 modulates the activity of CdGAP *in vivo* by inducing phosphorylation of T776 [349]. Additionally, GSK3 kinase activity is required for serum-induced CdGAP expression, as treatment of cells with LiCl prevents an increase in protein levels of CdGAP [349].

NOMA-GAP / ARHGAP33 / TCGAP

NOMA-GAP / ARHGAP33 / TCGAP is the closest homolog to CdGAPr with whom it shares the same topology. At the N-terminus of its GAP domain lies a PX domain followed by an SH3 domain (Figure 1.4). NOMA-GAP is able to increase the *in vitro* the GTPase activity of Cdc42, TC10 and Rac1, but not RhoA [350] while *in vivo* co-immunoprecipitation of its GAP domain with both Cdc42- and TC10-GTP and not with Rac1-GTP [350, 351], suggesting specificity towards proteins from the Cdc42 group. In adipocytes, NOMA-GAP translocates to the plasma membrane in response to insulin stimulation [350]. This ability is partly mediated by its PX domain, which has been shown *in vitro* to bind various phosphatidylinositol groups including PI(3)P, PI(4)P, PI(3,4)P_2 and PI(4,5)P_2, but also due to the C-terminus of NOMA-GAP, which associates with an SH3 domain of CrkII [352]. Recruitment of NOMA-GAP at the plasma membrane would block the insulin-stimulated glucose uptake of adipocytes. In

normal conditions, insulin stimulation promotes exocytosis of GLUT4 glucose-transporters containing endosomes. However, when NOMA-GAP and GLUT4 are coexpressed, NOMA-GAP prevents the translocation of GLUT4 upon insulin stimulation [350].

In neurons, NOMA-GAP is phosphorylated within its GAP domain by Fyn upon NGF stimulation [352]. This phosphorylation inhibits the GAP activity of NOMA-GAP and could be important for neurite outgrowth as PC12 cells stimulated by NGF could not grow neurites if TCGAP or a mutant lacking the phosphorylation site were expressed [352]. This analysis remains to be confirmed as a second study has revealed that NOMA-GAP associates with TrkA, the NGF receptor, and is required for neurite extension in PC12 cells [351]. According to this model, NOMA-GAP would serve as a scaffold protein to recruit other molecules required for neurite outgrowth (i.e., SHP2), and for differentiation (i.e., Erk5). Likewise, overexpression studies of NOMA-GAP constructs in developing chick spinal cord also revealed that its expression stimulates neuronal differentiation [351].

RICS / ARHGAP32 / GRIT / GC-GAP

RICS / ARHGAP32 / GRIT / GC-GAP shares PX, SH3 and GAP domains with TCGAP, but only in its longest isoform, named PX-RICS (Figure 1.4). If the longest isoform is expressed ubiquitously, the shortest version, termed RICS, is brain-specific, and lacks the PX and SH3 domains at the N-terminus [343, 344]. As with TCGAP, RICS proteins bind to the NGF receptor TrkA [345], but are not required for neurite outgrowth upon NGF stimulation, as siRNA treatment of PC12 cells had no effect on neurite induction rates [351]. The PX domain of RICS proteins is specific to phosphatidylinositol head groups phosphorylated at only one position (PI(3)P, PI(4)P and PI(5)P). Interestingly, a PX mutation that abolishes lipid interaction promotes the GAP activity of PX-RICS, suggesting a regulation mechanism where lipids would be required for GAP activation [353].

In resting cells, PX-RICS colocalizes with endoplasmic reticulum proteins [353, 354]. By its association with GABARAP and β-catenin, PX-RICS would facilitate the ER-to-Golgi transport of the N-cadherin/β-catenin complex, allowing it to enter the secretory pathway, and thereby regulating the amount of N-cadherin available at the plasma membrane for cell adhesion [354].

ARHGAP30

A third member of this family, ARHGAP30, has been the subject of only one study. It was identified in a screen for regulators of neurite outgrowth in N1E-115 neuroblastoma cells [355]. N1E-115 cells transfected with ARHGAP30 siRNA grow very long neurites. Time-lapse analysis suggests that neurites lacking ARHGAP30 form stronger focal adhesions and/or have focal adhesions whose turnover is slower [355]. ARHGAP30 contains, as for CdGAP, only one globular domain: the GAP domain.

RhoGAP containing proteins forms the 38th largest family of proteins expressed by human cells with 77 members [26], a number that is over 3.8 times larger than the number of 20 RhoGTPases [115]. Albeit the techniques available make it hard to determinate with precision if RhoGAPs have more specificity than what has been published to date, one could hypothesize a tight control in time and space of each GTPase by this large number of inactivators.

1.4 Rationale and Objectives

Considering their involvement in cell migration, neurite outgrowth and cell adhesion, Rho GTPases are interesting medical targets for researchers looking to limit cancer progression or to regenerate axon growth of neurons. However, the main problem with targeting these proteins comes from their central role in the homeostasis of the cell. Inhibiting or activating non-specifically these

molecular switches could cause more problems than benefits. Nevertheless, the number of modulators of the RhoGTPases (RhoGEFs and RhoGAPs) greatly exceeds that of RhoGTPases in humans, providing targets that could have more specific impacts given their specificity in space and time. Thus, the goal of this thesis is to have a better understanding of the molecular mechanisms of regulation of the activity of one specific RhoGAP, CdGAP. There are three main objectives in this thesis:

1. Given that CdGAP contains no known lipid binding domain but needs access to a membrane to perform its molecular task, the first objective aims to discover what region of CdGAP associates with lipids, and how important this region is for the regulation of the activity of CdGAP.

2. The activity of CdGAP has been shown to be inhibited by the binding of an SH3 domain of Intersectin. The second objective is to localize with precision what region of CdGAP is involved in this interaction.

3. CdGAP/ARHGAP31 mutations have been linked to a condition similar to the Adams-Oliver syndrome. The third objective is to have a better molecular understanding on how CdGAP function is modified in these protein mutants.

Preface to Chapter 2

Proteins of the Rho GTPase family are anchored at the membrane after the covalent addition of a lipid moiety to their C-terminus. Therefore, regulators of these proteins, including CdGAP, need to access the membrane in order to perform their task and control the activation state of these molecular switches. CdGAP harbors at the N-terminus of its GAP domain an evolutionarily conserved cluster of positively charged amino acids. Here, we investigate the possibility for this region to bind specific lipids of the phosphatidylinositol group and characterize the function of this positively charged cluster inside the cell.

Chapter 2 - A stretch of polybasic residues in CdGAP binds to Phosphatidylinositol-3,4,5-Trisphosphate and regulates its GAP activity

Martin Primeau, Fereshteh Karimzadeh, Driss Mountassif, Isabelle Rouiller and Nathalie Lamarche-Vane (2010), Submitted to Molecular Biology of the Cell.

Abstract

Rho GTPases are membrane associated molecular switches involved in the control of various cellular activities, including cell migration and proliferation. CdGAP/ARHGAP31 is a GTPase-activating protein (GAP) that regulates negatively Cdc42 and Rac1. In this study, we show that a polybasic cluster preceding the GAP domain, and found in numerous Rho family GAPs, is required for CdGAP specific association with phosphatidilinositol-3,4,5-trisphosphate (PI(3,4,5)P_3). *In vitro* reconstitution of a membrane context using multilamellar vesicles suggests that recruitment of CdGAP by PI(3,4,5)P_3 is mediated by its polybasic cluster, and is required for full GAP activation. In living cells, removal of the polybasic region or substitution of basic residues by uncharged amino acids reduced cell rounding stimulated by CdGAP and increased cell spreading rates despite having no effect on the intrinsic GAP activity of those mutant proteins. Taken together, these data suggest that the polybasic cluster found at the N-terminus of CdGAP recruits the GAP domain tightly to the membrane by its association with PI(3,4,5)P_3, an ability necessary for complete functionality of CdGAP.

Introduction

The Rho subfamily of small GTPases (Rho GTPases), mostly known by the studies on Cdc42, Rac1 and RhoA, are key regulators of cytoskeleton remodelling and play a central role in cell polarization, cell migration and invasion, vesicular trafficking and cell cycle progression [45, 59, 75, 115]. As most GTPases, these molecular switches cycle between active GTP- and inactive GDP-bound states. The transition between nucleotide-bound states is mediated by two classes of regulators. Guanine-nucleotide Exchange Factors (GEFs) activate GTPases by promoting the release of the nucleotide from GDP-bound GTPases, whereas GTPase-Activating Proteins (GAPs) inactivate the switch by increasing the intrinsic activity of GTPases to promote hydrolysis of GTP to GDP. Over 70 Rho family specific GAPs (RhoGAPs) have been identified in humans [26, 264]. Compared to the 20 genes encoding Rho GTPases, this large number suggests different specificities and localized functions of RhoGAPs within the cell. Therefore, these proteins are tightly controlled by different means ranging from protein-protein interactions to lipid interactions, post-translational modifications and proteolytic degradation [45].

CdGAP/ARHGAP31 is a ubiquitously expressed RhoGAP active towards Cdc42 and Rac1 [338, 342, 343, 346, 347]. It was originally identified in a yeast two-hybrid screen for its ability to bind an effector mutant form of Cdc42 ($Cdc42^{Q61L/Y40C}$) [338]. When overexpressed in various cell types, this GAP induces a reduction in cell spreading, and in lamellipodia formation [338, 346]. In U2OS osteoblast-like cells, CdGAP localizes to focal adhesion sites where it is activated following integrin engagement to prevent cell polarization and random cell motility [346]. We have previously shown that CdGAP is a substrate for Erk1/2 and GSK3α/β kinases which both phosphorylate it on multiple sites

including one, T776, which is critical for regulating its activity [342, 349]. Association of CdGAP with the SH3 domains of the scaffolding protein Intersectin has also been shown to inhibit both the *in vitro* and *in vivo* GAP activity of this protein [347].

To mediate signaling events, most Rho subfamily members are anchored to membranes after the addition of a prenyl and/or palmitoyl group to their C-terminus [75, 115]. This transformation, in combination with a positively charged cluster of amino acids, accounts for distinct intracellular localization of GTPases and is required for their activity *in vivo* [31, 65, 81]. Accordingly, regulators of Rho GTPases need to be targeted to the membrane in order to reach their targets, either through protein-protein or lipid-protein interactions [222, 264]. Lipid-binding globular domains are frequently found in RhoGEFs and RhoGAPs, but are not exclusively responsible for membrane association. A growing number of proteins have been shown to associate with lipids through a small polybasic region (PBR) [31, 65]. To date, a PBR was shown to be required by two RhoGAPs for their interaction with specific lipids. For p190RhoGAP, this region is required for binding to phosphatidylserine [284], whereas in DLC1, it interacts predominantly with PI(4,5,)P_2 [324].

In this study, we show that a PBR located at the N-terminus of CdGAP is responsible for its specific interaction with PI(3,4,5)P_3. *In vitro* reconstitution of membrane vesicles loaded with prenylated Rac1 suggests that this PBR is required for full activation of CdGAP in the presence of PI(3,4,5)P_3. *In vivo*, CdGAP protein mutants with altered PBR expressed in fibroblast cells have a reduced ability to induce cell rounding. Moreover, cells expressing PBR-deleted or PBR-neutralized mutants of CdGAP have increased cell spreading rates compared to WT expressing cells, in agreement with a decrease in GAP activity. Taken together, these data suggest that the polybasic cluster of CdGAP helps

recruiting the protein to membranes enriched in $PI(3,4,5)P_3$, and is required for normal CdGAP function.

Materials and Methods

Antibodies and Reagents

Antibodies used in these experiments were as follows: rabbit anti-GST (Santa Cruz Biotechnology, California), rabbit anti-GFP (A6455, Molecular Probes, Burlington, ON) and horseradish peroxidase (HRP)-labeled anti-rabbit IgG antibody (GE Healthcare, Piscataway, NJ). Other reagents used in immunofluoresence were phalloidin-tetramethylrhodamine B isothiocyanate (Sigma-Aldrich, Oakville, ON) and DAPI. Lipid Membrane Strips were purchased from Echelon-Biosciences (Salt Lake City, Utah).

DNA cloning

The plasmids pGEX-4T2-Cd(1-221), pGEX-4T2-Cd(17-221), pGEX-4T2-Cd(1-221)KQ were generated by using a modified version of pGEX-4T2 where a XbaI restriction site was inserted within the unique SalI site. Cd(1-221), Cd(17-221) and Cd(1-221)KQ fragments were amplified by PCR using pRK5myc-Cd(1-1425) as a template and were introduced in pGEX-4T3 using the BamHI and XbaI restriction sites. Forward primers used were 5'-CGGGATCCAAGAACAAGGGTGCCAAG-3' for Cd(1-221), 5'-AGAGGGATCCAGTGCGTTTGGATGTGACCTG-3' for Cd(17-221) and 5'-CGGGATCCGGTACCATGCAGAACCAGGGTGC-CCAGCAGCAGCTGCAACAACAGGGAGCCGCCAGTGCG-3' for Cd(1-221)KQ. The reverse primer was 5'-GCTCTAGATCATGGAGCACCGC-CATTGAAG-3'. The plasmids pGEX-Cdc42 and pGEX-Rac1 were described previously [348]. To generate the pEGFPC1-related plasmids, pEGFPC1

(Clontech, Mountain View, CA) and PCR amplified fragments for pEGFPC1-Cd(1-1425), pEGFPC1-Cd(17-1425), pEGFPC1-Cd(1-1425)KQ, pEGFPC1-Cd(219-1425) were ligated after digestion by BamHI and XbaI. Forward primers used to amplify Cd(1-1425), Cd(17-1425) and Cd(1-1425)KQ were the same used to generate Cd(1-221), Cd(17-221) and Cd(1-221)KQ, respectively. The forward primer 5'-CGGGATCCATGGGTGCTCCAGGGGCTCTG-3' was used for Cd(219-1425). The reverse primer for those four fragments was 5'-GCTCTAGATCATTCTATCTGTCTCCCACT-3'. The R56A and N169V double mutant construct was generated by taking advantage of the NheI restriction sites located 5' to the EGFP gene in pEGFPC1-mCd(1-820)R56A/N169V [346] and starting at base pair 1814 in the coding sequence of *M.m.*CdGAP. A fragment corresponding to the coding sequences of EGFP and of the first 1814 bases of CdGAP coding for substitutions R56A/N169V replaced a fragment removed by the same enzymes in pEGFPC1-mCd(219-1425) to generate pEGFP-mCd(1-1425)R56A/N169V.

Cell Culture and Transfection

COS-7 cells were cultured in Dulbecco's Modified Eagle Medium (DMEM, WISENT, Mississauga, ON) supplemented with 10% Fetal Bovine Serum (FBS, WISENT), 100ug/mL streptomycin sulphate and 100U/mL penicillin G sodium salt (Invitrogen) in a 5% CO_2 humidified environment at 37°C. COS-7 cells were transfected with linear polyethylenimine MW 25,000 (PEI, Polysciences, Pennsylvania) using a 1:5 ratio (µg DNA : µg PEI). Media was replaced 3 hours after transfection.

Purification of Recombinant Proteins from E.coli

pGEX-1λT-Rac1, pGEX-1λT-Cdc42, pGEX-4T2-Cd(1-221), pGEX-4T2-Cd(17-221) and pGEX-4T2-Cd(1-221)KQ vectors were transformed in BL21 bacteria.

For producing GST-Rac1 and GST-Cdc42, overnight cultures were used to inoculate Terrific Broth (TB) (1/20) and grown for 2 hours at 37°C. Protein production was induced by 0.4 mM IPTG (BioVectra, Charlottetown, PE) for 3 hours at 30°C. Bacteria were then harvested by centrifugation and washed in PBS followed by centrifugation. Aliquots were stored at -80°C. Production of GST-Cd(1-221), GST-Cd(17-221) and GST-Cd(1-221)KQ was achieved according to the same protocol, except that proteins were induced by 0.4 mM IPTG for 16 hours at 20°C. Bacteria pellets were resuspended and stired for 30 minutes at 4°C in buffer A (50 mM Tris-HCl pH 7.5, 50 mM NaCl, 5 mM MgCl2, 1mM DTT) supplemented with 0.2 mg/mL lysozyme, 20 ug/mL DNAse, 1 mM $MgCl_2$, 1 mM PMSF and Complete™ protease inhibitors (Roche). Bacteria were then lysed by sonication using a Sonic Dismembrator Model 100 (3 x 30 seconds, 10 W average power (RMS), Fisher Scientific). The cleared lysate obtained after centrifugation was incubated with Glutathione-Agarose beads (Sigma, Saint-Louis, MI) for 2 hours at 4°C. Beads were then washed five times with 10 bead volumes of Buffer B (50 mM Tris-HCl pH 7.5, 150 mM NaCl, 5 mM $MgCl_2$, 1mM DTT), and were eluted with 20 mM glutathione in Buffer D (50 mM Tris-HCl pH 8.0, 150 mM NaCl, 5 mM $MgCl_2$, 1 mM DTT) followed by concentration and replacement by buffer E (10 mM Tris-HCl pH 7.5, 2 mM $MgCl_2$, 1 mM DTT) with a Amicon Ultra-4 30K Centricon column concentrator (Sigma). Bacteria pellets containing GST-Rac1 and GST-Cdc42 were lysed in buffer A as described for GST-GAP related proteins, but without protease inhibitors and PMSF. Glutathione-agarose beads linked to GST-Rac1 or GST-Cdc42 were incubated 16 hours at 4°C with 5U thrombin (Calbiochem) to separate the GST moiety from the GTPases. Thrombin was later removed after incubation with ρ-aminobenzamidine-agarose (Sigma). All samples were aliquoted, snap frozen in liquid nitrogen and stored at -80°C. Purity and

concentration of the protein was determined by SDS-PAGE and Coomassie staining.

Lipid Strip overlay assay

Membrane Lipid Strips™ (Echelon-Biosciences, Salt-Lake City, Utah) overlay assays were performed according to the manufacturer recommendations. Briefly, membrane was blocked 1 hour at room temperature with 3% fatty-acid free bovine serum albumin (BSA, Sigma) dissolved in TBS (10 mM Tris-HCl, 150 mM NaCl pH 8.0) followed by incubation with GST-Cd(1-221) or GST-Cd(17-221) (10 nM) in TBS supplemented with 3% BSA at room temperature for 1 hour. Membrane was washed three times for 10 minutes in TBS + 0.1% Tween-20. That step was also repeated after successive incubations with rabbit polyclonal anti-GST (1:1000) and (HRP)-labelled anti-rabbit IgG antibodies (1:10000). HRP activity was detected by Western Lightning Plus-ECL detection kit (Perkin Elmer).

Multilamellar Vesicles (MLVs) preparation

Phosphatidylcholine (PC) and phosphatidylinositol-related lipids were all purchased from Avanti Polar Lipids (Alabaster, Alabama). PC and PI were bought as chloroform solubilized forms whereas PI(3)P, PI(4)P, PI(5)P, PI(4,5)P_2, PI(3,4,5)P_3 were obtained as ammonium salts and were dissolved at 1 mM in chloroform:methanol:water (80:18:2). Required amounts of lipids were measured using Hamilton syringes (Hamilton Company, Reno, NV), mixed and dried in a glass tube under an argon stream. To generate MLVs, lipids were rehydrated in 20 mM Tris-HCl pH 7.5, 25 mM NaCl and 4 mM EDTA for 1 hour on ice, followed by vigorous vortexing to a final lipid concentration of 1 mM. MLVs were stored at 4°C and used within 24 hours.

Multilamellar Vesicle Flotation Assay

GST-tagged proteins used in the MLV flotation assay were preliminary centrifuged at 436,000 x g for 15 minutes in an Optima™ TLX ultracentrifuge using a TLA-100 rotor (Beckman Coulter) in order to remove protein aggregates. Each MLV flotation experiment was performed as follows. A volume of 100 µL of the MLV solution (1 mM) was incubated with 25 µL of GST-tagged proteins (10 µM to 20 µM) and 25 µL of buffer (20 mM HEPES pH 7.2, 100 mM NaCl and 5 mM EDTA) for 30 minutes at 25°C. A volume of 100 µL of 75% sucrose was added to the mix in order to bring sucrose concentration to 30%. This suspension was moved to a thickwall centrifugation tube and overlaid by 200 µL of 25% sucrose in buffer followed by 50 µL of sucrose-free buffer. Samples were centrifuged at 259,000 x g for 1 hour with a TLS-55 rotor swinging-bucket rotor (Beckman Coulter). Bottom (250 µL) and middle (150 µL) fractions were removed from the bottom using a Hamilton syringue. The top fraction on which MLVs floated was adjusted to a volume of 100 µL before being resuspended. Lamelli buffer (6x) was added to each fraction, and 20% of the basal and top fractions was loaded on 10% SDS-PAGE gels prior to transfer and Western blotting detection. Band density was measured using Autoquant (Biorad) and the bound/unbound ratio calculated was compared to the reference value obtained for PC MLVs. Each condition was assessed at least 3 times.

Rac1 *in vitro* prenylation

Bacteria-purified Rac1 (1µg) was prenylated *in vitro* in 50mM HEPES pH 7.2, 150 mM KCl, 5 mM $MgCl_2$, 1 mM DTT, 3 mM NP-40, supplemented with 2 mM geranylgeranyl pyrophosphate ammonium salt (Sigma-Aldrich) and 2 µg/µL recombinant rat Geranylgeranyltransferase I (Merck Biosciences, Darmstadt, Germany) in a volume of 25 µL following a 16 hours incubation at 4°C. Rac1-geranylgeranyl ($Rac1_{GG}$) proteins were then purified as MLV-bound

components. The reaction mix was devided in two fractions, and each was incubated with 20µg of PC-based or PC:PI(3,4,5)P_3 (9:1) MLVs in a buffer constituted of Tris-HCl pH 7.5, 25 mM NaCl and 4 mM EDTA in a final volume of 150 µL for 30 minutes at room temperature. MLVs were then purified as described for the multilamellar vesicle flotation assay and were resuspended in a final volume of 50 µL. Western blot analysis confirmed that approximately 50% of Rac1 was copurified with MLVs (data not shown).

In Vitro RhoGAP Activity Assay

For *in vitro* GAP assays with GST-tagged GAP proteins, Rac1 (1 µg) was preloaded with 10 µCi γ^{32}P-GTP (Perkin Elmer) in binding buffer (20 mM Tris-HCl, pH 7.5, 25 mM NaCl, 4 mM EDTA, 0.1 mM DTT) to a final volume of 20 µL at 30°C for 10 minutes. $Rac1_{GG}$ bound to PC or PC:PI(3,4,5)P_3 (9:1) MLVs (~0.5 µg) was preloaded accordingly in a volume of 48 µL. Preloading was stopped by the addition of 20 mM $MgCl_2$ and by placing the samples on ice. Preloaded GTPases (4.5 µL) were added to 10.5 µL of the incubation buffer (20 mM TrisHCl pH 7.5, 0.1 mM DTT) supplemented with 1 mM GTP and 0.9 mg/mL BSA with or without GST-Cd(1-221), GST-Cd(17-221) or GST-Cd(1-221)KQ and shifted to 20°C for 10 minutes to start the reaction. Fractions of 5 µL of the reaction mix were taken at 0 and 10 minutes and added to 1 mL of ice-cold wash buffer (50 mM Tris-HCl pH 7.5, 50 mM NaCl, 5 mM $MgCl_2$) before being filtered through pre-humidified nitrocellulose membranes (Millipore) retaining macromolecules including Rac1-bound γ^{32}P-GTP. Filters were rinsed by 6 mL of wash buffer and the amount of radioactivity was measured by scintillation counting. For *in vitro* GAP assays using GFP-tagged proteins, COS-7 cells were transiently transfected with pEGFPC1-related vectors for 16 hours before being lysed in lysis buffer (25mM HEPES pH 7.5, 1% NP40, 100 mM NaCl, 10 mM $MgCl_2$, 5% glycerol, 5 mM Na_3VO_4, 5 mM NaF, 1 mM phenylmethylsulfonyl

fluoride (PMSF) and Complete™ protease inhibitors). Supernatant was cleared by centrifugation (14,000 x g, 5 minutes), and incubated with 20 µL bead volume of protein-A-sepharose (GE Healthcare) and 2 µL of anti-GFP antibodies for 2 hours at 4°C. Beads were then washed three times in lysis buffer followed by three washes in incubation buffer and were resuspended in a total volume of 100 µL with incubation buffer. To quantify the amount of GFP-tagged proteins present on the beads, 10 µL of this mix was added in duplicate to a flat bottom 96 wells polystyrene plate (Becton Dickinson). Levels of GFP fluorescence were measured using a Victor X3 2030 Multilabel Reader spectrofluorometer (PerkinElmer) with excitation and emission wavelength respectively of 485 nm and 535 nm. The GAP assay experiment itself was performed according to the protocol described previously, except that 10 µg of Rac1 and Cdc42 were loaded with γ^{32}P-GTP and that total reaction volumes were of 30 µL. Approximately 0.1 to 0.5 µg of immunoprecipitated GFP-tagged proteins were used in each experiment.

Immunofluorescence Microscopy

For cell rounding experiments, COS-7 cells grown on glass coverslips were transfected by pEGFPC1-related vectors. After 40 hours, cells were washed by PBS and fixed in 3.7% paraformaldehyde (PFA, Fisher Scientific) for 10 minutes. After washing with PBS, cells were permeabilized with 0.25% Triton X-100 (Fisher) for 5 minutes, washed and blocked by 0.2% BSA for 30 minutes followed by incubation with phalloidin-tetramethylrhodamine B isothiocyanate (Sigma) and DAPI for 15 minutes in blocking solution. Coverslips were washed twice in PBS, and once in deionized water before being mounted on glass slides using Prolong anti-fade mounting media (Invitrogen). Pictures were taken using a IX81-ZDC2 zero drift motorized inverted microscope (Olympus, Ontario, Canada) with a 40x NA 1.30 and 60x NA 1.35 U plan S-apo oil objectives used

in combination with Olympus type F immersion oil. For the cell spreading experiments, COS-7 cells transfected with plasmids for 16 hours were trypsinized and seeded on glass coverslips and on 6-well plates, both pre-coated after an overnight incubation with fibronectin 1 µg/mL in PBS followed by one wash with PBS. Fixation and mounting of the glass coverslips was performed as for the cell rounding experiment. Measurement of COS-7 cells spreading was carried out using the IX81-ZDC2 zero drift motorized inverted microscope with a 10x U plans S-apo oil objective NA 0.4 which allowed the tracking of individual cells during time. Images were analysed and used to measure the area covered by each cell throughout the experiment. At least 50 cells per condition were analysed in each of three independent experiments.

Statistical analysis

P values were determined by unpaired student's *t* test. *** $p \leq 0.001$, ** $p \leq 0.01$, * $p \leq 0.05$.

Results

A Polybasic region preceding the GAP domain of CdGAP is conserved in its orthologs and homologs

Amino acid sequence analysis of CdGAP vertebrate orthologs reveals 95% sequence identity conservation for a cluster of 20 amino acids located at the N-terminus of the GAP domain, which has a net charge of +7 (Figure 2.1A). A similar region enriched in positively charged amino acids is also present in the closest homologs of CdGAP (ARHGAP30, ARHGAP32 and ARHGAP33) and in their common relative homolog CdGAPr in *Drosophila melanogaster* (Figure

2.1B). The relatively high conservation of these basic residues in CdGAP homologs suggests they could be of great importance for protein function. PBRs found at the C-terminus of Rho GTPases have previously been shown to be important for their function in the cell and could have a similar impact on the function of RhoGAPs [284, 324].

CdGAP interacts with negatively charged lipids

To determine whether this stretch of basic residues is responsible for binding to negatively charged phospholipids, purified GST fusion proteins of CdGAP encoding amino acids 1-221 or 17-221 were generated (Figure 2.1C). Lipid overlay experiments using these recombinant proteins revealed that the first 16 amino acids of CdGAP are required for its association with phosphatidylinositol-4-phosphate PI(4)P, but also with phosphatidic acid (PA), phosphatidylinositol-4,5-bisphosphate $PI(4,5)P_2$, phosphatidylinositol-3,4,5-trisphosphate $PI(3,4,5)P_3$ and cardiolipins (Figure 2.1D). These lipids all bear at least one negative charge on their head group, which suggests that PBR positively-charged amino acids form electrostatic interactions with these lipids.

CdGAP Interacts with $PI(3,4,5)P_3$ on MLVs

To confirm this result in a more physiological context, multilamellar vesicles (MLVs) were generated using phosphatidylcholine (PC) as the primary substrate. MLVs containing no alternative lipid, or 10mol% of PI, PI(3)P, PI(4)P, PI(5)P, $PI(4,5)P_2$ or $PI(3,4,5)P_3$ were generated. Unbound and bound fractions were analysed by Western blot and revealed a marked association of GST-Cd(1-221) with $PI(3,4,5)P_3$-containing MLVs (Figure 2.2A). The intensity of each band was quantified and a ratio of bound to unbound measurements was calculated. By setting to 1 the ratio obtained with the 100%PC MLVs incubation,

we measured a 9.5 fold increase in binding of GST-Cd(1-221) to PI(3,4,5)P_3-containing MLVs (Figure 2.2B).

To determine whether an intact PBR is required for its association with PI(3,4,5)P_3, MLVs were incubated with GST-tagged Cd(1-221), Cd(17-221) or Cd(1-221)KQ, the last having the seven lysine residues in the PBR substituted by glutamine. Removal of the first sixteen amino acids of CdGAP or elimination of the basic charges of the PBR abolished the ability of CdGAP mutant proteins to associate with PI(3,4,5)P_3-containting MLVs (Figure 2.3A and 2.3B).

The GAP activity of CdGAP is stimulated by the presence of PI(3,4,5)P_3 on MLVs

The *in vivo* stimulation of small GTPases by GAPs occurs at the membrane. Therefore, it is important to consider the circumstances in which these proteins normaly interact. To assess if PI(3,4,5)P_3-containing MLVs contained the minimal requirements to bridge Rac1 and the GAP domain of CdGAP on a membrane, we loaded MLVs with prenylated Rac1 ($Rac1_{GG}$), and performed an *in vitro* GAP activity assay. To eliminate non-specific activity, both $Rac1_{GG}$ (100 nM) and GST-tagged (40 nM) proteins were used at relatively low concentrations. Consequently, incubation of GST-tagged Cd(1-221), Cd(17-221) and Cd(1-221)KQ proteins with 100%PC $Rac1_{GG}$–loaded MLVs induced a relatively low stimulation of $Rac1_{GG}$ GTPase activity. However, when using PI(3,4,5)P_3-containing MLVs, the activity of $Rac1_{GG}$ increased significantly in the presence of GST-Cd(1-221) but not by the other GST-tagged mutant proteins (Figure 2.4A).

To test if the PBR acts as an autoinhibitory domain that is displaced upon PI(3,4,5)P_3 association, we incubated a non-prenylated form of Rac1 without MLVs to compare the GAP activities of the CdGAP protein mutants. As shown in

Figure 2.4B, Cd(1-221), Cd(17-221) and Cd(1-221)KQ showed a similar GAP activity towards Rac1. Therefore, deletion of the first 16 amino acids of CdGAP or substitution of the lysines to glutamines had no effect on the capacity of stimulating the GTPase activity of Rac1 in the absence of lipids. Taken together, these results suggest that $PI(3,4,5)P_3$ is sufficient to recruit CdGAP to membranes and to help this GAP to associate and increase the GTPase activity of Rac1.

The PBR is required for CdGAP GAP-dependant effects in the cell

Overexpression of CdGAP in different cell types induces cell rounding in a GAP-activity dependant way [338, 342, 343]. To study the role of the PBR in CdGAP cellular functions, we generated GFP-tagged full-length proteins of CdGAP containing or lacking the PBR, GFP-Cd(1-1425) and GFP-Cd(17-1425), respectively, with PBR lysine-to-glutamine substitutions, GFP-Cd(1-1425)KQ, with GAP activity alteration by R56A and N169V double substitution (GD for gap dead), GFP-Cd(1-1425)GD, or with complete removal of the PBR and of the GAP domain, GFP-Cd(219-1425). As expected, overexpression of Cd(1-1425) produced a strong cell rounding phenotype compared to GFP-transfected cells, increasing the proportion of round cells by 28% (Figure 2.5A, 2.5B). Removal of the PBR and GAP domain completely abolished this effect, while the GAP-dead mutant showed a statistically non-significant increase of 5% in the number of round cells. Mutants Cd(17-1425) and Cd(1-1425)KQ were able to induce cell rounding but not to the same extent as the wild-type protein. Therefore, the stretch of basic residues is required for CdGAP to induce cell rounding.

Then, we assessed the role of CdGAP protein mutants in cell spreading experiments by quantifying the ability of transfected cells to spread and adhere on fibronectin. Cells expressing CdGAP have previsouly been shown to spread at a lower rate than control cells on extracellular matrix [346]. COS-7 cells

expressing CdGAP were able to attach to the matrix but could not spread as rapidly as normal cells (Figure 2.6A, 2.6B). Cells expressing the PBR mutants Cd(17-1425) and Cd(1-1425)KQ or the GAP defective mutant Cd(1-1425)GD had similar spreading profiles, covering at least 40% more area from 15 to 60 minutes after being plated. Complete removal of the GAP domain provided an even stronger spreading capacity, with cells covering a surface three times larger than Cd(1-1425) transfected cells after 60 minutes (Figure 2.6B). Taken together, these results suggest a key role for the PBR to mediate CdGAP function in the cell.

To assess if these effects were directly linked to the GAP activity of these proteins, GFP-tagged proteins expressed in COS7 cells were isolated by immunoprecipitation, quantified by GFP-light emission and used in an *in vitro* GAP assay with Cdc42 and Rac1 (Figure 2.7A, 2.7B). Expression of GFP itself, or GFP-Cd(219-1425) showed no GAP activity, whereas the GAP-defective mutant provided marked reduction of RhoGTPase-GTP levels over the controls. However, wild-type, PBR-deleted or PBR-neutralized GFP-tagged proteins all kept a strong intrinsic GAP activity. Therefore, these results suggest that the PBR is required for the CdGAP induced cell-rounding phenotype by acting indirectly on the GAP activity.

Discussion

In this study, we demonstrated the presence of a PI(3,4,5)P_3 specific binding region at the N-terminus of CdGAP which is absolutely required for its full GAP activation *in vivo*. The fact that nearly all Rho GTPases are anchored at the membrane suggests the need for effector and regulatory proteins to be recruited within close proximity to their cognate molecular switches. Numerous effector proteins comprising the WASP, Pak and Cdc42-effector protein (CEP)

families of effectors enclose a region enriched in basic residues preceding their GTPase-binding domain [125, 356][159]. Each RhoGEF of the Dbl family includes a PH domain, which associates with low affinity to phosphatidylinositol groups [222]. Moreover, some RhoGAP proteins contain potential lipid-binding regions such as PH, C1, C2, Sec14, PX and BAR domains [264]. For others like CdGAP, a polybasic amino acid cluster seems sufficient to fulfill this requirement [284, 324].

Discovery of a lipid-binding region in CdGAP draws several comparisons with two previously published studies on p190RhoGAP and DLC1 [284, 324]. In all three cases the PBR precedes the GAP domain, at a site that fits a model in which the GAP domain could simultaneously bind a GTPase and associate with the membrane through the PBR. The specificity and activity of p190RhoGAP have previously been shown to be modulated *in vitro* by the presence of phosphatidylserine, PI and PI(4,5)P_2 [283]. Although the PBR in p190RhoGAP was strictly shown to be required for p190RhoGAP association with PS, there is a possibility that it could also serve as a PI and/or PI(4,5)P_2 binding site [284]. In the case of DLC1, specificity of the PBR was addressed in an experiment using immobilized lipids and demonstrated a strong preference for PI(4,5)P_2 [324]. For CdGAP, a similar experiment performed with lipid-blotted strips suggested association of the PBR with PI(4)P, PI(4,5)P_2, PI(3,4,5)P_3, phosphatidic acid (PA) and cardiolipins. However, when these lipids were inserted in vesicular membranes, PI(3,4,5)P_3 specifically bound to CdGAP. To our knowledge, this is the first example of a RhoGAP binding PI(3,4,5)P_3 specifically through a polybasic amino acid cluster.

The relative specificity shown by the PBR of CdGAP, DLC1 and p190RhoGAP can not be explained strictly by electrostatic forces between the positively charged PBR and its association with the negatively charged head

group of the lipid. The fact that $PI(3,4,5)P_3$, with a net charge of -3, does not bind to DLC1 with greater affinity than $PI(4,5)P_2$ and that CdGAP does not show more affinity towards $PI(4,5)P_2$ than it does for PI(3)P, PI(4)P or PI(5)P suggests that these regions adopt a three-dimensional conformation that provides lipid binding specificity. Conserved hydrophobic residues in the PBR were proposed to induce the formation of an amphipatic alpha-helix upon membrane association as in Arf GTPases and ArfGAPs [51, 52, 357, 358]. In CdGAP, relative conservation of lysine and phenylalanine residues respectively at positions 10 and 19 suggest that these residues could behave in a similar way, forcing the positioning of positively charged side chains within the PBR after their insertion into a membrane. Alternatively, the nearby globular GAP domain could stabilize the PBR in a conformation allowing particular positioning of its positively charged side chains.

To date, most *in vitro* experiments involving Rho GTPases and their relative GAPs have been performed in an environment that did not account for the membrane context of their interaction. Although their composition does not reflect precisely the *in vivo* nature of cellular membranes, PC-constituted MLVs used with prenylated RhoGTPases provide a framework that gives the opportunity to study the effect of different lipids on the activity of GTPases in the presence of their regulators. As for DLC1 with $PIP(4,5)P_2$, the GAP activity of CdGAP was activated by the presence of $PIP(3,4,5)P_3$ on MLVs. Considering that the intrinsic GAP activity of CdGAP is not changed by removal of the PBR or substitution of its lysines to glutamines, we suggest that $PI(3,4,5)P_3$ recruits CdGAP to the membrane of MLVs where it can interact with GTPases.

Because of their low lipid binding affinity, PBRs are not sufficient to target proteins to specific localizations in the cell [31]. Protein-protein or lipid-protein interactions mediated by other regions are thought to be first involved in the

specific subcellular localization of a protein. This could explain the absence of a change in the distribution of GFP-tagged CdGAP mutant proteins in COS-7 cells after removal or alteration of the PBR. However, differences in their cellular functions were observed. Overexpression of CdGAP induces cell rounding [338, 343, 346] and prevents cell spreading on extracellular matrix [346] both in a GAP-dependant manner. Cells expressing CdGAP mutant proteins lacking the PBR or containing a PBR containing lysine-to-glutamine substitutions produced a reduced number of round cells in agreement with an altered, but not abrogated, GAP activity. In addition, expression of CdGAP(17-1425) or CdGAP(1-1425)KQ mutant proteins increases the capacity of COS-7 cells to spread on fibronectin similar to the GAP inactivated mutant protein. Taken together, these results suggest the importance of an intact PBR for CdGAP cellular functions.

The specificity of CdGAP for $PI(3,4,5)P_3$ suggests that its GAP activity may be restricted to sites of $PI(3,4,5)P_3$ production. Cellular abundance of $PI(3,4,5)P_3$ is estimated to be under 0.15% of all PI species whereas PI(4)P and $PI(4,5)P_2$ each represent around 5% of these lipids [356]. This low abundance of $PI(3,4,5)P_3$ suggests that it may be the clutch that controls CdGAP activity at specific cellular locations. This phospholipid is known as a secondary messenger generated after growth factor receptor stimulation, but is also involved in endocytosis and phagocytosis. $PI(3,4,5)P_3$ also stimulates cell migration and generation of membrane ruffles upon activation of Rac-specific GEFs [359], and works in combination with Rac1 in inducing F-actin synthesis and branching [360]. It will be of interest to assess the role of CdGAP-$PI(3,4,5)P_3$ interaction in these cellular functions. CdGAP has been shown to bind to actopaxin, which promotes its localization to focal adhesion complexes and its activation following integrin engagement [346]. Considering that integrins

activate PI3K to produce $PI(3,4,5)P_3$, it is tempting to propose that integrin activation of CdGAP could be partly mediated by local production of $PI(3,4,5)P_3$.

Analysis of the amino acid sequences preceding the GAP domain of mammalian RhoGAPs suggests a high prevalence of PBRs in RhoGAPs. In 23 proteins, a stretch of basic amino acids is easily localized. Interestingly, GAP domains preceded by a lipid binding domains (PH, C1, C2 or sec14 domains) do not possess a PBR, which increases the possibility that PBRs are indeed able to have the same function. This could suggest that as for CdGAP, DLC1 and p190RhoGAP, a number of mammalian RhoGAP proteins contain a lipid binding region near their GAP domain. In the end, PBRs in both GTPase and GAP families could provide an additional step for specificity between GAPs and GTPases by bridging GAPs and GTPases that associate with the same phosphoinositide.

Acknowledgments

This work was supported by the Canadian Cancer Society through the National Cancer Institute of Canada. M.P was a recipient of a Canada Graduate Scholarship administered by the Canadian Institutes of Health Research (CIHR) and of an Internal Scholarship Award provided by McGill University Faculty of Medicine. I.R. received funding from CIHR (grant MOP-86693). N.L.-V. and I.R. are recipient of a CIHR New Investigator Award.

Figure 2.1 – A conserved polybasic cluster in CdGAP binds to phospholipids. (A) Sequence alignment of the PBR in CdGAP from different species. Positively charged amino acids are highlighted in bold and marked (+) whereas amino acids forming the first alpha-helix of the GAP domain are underlined (H). (B) Sequence alignment of the PBR in CdGAP homologs in human and in fruit fly. (C) Coomassie stained SDS-PAGE gel showing recombinant Glutathione-S-Transferase (GST)-tagged Cd(1-221) and Cd(17-221) purified from bacteria. (D) Lipid overlay assay of GST-fused proteins showing selective binding of GST-Cd(1-221), but not GST-Cd(17-221), to nitrocellulose-bound phosphoinositides. *M.m.*, *Mus musculus*; *H.s.*, *Homo sapiens*; *R.n.*, *Rattus norvegicus*; *G.g.*, *Gallus gallus*, *T.n.*, *Tetraodon nigroviridis*, *D.m.*, *Drosophila melanogaster.* DAG, Diacylglycerol; PA, phosphatidic acid; PS, phosphatidylserine; PE, phosphatidylethanolamine; PC, phosphatidylcholine; PG, phosphatidylglycerol; PI, phosphatidylinositol; PI(4)P, phosphatidylinositol-(4)-phosphate; $PI(4,5)P_2$ phosphatidylinositol-(4,5)-bisphosphate; $PI(3,4,5)P_3$, phosphatidylinositol-(3,4,5)-trisphosphate; GalS, 3-sulfogalactosylceramide .

A

```
M.m.  CdGAP      1-MKNKGAKQKLKRKGAASAFGCDLTEYLESSGQDVP
H.s.  CdGAP      1-MKNKGAKQKLKRKGAASAFGCDLTEYLESSGQDVP
R.n.  CdGAP      1-MKNKGAKQKLKRKGAASAFGCDLTEYLESSGQDVP
G.g.  CdGAP      1-MKNKGAKQKLKRKGATSAFGCDLTEHLESSGQDVP
T.n.  CdGAP      1-MKNKGIKQKSKKKGSDNAFGCDLIEHLESSGQDVP
consensus           + +   + + +++         HHHHHHHHH
```

B

```
H.s.CdGAP              1-MKNKGAKQKLKRKGAA--SAFGCDLTEYLESSG
H.s.ARHGAP30           1-MKSRQ---KGKKKGSAKERVFGCDLQEHLQHSG
H.s.ARHGAP32-short     1-MKSRPTKQKLKQRGILKERVFGCDLGEHLLNSG
H.s.ARHGAP32-long    350-MKSRPTKQKLKQRGILKERVFGCDLGEHLLNSG
H.s.ARHGAP33         293-MRSRPSRQRLRQRGILRQRVFGCDLGEHLSNSG
D.m.CdGAPr           409-ILSRPSRRRLKQSGIYRERVFNCDLSEHLLNSG
```

C

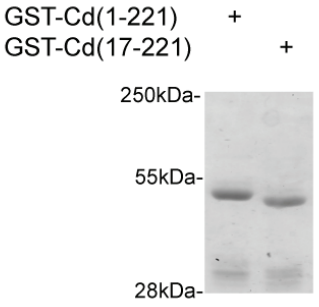

D

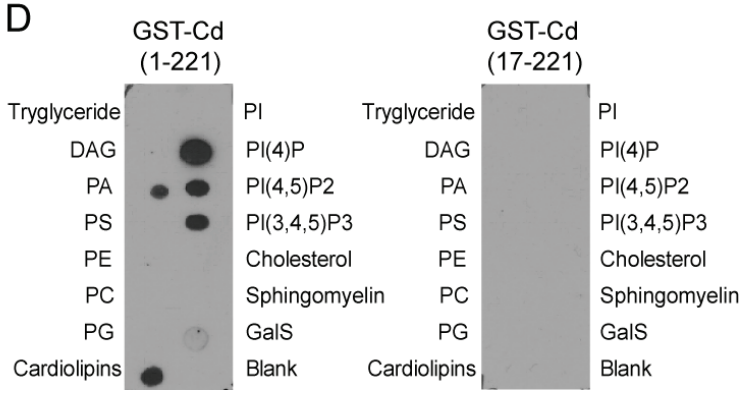

Figure 2.2 – CdGAP preferentially associates with phosphatidylinositol-(3,4,5)-trisphosphate.(A) Multilamellar vesicles (MLVs) constituted of phosphatidylcholine or of a mix of 90mol% phosphatidylcholine (PC) with 10mol% of phosphatidylinositol (PI), phosphatidylinositol-(3)-phosphate (PI(3)P), phosphatidylinositol-(4)-phosphate (PI(4)P), phosphatidylinositol-(5)-phosphate (PI(5)P), phosphatidylinositol-(4,5)-bisphosphate ($PI(4,5)P_2$) or phosphatidylinositol-(3,4,5)-trisphosphate ($PI(3,4,5)P_3$) were incubated with GST-Cd(1-221) in a MLV flotation assay. MLV-associated proteins were separated from unbound proteins by density sucrose-gradient centrifugation. Unbound and bound material were subjected to SDS-PAGE and analyzed by Western blotting with GST-specific antibodies (U, unbound material; B, bound material) (B) Ratio of bound to unbound GST-Cd(1-221) were compared after measurement of band density obtained by Western blot. The value obtained for PC MLVs was set to 1 and used as the reference point. Values represent an average of at least three independent experiments for each condition; error bars, S.E.M.

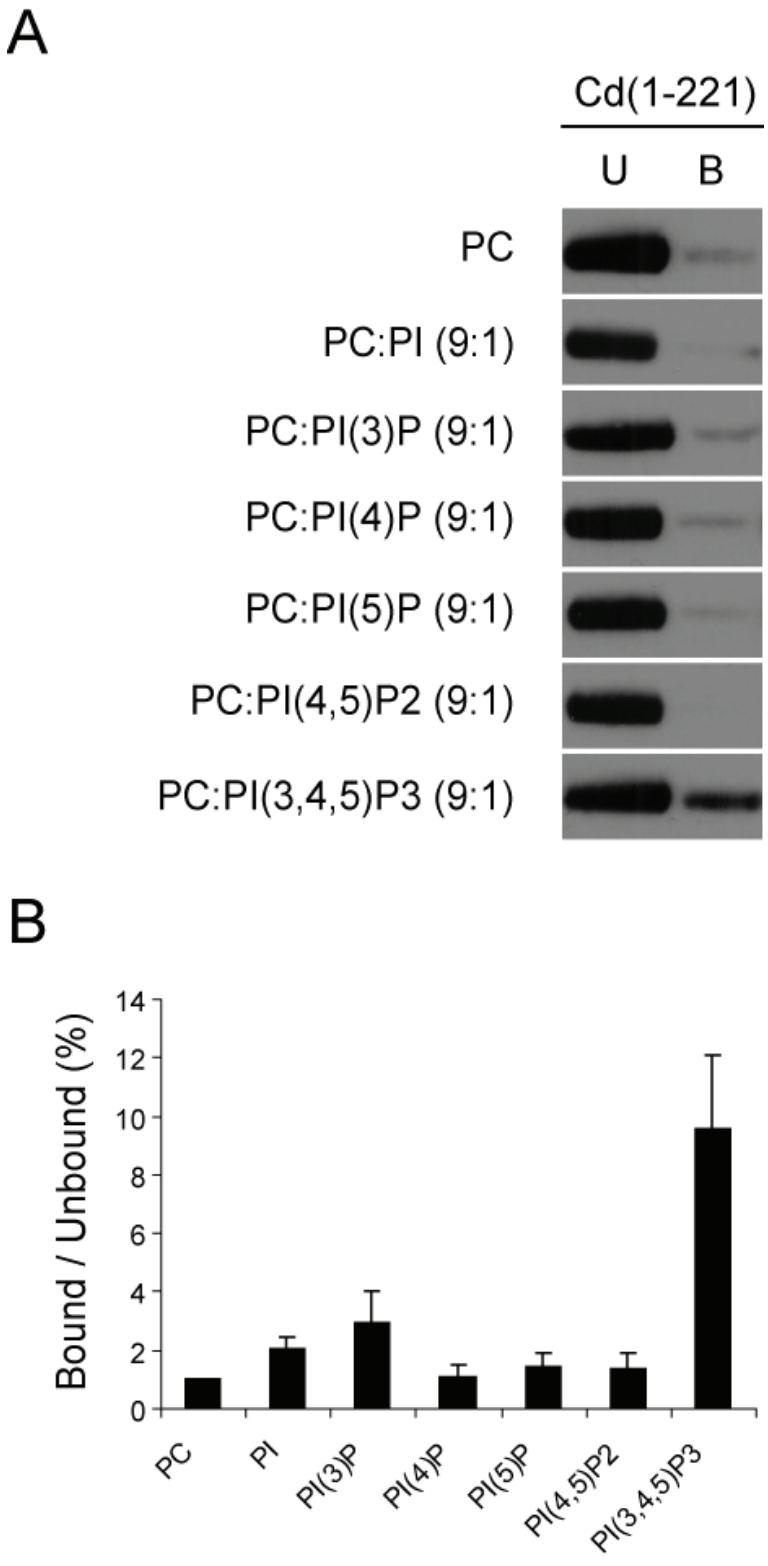
A
Cd(1-221)
U
B
PC
PC:PI (9:1)
PC:PI(3)P (9:1)
PC:PI(4)P (9:1)
PC:PI(5)P (9:1)
PC:PI(4,5)P2 (9:1)
PC:PI(3,4,5)P3 (9:1)
B
Bound / Unbound (%)
14
12
10
8
6
4
2
0
PC
PI
PI(3)P
PI(4)P
PI(5)P
PI(4,5)P2
PI(3,4,5)P3

Figure 2.3 – The polybasic cluster (PBR) of CdGAP is required for PI(3,4,5)P3 interaction. (A) Multilamellar vesicles (MLVs) constituted of phosphatidylcholine or of a mix of phosphatidylcholine (PC) and phosphatidylinositol-(3,4,5)-trisphosphate (PI(3,4,5)P_3) (9:1, mol:mol) were incubated with GST-tagged proteins containing the GAP domain with, Cd(1-221), or without the PBR, Cd(17-221), or with a PBR bearing a neutralized charge, Cd(1-221)KQ. Unbound and bound samples obtained after the MLV flotation experiments were subjected to SDS-PAGE and Western blotting (U, unbound material; B, bound material). (B) Ratios of bound to unbound GST-tagged proteins were compared after measurement of band density. The value obtained for GST-Cd(1-221) incubated with PC MLVs was set to 1 and used as the reference point. Values represent an average of at least three independent experiments for each condition; error bars, S.E.M.

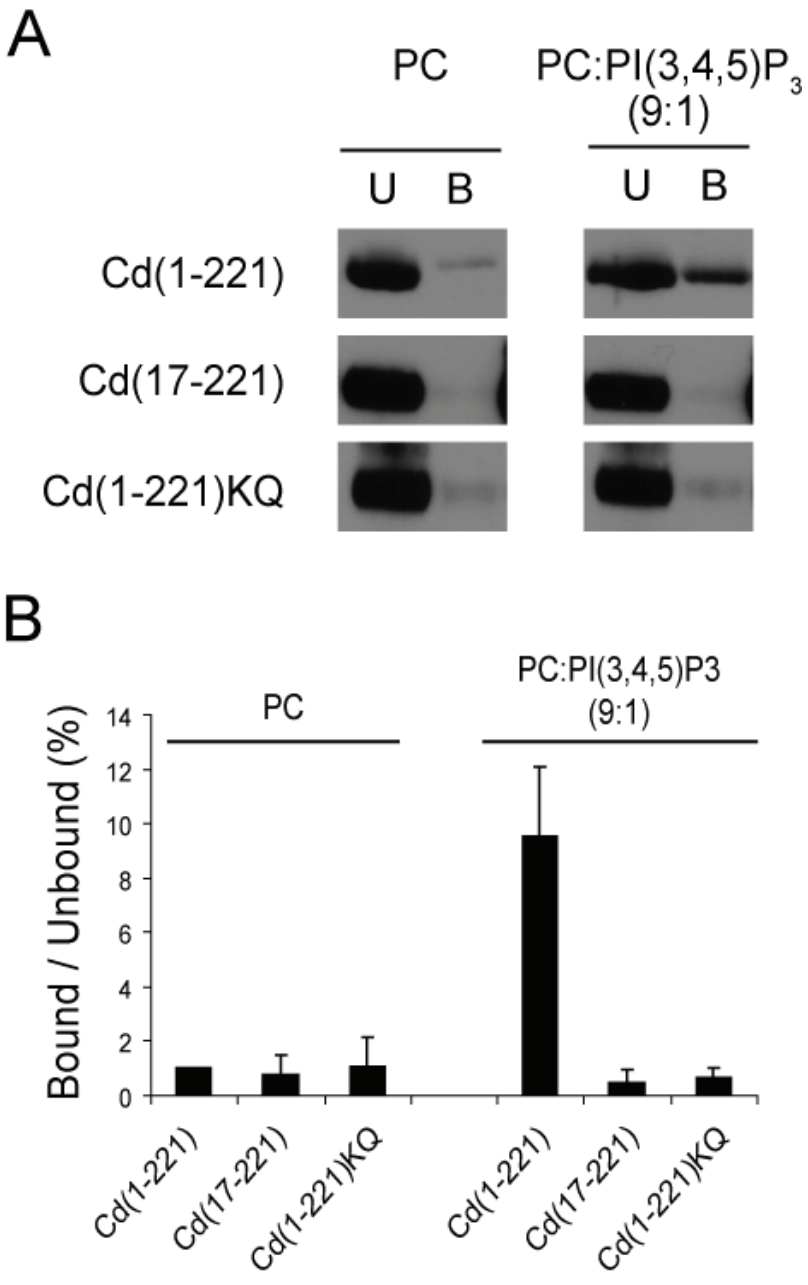
A
PC
PC:PI(3,4,5)P3
(9:1)
U B
U B
Cd(1-221)
Cd(17-221)
Cd(1-221)KQ
B
PC:PI(3,4,5)P3
(9:1)
PC
Bound / Unbound (%)
14
12
10
8
6
4
2
0
Cd(1-221)
Cd(17-221)
Cd(1-221)KQ
Cd(1-221)
Cd(17-221)
Cd(1-221)KQ

Figure 2.4 – Presence of PI(3,4,5)P3 on multilamellar vesicles loaded with prenylated Rac1 stimulates the GAP activity of CdGAP. (A) Geranylgeranylated Rac1 (Rac1GG) purified by its association to PC-based or PC+PI(3,4,5)P3-based MLVs was loaded with γ32P-GTP and incubated with equal amounts of GST-tagged CdGAP deletion mutants Cd(1-221), Cd(17-221) or Cd(1-221)KQ for 10 minutes at 20°C. Levels of Rac1GG-bound γ32P-GTP were measured after 0 and 10 minutes and the intrinsic Rac1GG GTPase activity was set to 100%. The graph shows a representative experiment performed in triplicate. (B) Non-geranylgeranylated Rac1 was incubated in the absence of lipids with GST-tagged Cd(1-221), Cd(17-221) or Cd(1-221)KQ for 10 minutes at 20°C. Levels of Rac1-bound γ32P-GTP were measured after 0 and 10 minutes and the intrinsic Rac1 GTPase activity was set to 100%. The graph shows a representative experiment performed in triplicate.

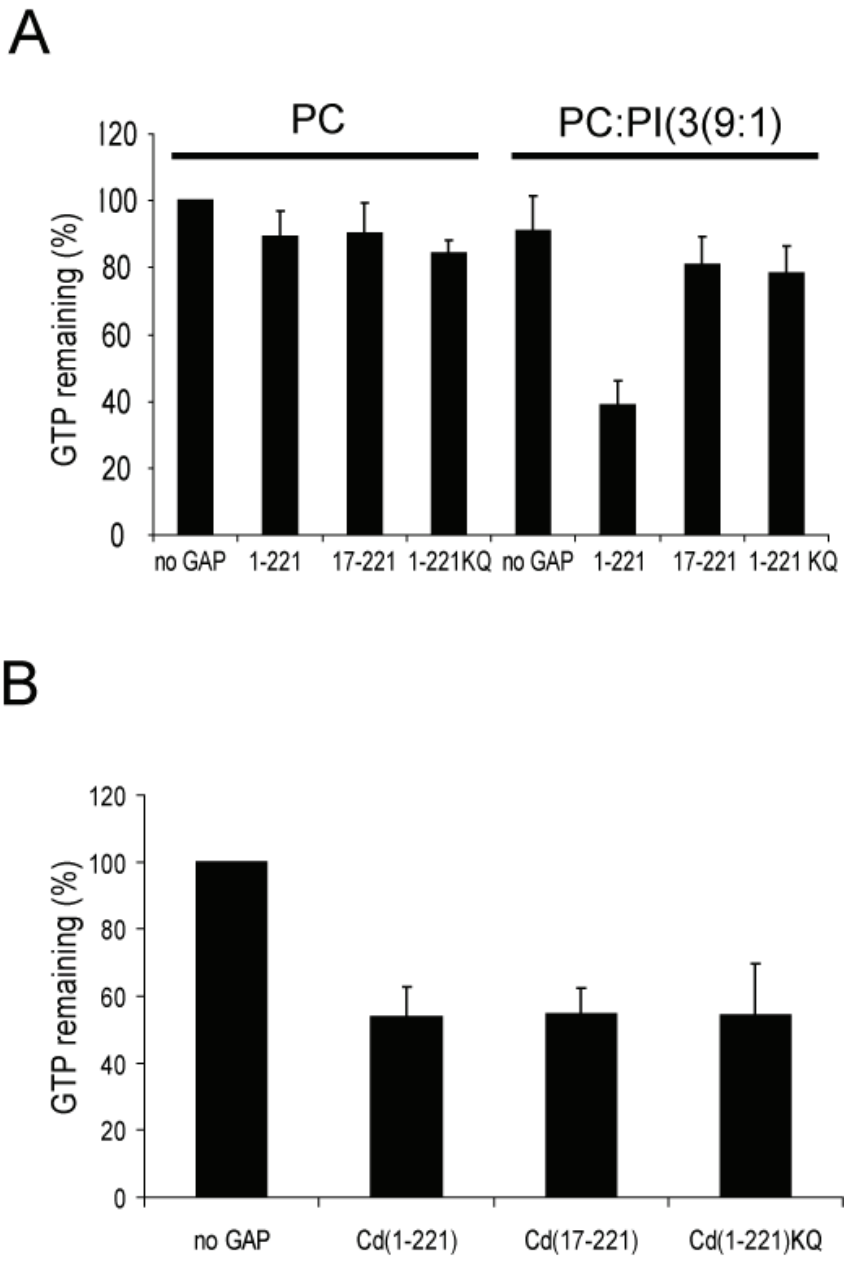
A
PC
PC:PI(3(9:1)
GTP remaining (%)
120
100
80
60
40
20
0
no GAP
1-221
17-221
1-221KQ
no GAP
1-221
17-221
1-221 KQ
B
GTP remaining (%)
120
100
80
60
40
20
0
no GAP
Cd(1-221)
Cd(17-221)
Cd(1-221)KQ

Figure 2.5 – Alteration of the polybasic cluster (PBR) in CdGAP prevents GAP-mediated cell rounding in vivo without changing its intrinsic GAP activity. (A) COS-7 cells transfected with GFP or GFP-tagged ARHGAP mutants corresponding to CdGAP, Cd(1-1425), GAP-defective CdGAP (R56A/N169V), Cd(1-1425)GD, PBR-deleted CdGAP, Cd(17-1425), PBR-neutralized CdGAP, Cd(1-1425)KQ or PBR- and GAP-deleted CdGAP (219-1425) and fixed 36 hours after transfection with phalloidin-actin and dapi staining. (B) The number of round and spread COS-7 cells was measured. Cells counted as round had a nucleus covering more than 50% of the cell surface. These values represent an average of three independent experiments, with at least 100 cells counted per condition and per experiment; scalebar, 15 µm.

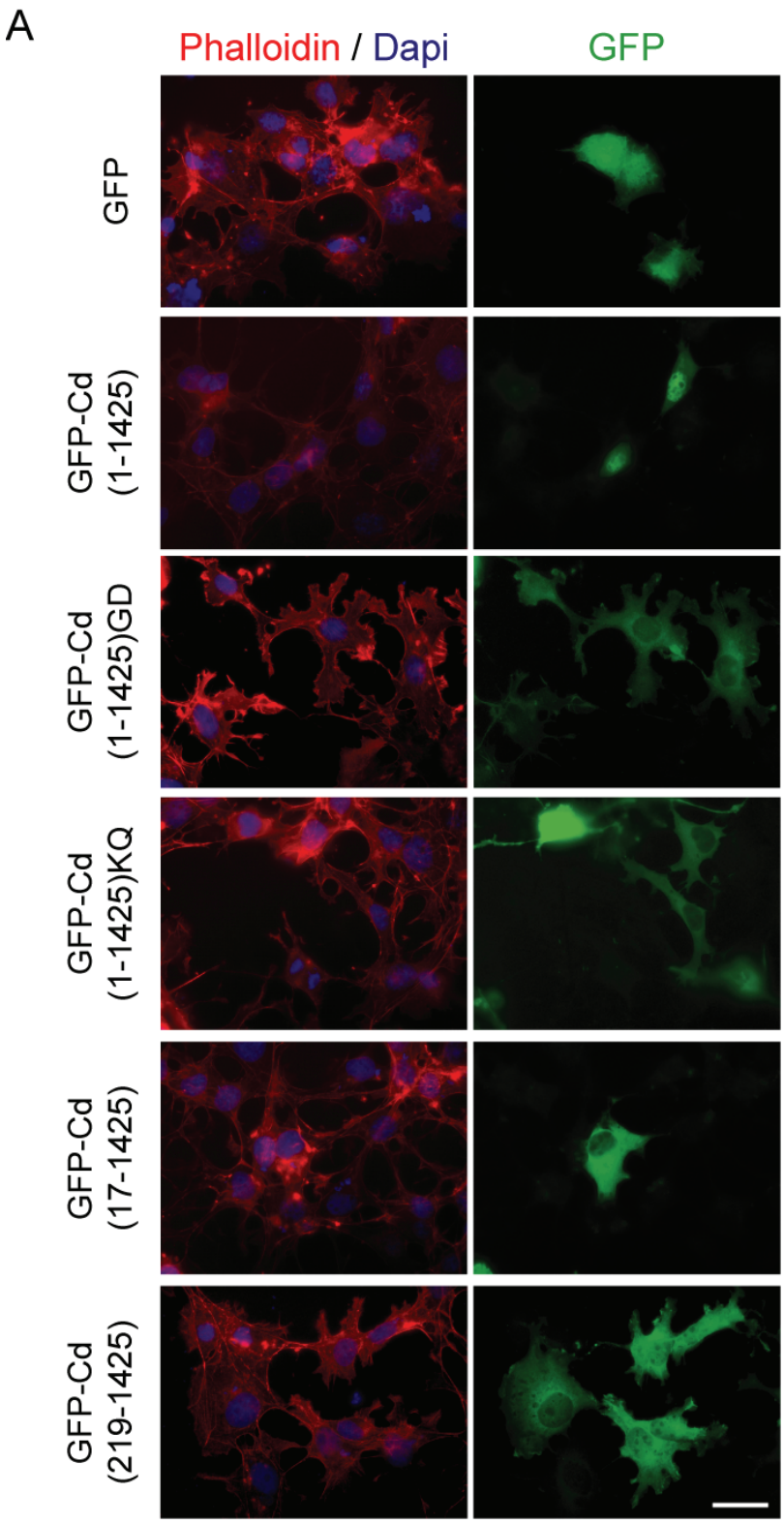
A
Phalloidin / Dapi
GFP
GFP
GFP-Cd (1-1425)
GFP-Cd (1-1425)GD
GFP-Cd (1-1425)KQ
GFP-Cd (17-1425)
GFP-Cd (219-1425)

B

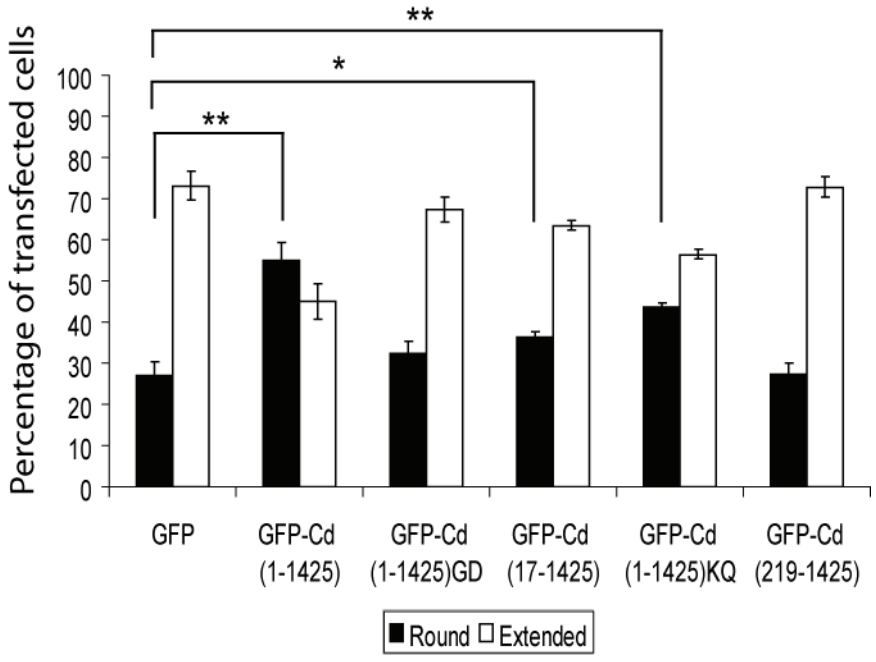
**
*
**
Percentage of transfected cells
100
90
80
70
60
50
40
30
20
10
0
GFP
GFP-Cd (1-1425)
GFP-Cd (1-1425)GD
GFP-Cd (17-1425)
GFP-Cd (1-1425)KQ
GFP-Cd (219-1425)
Round
Extended

Figure 2.6 – CdGAP polybasic cluster (PBR) is required for GAP activity mediated effects of CdGAP in vivo. (A, B) COS-7 cells transfected with GFP- or GFP-CdGAP constructs expressing plasmids were resuspended 16 hours post-transfection and either plated on fibronectin-coated coverslips (A) or fibronectin-coated 6-well plates (B). (A) Cells spreading on coverslips were fixed 15 and 60 minutes after being platted and were stained with rhodamin-phalloidin and dapi. (B) Cells spreading in 6-wells plates were individually tracked from 15 to 60 minutes after plateing, with pictures taken at 15, 30, 45 and 60 minutes. Images were analysed using Metamorph and the area covered by each cell was measured throughout the experiment. The graph showed is representative of one out of three independent experiments where the area of at least 50 cells was analysed per condition; scalebar, 15 μm; error bars, S.E.M.

A

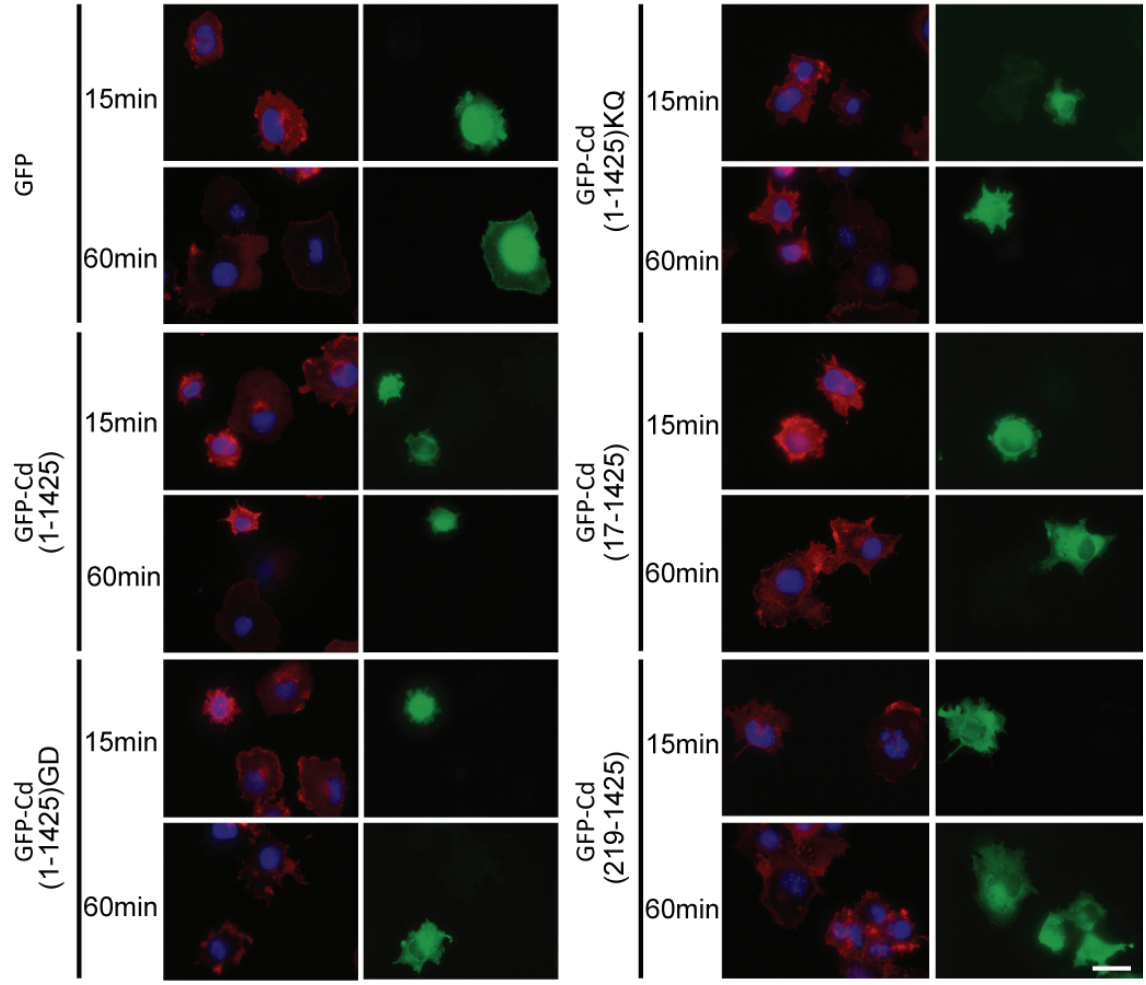
GFP
15min
60min
GFP-Cd (1-1425)KQ
15min
60min
GFP-Cd (1-1425)
15min
60min
GFP-Cd (17-1425)
15min
60min
GFP-Cd (1-1425)GD
15min
60min
GFP-Cd (219-1425)
15min
60min

B

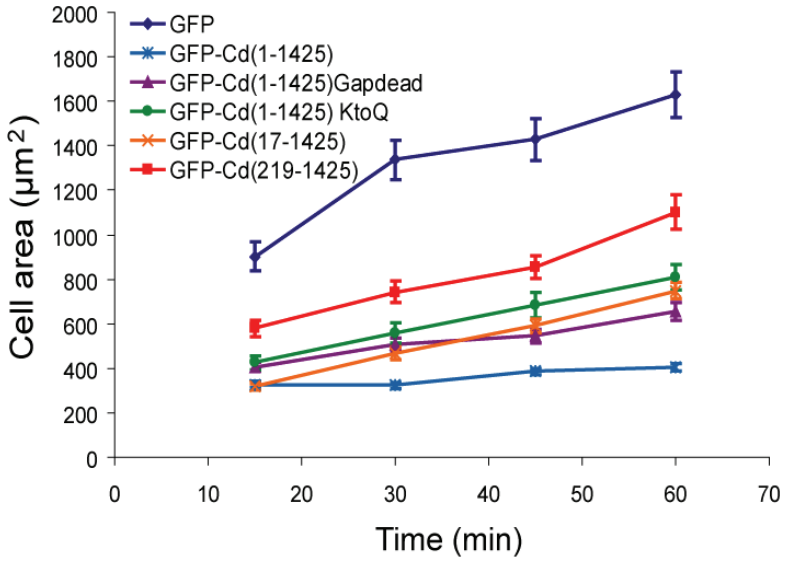
GFP
GFP-Cd(1-1425)
GFP-Cd(1-1425)Gapdead
GFP-Cd(1-1425) KtoQ
GFP-Cd(17-1425)
GFP-Cd(219-1425)
Cell area (μm2)
Time (min)
0
200
400
600
800
1000
1200
1400
1600
1800
2000
0
10
20
30
40
50
60
70

Figure 2.7 – CdGAP polybasic cluster (PBR) alteration does not affect the GAP activity of CdGAP in vitro. GFP-tagged CdGAP proteins isolated by immunoprecipitation using a GFP-specific antibody from transiently-transfected COS-7 cells were used in an *in vitro* GAP assay with γ^{32}P-GTP-loaded Cdc42 (A) or Rac1 (B). Levels of Cdc42- and Rac1-bound γ^{32}P-GTP were measured after 0 and 10 minutes. The graph is a representative of three independant experiments performed in triplicate.

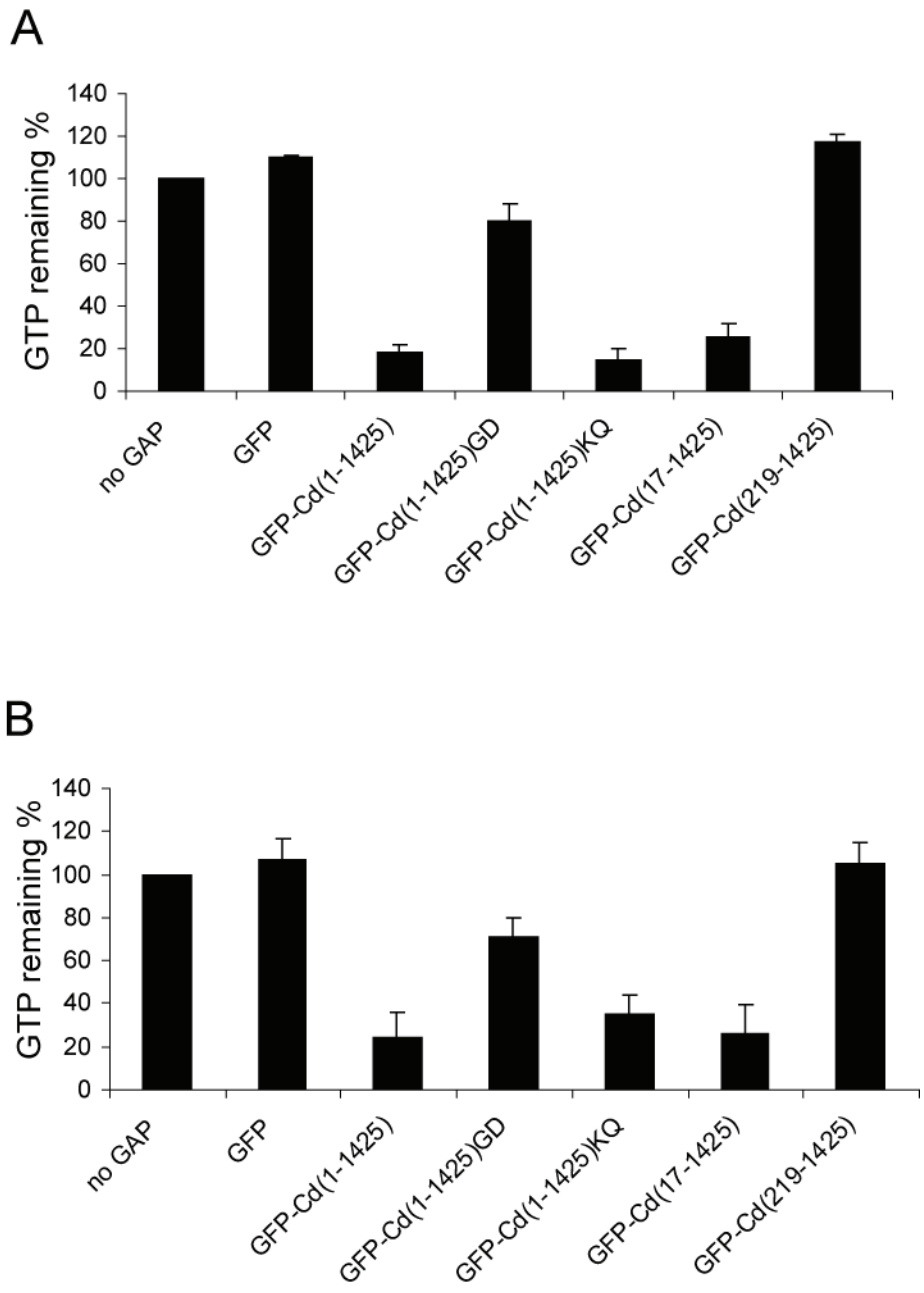
A
GTP remaining %
140
120
100
80
60
40
20
0
no GAP
GFP
GFP-Cd(1-1425)
GFP-Cd(1-1425)GD
GFP-Cd(1-1425)KQ
GFP-Cd(17-1425)
GFP-Cd(219-1425)
B
GTP remaining %
140
120
100
80
60
40
20
0
no GAP
GFP
GFP-Cd(1-1425)
GFP-Cd(1-1425)GD
GFP-Cd(1-1425)KQ
GFP-Cd(17-1425)
GFP-Cd(219-1425)

Preface to Chapter 3

Besides lipid association, protein binding is another way by which proteins can be regulated. Protein association is predominantly mediated by evolutionary conserved globular domains which recognize specific protein folds, particular secondary modifications or peptide motifs. The SH3 module falls in the latter category. This domain commonly associates with small peptide motifs of different amino acid composition. CdGAP was previously shown to associate with the SH3 domains of the endocytic protein Intersectin. Given that preliminary results suggested that this interaction is mediated in a region that contains no common SH3 binding motif, we refine the location of this interaction in the amino acid sequence of CdGAP, and identify critical residues implicated in this interaction.

Chapter 3 - The SH3D domain of Intersectin binds to CdGAP through a novel basic-rich motif

Martin Primeau, Nathalie Lamarche-Vane (2010), Submitted to FEBS Letters, 2010.

Abstract

The small GTPase Cdc42 is a key regulator of the cytoskeleton, which is involved in the control of cellular activities ranging from cell polarization and migration to endocytosis and proliferation. Two opposite regulators have previously been shown to associate with this GTPase. The endocytic protein Intersectin is a brain-specific GEF for Cdc42 and also interacts with Cdc42 GTPase-activating protein (CdGAP) with activity towards Rac1 and Cdc42. We have previously shown that the SH3D domain of Intersectin1 interacts with the central domain of CdGAP and inhibits its GAP activity both *in vitro* and *in vivo*. This domain of CdGAP is highly enriched in basic residues and contains no proline-rich domain. Here, we determined that Intersectin-SH3D interacts directly with the basic region of CdGAP. Moreover, we identified a conserved xKx(K/R) motif within this basic region that is required for the association of CdGAP and Intersectin-SH3D.

Introduction

The Rho family of GTPases, comprising 20 gene members in mammals including the well studied proteins Cdc42, Rac1 and RhoA, are master regulators of the cytoskeleton. Consequently, they coordinate many cellular processes including cell polarization, proliferation, motility, adhesion and intracellular membrane trafficking [45, 59, 75, 115]. These proteins function as molecular switches that cycle between different conformations according to the nature of the nucleotide they bind to. Under their active GTP-bound state, Rho GTPases can interact with downstream effectors and transduce signal, whereas hydrolysis of GTP to GDP turns off this ability.

This cycle is tightly controlled by two groups of regulators: guanine nucleotide-exchange factors (GEFs) activate GTPases by inducing the exchange of GDP for GTP, whereas GTPase-activating proteins (GAPs) increase the intrinsic GTPase activity to inactivate Rho GTPases [263]. These regulators link diverse upstream signals to control GTPases at various times and regions throughout the cell. Therefore, their activity is regulated by mechanisms such as post-translational modifications, lipid- and protein-protein interactions which either change their localization or disrupt an autoinhibited state [222, 264]. Remarkably, GEFs and GAPs can directly regulate each other. The Rho specific GEF Ect2 and GAP MgcRacGAP association during cytokinesis induces Ect2 activation, which promotes cortical actomyosin contractility through RhoA [361, 362]. Likewise, Intersectin-1, which also exists as a brain Cdc42 GEF splice-variant [228, 363], was shown to associate with CdGAP/ARHGAP31 to inhibit its GAP activity [347].

Intersectin is a ubiquitously expressed modular endocytic scaffolding protein composed of two N-terminal Eps-homology (EH) domains, a putative

coil-coiled domain and five SH3 domains (SH3 A, B, C, D, E) [364]. Its neuronal splice-variant, Intersectin-1L, contains additional Dbl-homology (DH), Pleckstrin-homology (PH) and C2 domains [228, 363]. Overexpression of Intersectin or its SH3 domains alone has been shown to inhibit clathrin-mediated endocytosis, presumably by sequestration of proteins required for this event [365, 366]. Indeed, Intersectin is targeted to clathrin-coated pits through the EH domains by their interaction with epsins. Subsequently, it recruits dynamin, synaptojanin, Numb and Wiskott-Aldrich syndrome protein (WASP) by a subset of its SH3 domains [228, 365, 366]. Based on this information, it is proposed to act as a scaffolding molecule that targets proteins of the endocytic machinery at specialized zones of the plasma membrane.

CdGAP association with Intersectin-1 is primarily mediated by the fourth SH3 domain (SH3D) of Intersectin, which inhibits its GAP activity [347]. Whereas the majority of RhoGAPs are multidomain proteins, CdGAP only contains an N-terminal GAP domain, which is preceeded and followed by two evolutionarily conserved basic-rich regions [338]. The remaining C-terminus of CdGAP is enriched in serine and proline residues, which form several potential PxxP putative SH3 binding sites [338, 347]. CdGAP is ubiquitously expressed and promotes the inactivation of Cdc42 and Rac1, but not RhoA [338, 343, 345]. This activity translates *in vivo* by a reduction in cell spreading and in lamellipodia formation [338, 346]. In U2OS osteoblast-like cells, CdGAP is found associated with focal adhesion sites through its interaction with actopaxin [346]. It is activated following integrin engagement and prevents cell polarization and random cell motility [346]. Phosphorylation by Erk1/2 and GSK3α/β also negatively regulates CdGAP, given that both kinases target a critical site for modulating its activity [351, 357]. The role of CdGAP in endocytosis remains to be clarified, but its association with the SH3D domain of Intersectin is of particular interest for two reasons. First, in contrast to the other SH3 domains of

Intersectin, SH3D is not predicted to associate with conventional class I ([R/K]xXPxXP) or class II (XPxXPx[R/K]) SH3 binding motifs, because of the absence of a key negatively charged amino acid in its primary sequence (Q1085 in *M.m.*Intersectin-1). Secondly, this domain binds to the DH domain of Intersectin-1L to maintain the GEF in an autoinhibited conformation, which is released by the binding of SH3D with the protein Numb [3, 367]. Therefore, we seek to determine which residues of CdGAP are responsible for the binding to the Intersectin SH3D.

In this study, we show that the Intersectin-SH3D directly associates with the CdGAP basic rich (BR) domain through an evolutionary conserved SKSK motif. The BR domain is evolutionarily conserved in CdGAP closest homologs and our data suggest that one of these, ARHGAP30, also associates with Intersectin-1.

Materials and Methods

Antibodies

Antibodies used in these experiments were as follows. Monoclonal anti-myc 9E10 antibody was kindly provided by Dr. Nicole Beauchemin (McGill University, Montreal, Canada) and was detected by horseradish peroxidase (HRP)-labeled anti-mouse IgG antibody (GE Healthcare, Piscataway, NJ). GST-tagged proteins were detected by using a HRP-conjugated mouse monoclonal anti-GST antibody (Upstate, Lake Placid, NY).

DNA cloning

The pRK5myc-Cd(1-1425), pRK5myc-Cd(1-515) and pGEX4T1-actopaxin were described elsewhere [342, 346, 347]. The DNA sequence encoding the mouse SH3D domain of Intersectin, ITSN(1070-1131), was cloned by polymerase chain reaction (PCR) from mouse pEGFP-Intersectin-1 [228] using the 5' primer 5'-CGGGATCCGAAATT-GCCCAGGTTATTGCT-3' and the 3' primer 5'-GAGAGAGAGCGGCC-GCTCAGGGCTTAGAAGTTTGACATAAT-3' and was inserted using BamHI and NotI restriction sites in pGEX-4T3 to generate the plasmid pGEX-4T3-ITSN(1070-1131). The Cd(1-515) fragment was amplified with 5' and 3' primers 5'-CGGGATCCGGTACCATGAAGAACAAGGGT-GCCAAG-3' and 5'-GCTCTAGAGCTCAGAAAGAAAACTCTTC-3' and inserted using BamHI and XbaI in pCDNA3.1 to constitute pCDNA-Cd(1-515). CdGAP deletion mutants were amplified by polymerase chain reaction using pRK5myc-Cd(1-820) as a template [347] and were introduced in pRK5myc using BamHI and XbaI restriction sites. Forward primers used were 5'-CGGGATCCAAGAAC-AAGGGTGCCAAG-3', termed *Primer1*, for Cd(1-358) and Cd(1-312), 5'-CGGGATCCCAGGCCCGAAGCTTGGCG-3' for Cd(254-515), 5'-CGGGATCCGACTCGAAGTCCAAGCTGAG-3' for Cd(313-515) and 5'-CGGGATCCAGTAAGAAAATCGAAGCC-3' for Cd(181-358). Reverse primers used were 5'-GCTCTAGATCATTTGTTTTCTTTCCCTTCCACA-3' for Cd(1-358) and Cd(181-358), 5'-GCTCTAGAGCTCAGAAAGAAAACTCTTC-3', termed *Primer2*, for Cd(254-515) and Cd(313-515) and 5'-GCTCTAGATCACGATCCA-GAACGTCCCAGG-3' for Cd(1-312). ARHGAP30 and ARHGAP30 deletion mutants were amplified by polymerase chain reaction using ARHGAP30 mouse cDNA (MGC:99989, Mammalian Gene Collection, NIH) and were digested with BglII and XbaI to be introduced in pRK5myc primarily digested with BamHI and XbaI. Forward primers used were 5'-GGGGTACCAGATCTACCATGAAGTCTC-GGCAGAAAGG-3' for Ar30(1-1093) and Ar30(1-334) and 5'-

GGGGTACCAGATCTACCATGGCCGCTGGGGCCAGTG-3' for Ar30(335-1093). Reverse primers were 5'-GCTCTAGAGCGGCCGCTCAAACCGGTCCT-ACCCCTTCATCTTTCCCATG-3' for Ar30(1-1093) and Ar30(335-1093) and 5'-GCTCTAGAGCGGCCGCTCAAACCGGTCCAGCACTCAGCGAGTCCATG-3' for Ar30(1-334). Fragments coding for CdGAP point mutants were generated by overlap extension PCR, which involved a two-step PCR. In the first step, using pRK5myc-Cd(1-515) as a template, the 5' arm of each mutant was amplified with the 5' primer *Primer1* and with mutant-specific 3' primers, whereas the 3' arm was obtained by the combination of the 3' primer *Primer2* with 5'-specific primers. Corresponding 5'- and 3'-arms generated in the first step were purifed and combined for a second PCR with Primer1 and Primer2. For each mutant, the specific 3' and 5' primers were: 5'-GAAAGCGCGGCGGCGTTGTCTGGTA-ACTCAAGGAC-3' and 5'-CAACGCCGCCGCGCTTTCCAGCAAATCAA-AGAAG-3' for Cd(1-515) (K291A, R292A, K293A), 5'-CCACGCGGCTGAGGCGCTGGAAAGCTTTCTCTTGT-3' and 5'-GCGCCTCAGCCGCGTGGAAATCGATATTTAACCTG-3' for Cd(1-515) (K297A, K299A, K300A), 5'-ATCGATTTGGCCTTCTTTGATTTGCTGGAAAGC-3', 5'-ATCAAAGAAGGCCAAATCGATATTTAACCTGGGAC-3' for Cd(1-515) (W301A), 5'-ATCGCGGCCCACTTCTTTGATTTGCTGGA-3' and 5'-CAAAGAAGTGGGCCGCGATATTTAACCTGGGACGT-3' for Cd(1-515) (K302A, S303A), 5'-CCGCGTTAGCGGCCGATTTCCACTTCTTTGATTTG-3' and 5'-TCGGCCGCTAACGCGGGACGTTCTGGATCGGAC-3' for Cd(1-515) (I304A, F305A, L307A), 5'-TCCAGAAGCTCCCAGGTTAAATATCGATTTC-3' and 5'-TTAACCTGGGAGCTTCTGGATCGGACTCGAAGT-3' for Cd(1-515) (R309A), 5'-GGCGGCAGCGGCGGCCGATCCAGAACGTCCCAGG-3' and 5'-CCGCTGCCGCCGCGAGTAGAAACGGGAGTGTGTTC-3' for Cd(1-515) (D313A, S314A, K315A, S316A, K317A, L318A), 5'-CGCGGCGGCAGCGGCT-TCCACTGACAGCCTCTGG-3' and 5'-GCCGCTGCCGCCGCGCCAGCAAAAA-

GCATGGACT-3' for Cd(1-515) (K335A, T337A, I338A, R339A) and 5'-CGCGGCGGCCATGGCGGCTGCTGGCCGGATAGTA-3' and 5'-CGCCATGG-CCGCCGCGTGTTCGGTGCCTGTGGAA-3' for Cd(1-515) (K342A, S343A, D345A, S346A, L347A). Plasmid pRK5myc and PCR fragments were digested with BamHI and XbaI restriction sites before ligation. All mutants were verified by sequencing.

Cell Culture and Transfection

HEK 293 cells were cultured in Dulbecco's Modified Eagle Medium (DMEM, WISENT, Mississauga, ON) supplemented with 10% Fetal Bovine Serum (FBS, WISENT), 100 µg/mL streptomycin sulphate and 100 U/mL penicillin G sodium salt (Invitrogen) in a 5% CO_2 humidified environment at 37°C. Cells were either transfected with linear polyethylenimine MW 25,000 (PEI, Polysciences, Pennsylvania) using a 1:5 ratio (µg DNA : µg PEI) with media was replaced 3 hours after transfection or by calcium phosphate transfection [368].

Purification of Recombinant Proteins from E.coli

GST, GST-SH3D and GST-actopaxin proteins were purified as follows. pGEX4T3, pGEX4T3-ITSN(1070-1131) and pGEX4T1-actopaxin vectors were transformed in BL21 bacteria. Overnight cultures were used to inoculate M9 broth (1/20) and grown for 3 hours at 37°C. Protein production was induced by 0.4 mM IPTG (BioVectra, Charlottetown, PE) for 3 hours at 37°C. Bacteria were then harvested by centrifugation, washed in PBS followed by centrifugation. Aliquots were stored at -80°C. Bacteria pellets were resuspended and stirred for 30 minutes at 4°C in buffer A (50 mM Tris-HCl pH 7.5, 50 mM NaCl, 5 mM MgCl2, 1mM DTT) supplemented with 0.2 mg/mL lysozyme, 20 ug/mL DNAse, 1 mM $MgCl_2$, 1 mM PMSF and Complete™ protease inhibitors (Roche). Bacteria were then lysed by sonication using a Sonic Dismembrator Model 100 (3 x 30

seconds, 10 W average power (RMS), Fisher Scientific). The cleared lysate obtained after centrifugation was incubated with Glutathione-Agarose beads (Sigma, Saint-Louis, MI) for 2 hours at 4°C. Beads were then washed five times with 10 bead volumes of Buffer B (50 mM Tris-HCl pH 7.5, 150 mM NaCl, 5 mM $MgCl_2$, 1mM DTT) and were eluted with 20 mM glutathione in Buffer D (50 mM Tris-HCl pH 8.0, 150 mM NaCl, 5 mM $MgCl_2$, 1 mM DTT) followed by concentration and replacement by buffer E (10 mM Tris-HCl pH 7.5, 2 mM $MgCl_2$, 1 mM DTT) with a Amicon Ultra-4 30K Centricon column concentrator (Sigma). All samples were aliquoted and stored at -80°C after snap freezing in liquid nitrogen.

GST-pulldown

HEK 293 cells transfected in 100-mm dish were lysed 24 hours post-transfection in 500 µL of lysis buffer (20 mM HEPES pH 7.4 and 1% Triton X-100) supplemented with 5 mM Na_3VO_4, 5 mM NaF, 1 mM phenylmethylsulfonyl fluoride (PMSF) and Complete™ protease inhibitors for 20 minutes on ice. Supernatant was cleared following a 10 minutes centrifugation (14,000 x g), and was incubated with 0.6 nmol of GST or GST-SH3D and 40 µL glutathione-agarose beads (1:1) (Sigma) for 2 hours at 4°C. Samples were washed three times in lysis buffer, and bound proteins were submitted to SDS-PAGE and Western blot analysis using anti-myc antibody.

Coupled transcription/translation

In vitro transcription and translation was performed using TNT® Quick Coupled Transcription/Translation Systems (Promega, Madison, WI). Briefly, TNT Quick Master mix was incubated with 1 µg of pCDNA-Cd(1-515) and 63 µCi of [^{35}S]-methionine in a total volume of 50 µL at 30°C for 90 minutes. Fractions of 15 µL of the reaction mix were either incubated with 20 µg of GST, GST-SH3D and

GST-actopaxin already attached to gluthatione-agarose beads, and GST-pulldown was performed as described previsouly. Samples were loaded on an SDS-PAGE gel, and the membrane was stained with Coomassie. Radioactivity was detected by PhosphoImager analysis (PerkinElmer).

Peptide overlay assay

A total of 20 chemically peptides of 15 amino acid each and overlapping by 10 amino acid to span the protein sequence of *M.m.*ARHGAP(249-358) were synthesized directly on a cellulose membrane through their C-terminus (JPT Peptide Technologies GmbH, Berlin, Germany). Each spot contains 5 to 10 nmol of synthetic peptide. The membrane was washed once in 100% ethanol for five minutes, and three times for 10 minutes in TBS buffer (50 mM TrisHCl pH 8.0, 137 mM NaCl and 2.7 mM KCl) before being blocked for 3 hours at room temperature with blocking buffer (BSA 2% w/v in TBS buffer). The blocked membrane was incubated overnight at 4°C either with GST or GST-SH3D (1.4 µmol/mL) in blocking buffer. Subsequently membrane was washed three times for ten minutes in T-TBS buffer (TBS buffer supplemented with 0.05% Tween-20) and incubated for one hour with mouse monoclonal anti-GST-HRP antibody diluted 1:1000 in blocking buffer plus 0.05% Tween-20. Membrane was washed twice for 10 minutes with T-TBS buffer, followed by one wash with TBS buffer and was then subjected to chemiluminescent reaction using Western Lightning Plus-ECL detection kit (Perkin Elmer).

Statistical analysis

P value was determined by unpaired student's *t* test.

Results

CdGAP contains a proline-rich domain with 6 consensus SH3-binding sites. However, we have previously found that the SH3D of Intersectin does not bind to this domain, but interacts with the central region of CdGAP enriched in basic residues. To further define this region binding to SH3D, lysates of HEK 293 cells expressing myc–tagged CdGAP deletion mutant proteins were incubated with Intersectin SH3D domain expressed as a GST fusion protein and immobilized on glutathione-agarose beads (Figure 3.1). Myc-tagged proteins binding to GST-SH3D were detected by Western blot using anti-myc antibodies. We found a strong association of the SH3D domain of Intersectin with CdGAP deletion mutant proteins Cd(1-515), Cd(1-358), Cd(254-515) and Cd(181-358) which all span a region of CdGAP termed the basic rich (BR) domain. In contrast, constructs Cd(1-312) and Cd(313-515) did not bind to the SH3D. Since SH3 domains are known to bind specific linear peptides, this result may suggest that the binding site for SH3D is located near the junction of proteins Cd(1-312) and Cd(313-515). Alternatively, requirement for an intact BR region may suggest that a precise secondary fold is necessary for the interaction to take place.

The focal adhesion protein actopaxin has previously been shown to bind to the N-terminus of CdGAP within amino acids 1 to 515 [346]. Taking advantage of this interaction, we next performed an experiment to evaluate if the association between CdGAP and Intersectin SH3D domain was direct, using actopaxin binding as a positive control. A fragment corresponding to the N-terminal 515 amino acids of CdGAP was expressed as a ^{35}S-methionine-labeled protein in an *in vitro* transcription/translation rabbit reticulocyte system and used in a GST-pulldown binding assay with GST-SH3D and GST-actopaxin fusion proteins (Figure 3.2A). Both GST-SH3D and GST-actopaxin, but not GST, were found to associate with Cd(1-515) in this assay, providing evidence that the

interaction between CdGAP and the SH3 domain is direct. We then investigated the possibility that the SH3D domain of Intersectin could recognize a specific amino acid motif within the sequence of CdGAP. To do so, a library of 20 overlapping peptides (15-mers), each shifted by 5 amino acids across the entire sequence of the BR region (a.a. 249 to 358) was immobilized on a cellulose membrane and probed in a protein-peptide overlay assay with recombinant GST-SH3D and GST proteins. Association between GST-tagged proteins and membrane-attached peptides was revealed by an anti-GST-HRP antibody (Figure 3.2B). Interestingly, 8 consecutive peptides spanning amino acids 286 to 335 could specifically bind to the SH3D domain. This result initially suggested the presence of multiple binding sites within the BR domain for SH3D, but close analysis of the peptide amino acid sequences revealed that the peptides binding with the strongest affinity to SH3D were all containing a SKSK motif which is found twice in that area of the BR domain at positions 298-301 and 316-319 (Figure 3.2C). This observation is reinforced after considering that peptides were covalently attached to the cellulose membrane by their C-terminus. Indeed, the four peptides binding to the SH3D domain with the highest affinity, no. 9, 10, 13 and 14, all have a SKSK motif located either at their N-terminus or in the middle of their sequence. Nevertheless, association of SH3D with peptides no. 11 and no. 15 suggests that the SKSK motif is not sufficient to mediate the interaction and implies the possibility that a structural fold of the BR domain is required for the interaction to take place.

CdGAP BR region was initially defined based on amino acid sequence homology between CdGAP and its homologs ARHGAP30, ARHGAP32 and ARHGAP33. These evolutionary related RhoGAPs all share a region enriched in positively charged amino acids at the C-terminus of their GAP domain (Figure 3.3A). Considering the possibility that key residues required for SH3D association with CdGAP are conserved within its homologs, we investigated the

possibility that ARHGAP30 could also bind Intersectin SH3D. To assess this possibility, lysates of HEK 293 cells expressing either myc–tagged CdGAP or ARHGAP30, or ARHGAP30 deletion mutant proteins were incubated with Intersectin SH3D domain expressed as a GST fusion protein and immobilized on glutathione-agarose beads (Figure 3.3B). Indeed, ARHGAP30 also associates with the SH3D domain. Moreover, this interaction is mediated by its N-terminal amino acids 1-334, which suggests the possibility that its BR region is also important for this interaction.

Since the results obtained with the protein-peptide overlay assay could not allow us to eliminate the idea that SH3D binds to a folded BR domain instead of a linear peptide, we took an alternative approach to localize which residues in CdGAP mediate the interaction with SH3D. The BR domains of CdGAP and ARHGAP30 share 70% identity, with 85% amino acid sequence similarity. Based on the hypothesis that residues mediating the interaction between CdGAP and Intersectin SH3D are also found in ARHGAP30, the amino acid sequences of these BR domains were aligned. Single amino acid or clusters of conserved residues were then substituted to alanine residues within the CdGAP sequence to perform an alanine scanning mutagenesis analysis of the BR domain (Figure 3.4A). Lysates of HEK 293 cells expressing myc–tagged CdGAP alanine mutant proteins were incubated with GST-SH3D recombinant protein and immobilized on glutathione-agarose beads (Figure 3.4B). Bound proteins were analysed by SDS-PAGE followed by Western blotting. Out of 9 different mutants, the triple mutant K297A + K299A + K300A lost over 80% of its capacity to associate with the SH3D domain. This result was confirmed by density quantification of the bands obtained after Western blot in five different experiments (Figure 3.4C). Interestingly, lysines K297 and K299 were previously identified in the protein-peptide overlay assay as being part of the first SKSK motif targeted by the SH3 domain. However, mutation of the residues 314-

SKSK-317 did not change the ability of the SH3 domain to bind to the BR domain.

Discussion

In this study, we have identified key amino acid residues involved in the direct binding of the SH3D domain of Intersectin-1 to CdGAP. These findings suggest that evolutionary conserved lysine residues located in the BR region of this GAP protein are central to a novel atypical SH3 binding motif, SKSK, or more precisely xKx(K/R), recognized by the SH3D domain of Intersectin. The majority of SH3 domains characterized to date bind, through a set of evolutionary conserved surface residues, to conventional class I ([R/K]xXPxXP) or class II (XPxXPx[R/K]) motifs [74, 339]. However, a growing number of atypical motifs with or without a proline have been discovered over the years. These include the PxxxPR motif recognized by CIN85 in a number of proteins [369], the PxxDY motif which associates with Eps8 SH3 domain [370], the RKxxY motif in SKAP-55 that mediates its interaction with the C-SH3 domain of SLAP [371] and the RxxK motif in SLP-76 bound by the C-SH3 domain of Gads [372]. Most of these motifs share with xKx(K/R) the presence of key basic amino acids in their sequence. However, if some of these atypical motifs associate with their respective SH3 domain through the canonical ligand-binding site, association of the xKx(K/R) motif with the SH3D domain probably occurs on another binding surface of the SH3 domain because of the lack of negatively charged residues in its canonical ligand-binding site. Interestingly, the four amino acids of the SKSK motif are also found at the C-terminus of the protein Numb, within the region that was originally established to associate with the SH3D domain of Intersectin and in between DPF and NPF motifs which link

Numb to endocytic components [3]. This observation gives weight to the idea that lysines of the SKSK motif are required for SH3D association.

The SKSK motif is localized in the BR region of CdGAP. This region is not expected to adopt a globular fold based on secondary structure prediction (data not shown). Therefore, binding of the SH3 domain to the SKSK motif might not involve tertiary structural contacts. This hypothesis is not fully supported by our data. Indeed, the protein-peptide overlay experiment (Figure 3.2B) suggests that residues outside of the SKSK motif could also mediate the SH3D interaction. However, partial alanine scanning analysis revealed that point mutations in only one area of the BR region affected SH3D association with CdGAP (Figure 3.4B, C). Discrepancy between the results provided by these two methods could come from a number of factors. First, only evolutionarily conserved amino acids were substituted in the alanine scanning analysis. Therefore, important alternative amino acids involved in tertiary contacts could have been missed with this approach. Moreover, the transient expression of the BR in mammalian cells exposed the protein to secondary modifications. Interestingly, it was previouly demonstrated that SH3 domains of the endocytic proteins CIN85 and amphyphisin do not directly bind to a lysine containing motif on their substrates, but recognize instead the ubiquitin group that is covalently linked to a lysine [373]. Therefore, there is a possibility that secondary modifications enhance the affinity of the BR region for the SH3D domain. Nevertheless, it seems that the xKx(K/R) motif is the main contributor to the interaction between CdGAP and SH3D. It is noteworthy that the xKx(K/R) motif is also conserved in the BR domains of three mammalian and one drosophila homologs of CdGAP at the same position (Figure 3.3A). Although we have shown that ARHGAP30 could also associate with the SH3D domain (Figure 3.3B), direct association of these proteins with Intersectin remains to be shown.

The SH3 domains of Intersectin-1L were suggested to keep this GEF in an autoinhibited conformation by sterically blocking the DH domain [3, 367]. Interestingly, out of the five SH3 domains of Intersectin, SH3D binds with the strongest affinity to the DH domain and is believed to be central to Intersectin-L activation [3, 367] although this idea was recently challenged [374]. Therefore, proteins which associate with SH3D are thought to mediate the activation of Intersectin-L. This hypothesis was verified for Numb, which enhances the GEF activity of Intersectin-L *in vivo* and which competes with its C-terminus *in vitro* for binding the SH3D domain [3]. Since no structure of these binding partners yet exists, it is difficult to explain how Numb and the DH domain compete for SH3D. However, Asef, a Rac-specific GEF, was previously shown to be maintained in an autoinhibited state through an intramolecular interaction mediated by tertiary contacts between its SH3 and DH domains [375]. Interestingly, the association of both domains partially hides the canonical ligand-binding groove of the SH3 domain, which suggests that the interaction could be competed by a protein containing the correct SH3-binding motif. Although most experiments performed at this point with CdGAP and Intersectin involved its short form, CdGAP co-immunoprecipitates with both the short and long forms of Intersectin [347]. Therefore, CdGAP could not only be inhibited by its association with Intersectin-L, but it could in turn activate this GEF, providing a “double switch” system leading to Cdc42 activation. Considering the involvement of Cdc42 in vesicle trafficking [376] and the contribution of Intersectin-L to dentritic spine development and synaptic functions [3], tight control of the activation state of Cdc42 in neurons could require such a mechanism. Further characterization of the interaction between CdGAP and Intersectin-1L in a cellular context is needed to better understand how these proteins affect each other, and how this interaction influences neuronal development.

Acknowledgments

This work was supported by the Canadian Cancer Society through the National Cancer Institute of Canada. M.P was a recipient of a Canada Graduate Scholarship administered by the Canadian Institutes of Health Research (CIHR) and an Internal Scholarship Award provided by McGill University Faculty of Medicine. N.L.-V. and is a recipient of a CIHR New Investigator Award.

Figure 3.1 – Intersectin SH3D domain binds to the BR domain of CdGAP. (A) Schematic representation of full-length CdGAP, Cd(1-1425), and of its deletion mutants. A polybasic cluster (+) and a basic-rich region (BR) are respectively located N- and C-terminally to the GAP domain (GAP). The C-terminal sequence contains several PxxP motifs which are all conventional class I and class II SH3 binding sites. (B) Myc-tagged deletion mutants of CdGAP expressed in HEK 293 cells were incubated with GST or GST-SH3D proteins coupled with glutathione-agarose in a GST-pulldown assay. Proteins specifically bound to the beads were revealed by Western blotting. A volume corresponding to 2% of starting material (S.M.) was loaded as a control.

A)

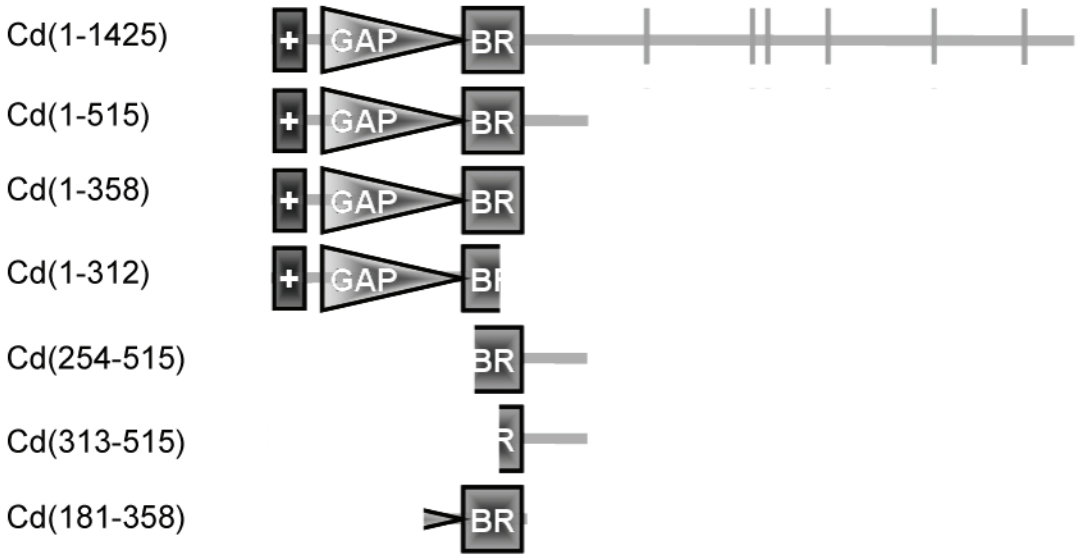
Cd(1-1425)
Cd(1-515)
Cd(1-358)
Cd(1-312)
Cd(254-515)
Cd(313-515)
Cd(181-358)
GAP
BR

B)

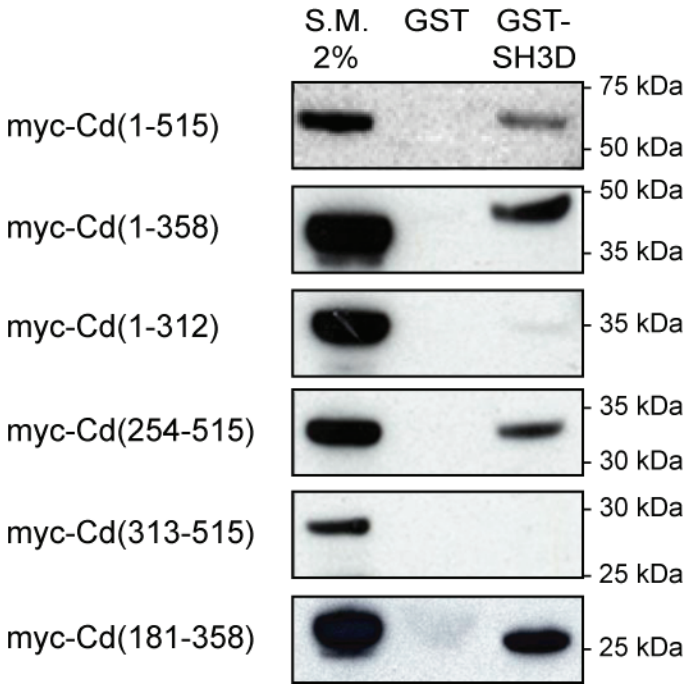
S.M. 2%
GST
GST-SH3D
myc-Cd(1-515)
myc-Cd(1-358)
myc-Cd(1-312)
myc-Cd(254-515)
myc-Cd(313-515)
myc-Cd(181-358)
75 kDa
50 kDa
50 kDa
35 kDa
35 kDa
35 kDa
30 kDa
30 kDa
25 kDa
25 kDa

Figure 3.2 – The association between Intersectin SH3D and CdGAP is direct. (A) *In vitro* transcribed and translated CdGAP(1-515) which incorporated [^{35}S]-methionine was incubated with GST, GST-SH3D or GST-actopaxin coupled to glutathione-agarose in a GST-pulldown assay. Material associated to the beads was revealed by autoradiography and coomassie staining. (B) Twenty 15-mer peptides spanning the amino acids 249 to 358 of *M.m.*ARHGAP were blotted on a nitrocellulose membrane that was incubated with GST or GST-SH3D. Association of GST-tagged proteins to the peptides was revealed by an anti-GST-HRP antibody. (C) Protein sequence alignement of peptide 8 to 15. Amino acids forming two distinct SKSK motifs were highlighted in bold.

A)

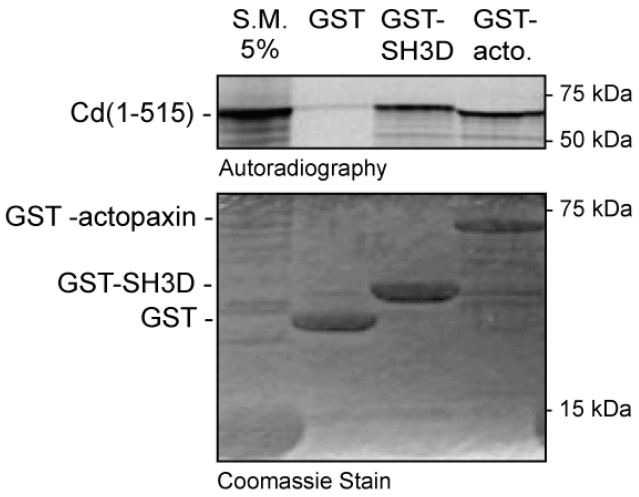

B)

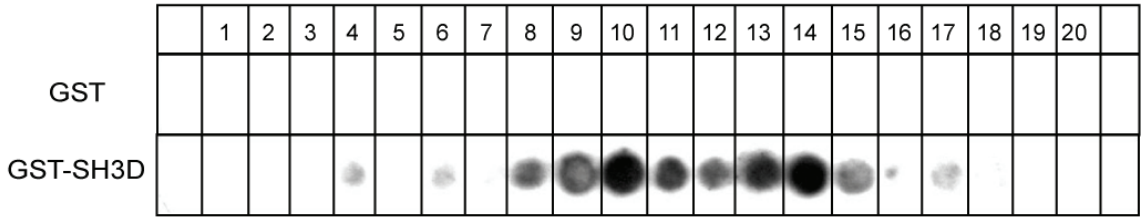

C)

```
249-LVSLEEAQARSLATNHPARKERRENSLPEIVPPPFHTVLELPDNKRKLSSKSKKWKSIFNLGRSGSDSKSKLSRNGSVFVRGQRLSVEKATIR-339
  8  ------------------------------------VLELPDNKRKLSSKS
  9  ----------------------------------------DNKRKLSSKSKKWKS
  10 ---------------------------------------------LSSKSKKWKSIFNLG
  11 ------------------------------------------------KKWKSIFNLGRSGSD
  12 ----------------------------------------------------IFNLGRSGSDSKSKL
  13 ------------------------------------------------------------RSGSDSKSKLSRNGS
  14 ----------------------------------------------------------------SKSKLSRNGSVFVRG
  15 ------------------------------------------------------------------SRNGSVFVRGQRLSV
```

Figure 3.3 – Association between Intersectin SH3D and ARHGAP30. (A) Schematic representation of the homologs of human CdGAP/ARHGAP31. ARHGAP30, ARHGAP32/RICS short and long isoforms and ARHGAP33/NOMA-GAP all contain a basic cluster of positively charged residues and a basic-rich region respectively at the N-terminus and C-terminus of their GAP domain. Each protein contains multiple potential SH3 binding sites at their C-terminus (bars). ARHGAP32 long form, ARHGAP33 and the drosophilia homolog CdGAP-r all contain extra PX and SH3 domains at their N-terminus. (B) Myc-tagged ARHGAP30 full-length and deletion mutants and CdGAP full-length were transiently expressed in HEK 293 cells with GST or GST-SH3D proteins coupled with glutathione-agarose in a GST-pulldown assay. Proteins associated with the beads were revealed by Western blotting. A volume corresponding to 2% of starting material (s.m.) used for the incubation was loaded as a control.

A)

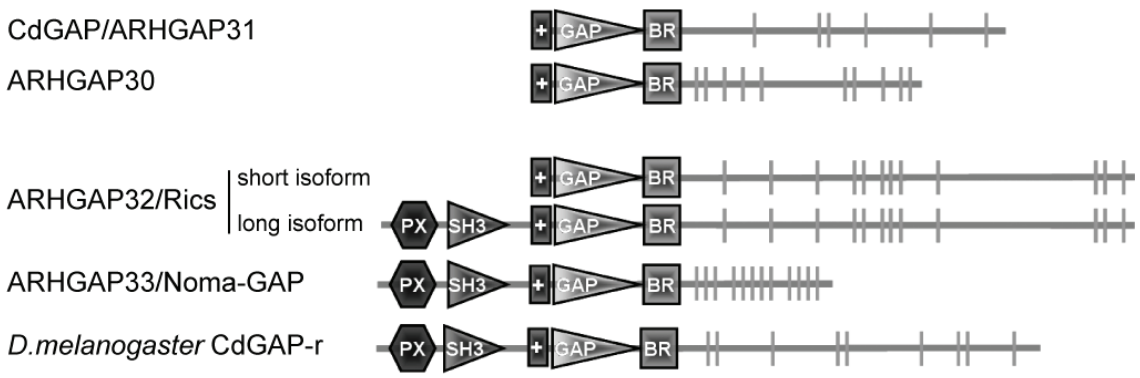
CdGAP/ARHGAP31
ARHGAP30
ARHGAP32/Rics
short isoform
long isoform
ARHGAP33/Noma-GAP
D.melanogaster CdGAP-r
PX
SH3
GAP
BR

B)

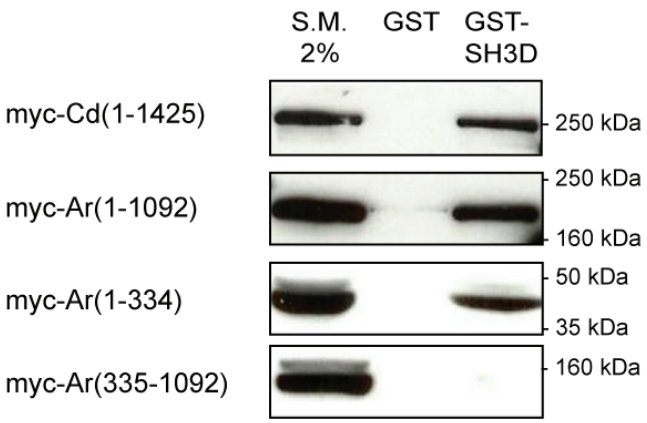
S.M. 2%
GST
GST-SH3D
myc-Cd(1-1425)
myc-Ar(1-1092)
myc-Ar(1-334)
myc-Ar(335-1092)
250 kDa
250 kDa
160 kDa
50 kDa
35 kDa
160 kDa

Figure 3.4 – Localization of SH3D binding site by alanine scanning mutagenesis. (A) Amino acid sequence alignment of the BR domains of CdGAP and ARHGAP30 with 9 alanine mutants generated based on their conservation in CdGAP and ARHGAP30 sequences. (B) Myc-tagged CdGAP(1-515) wild-type and alanine mutants (1 to 9) were expressed in HEK 293 cells were incubated with GST or GST-SH3D proteins coupled with glutathione-agarose. Proteins specifically bound to the beads were revealed by Western blotting using an anti-myc antibody. A volume corresponding to 2% of starting material (S.M.) was loaded as a control. (C) The proportion of myc-tagged proteins bound to SH3D was calculated by measuring the levels of myc-Cd associated with GST-SH3D or found in the lysate as visualized in (B). A ratio of bound to total proteins was calculated for each myc-tagged construct and was compared to the ratio obtained for myc-Cd(1-515)WT, which was set to 100%. Data shown are the mean of five experiments; error bars, S.E.M.

A)

CdGAP	288-PDNKRKLS**SKSK**KWKSIFNLGRSGSD**SKSK**LSRNGSVFVRGQRLSVEKATIRPAKSMDSLCSVPVEGKENK-358
ARHGAP30	276-AEHKRKGS**LKVR**KWRSIFNLGRSGHE**TKRK**LPLR----VEDREEKSSKGTLRPAKSMDSLSAAAGASDEPE-343
1. CdGAP (K291A, R292A, K293A)	288-PDN**aaa**LS**SKSK**KWKSIFNLGRSGSD**SKSK**LSRNGSVFVRGQRLSVEKATIRPAKSMDSLCSVPVEGKENK-358
2. CdGAP (K297A, K299A, K300A)	288-PDNKRKLS**SaSaa**WKSIFNLGRSGSD**SKSK**LSRNGSVFVRGQRLSVEKATIRPAKSMDSLCSVPVEGKENK-358
3. CdGAP (W301A)	288-PDNKRKLS**SKSK**K**a**KSIFNLGRSGSD**SKSK**LSRNGSVFVRGQRLSVEKATIRPAKSMDSLCSVPVEGKENK-358
4. CdGAP (K302A, S303A)	288-PDNKRKLS**SKSK**KW**aa**IFNLGRSGSD**SKSK**LSRNGSVFVRGQRLSVEKATIRPAKSMDSLCSVPVEGKENK-358
5. CdGAP (I304A, F305A, L307A)	288-PDNKRKLS**SKSK**KWKS**aa**N**a**GRSGSD**SKSK**LSRNGSVFVRGQRLSVEKATIRPAKSMDSLCSVPVEGKENK-358
6. CdGAP (R309A)	288-PDNKRKLS**SKSK**KWKSIFNLG**a**SGSD**SKSK**LSRNGSVFVRGQRLSVEKATIRPAKSMDSLCSVPVEGKENK-358
7. CdGAP (D313A, S314A, K315A, S316A, K317A, L318A)	288-PDNKRKLS**SKSK**KWKSIFNLGRSG**S**a**aaaaa**SRNGSVFVRGQRLSVEKATIRPAKSMDSLCSVPVEGKENK-358
8. CdGAP (K335A, T337A, I338A, R339A)	288-PDNKRKLS**SKSK**KWKSIFNLGRSGSD**SKSK**LSRNGSVFVRGQRLSVE**a**A**aaa**PAKSMDSLCSVPVEGKENK-358
9. CdGAP (K342A, S343A, D345A, S346A,L347A)	288-PDNKRKLS**SKSK**KWKSIFNLGRSGSD**SKSK**LSRNGSVFVRGQRLSVEKATIRPA**aa**M**aaa**CSVPVEGKENK-358

B)

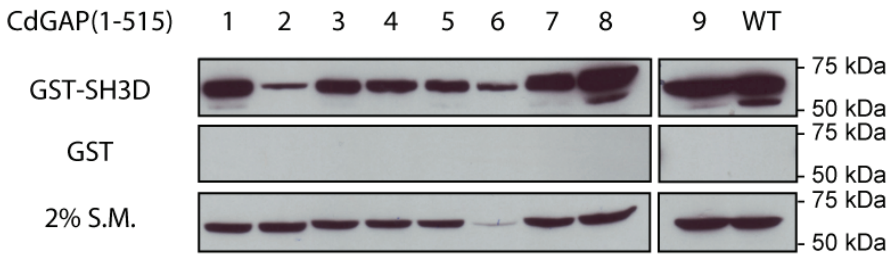

C)

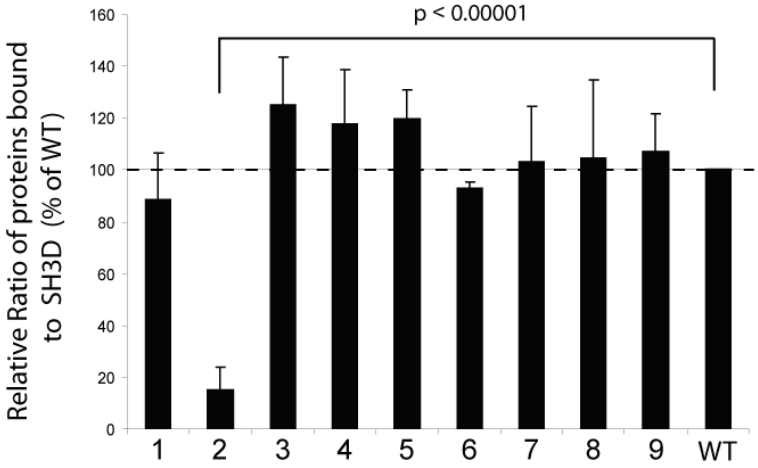

Preface to Chapter 4

Regulation of protein activity by lipid or protein association often involves a conformational change in the structure of the regulated protein that modulates its intrinsic activity. For many enzymes, the domain providing activity is concealed by an internal regulatory domain. Modifications to this region are frequently associated with aberrant activation of the protein and can be related with different development defects. A number of RhoGAP gene mutations are associated with human developmental disorders. CdGAP mutations have also been recently associated with a rare syndrome characterized by missing skin on the forehead at birth (aplasia cutis congenita, ACC) and abnormal development of fingers and/or toes (terminal transverse limb defects, TTLD). We investigate the possibility for these mutants to be gain- and loss-of-function mutations. We also seek to reveal a molecular explanation to account for human development defects induced by these mutations.

Chapter 4 - Mutations in ARHGAP31, a regulator of Cdc42 and Rac1 GTPases, cause scalp and transverse limb birth defects

Laura Southgate[1,12], Rajiv D Machado[1,12], Katie M Snape[1,12], Martin Primeau[2], Dimitra Dafou[1], Deborah M Ruddy[3], Malcolm Fisher[4], Grace J Lee[1], Yi He[2], Teisha Y Bradshaw[1], Bettina Blaumeiser[5], William S Winship[6], Willie Reardon[7], Eamonn R Maher[8,9], David R FitzPatrick[4], Wim Wuyts[5], Martin Zenker[10,11], Nathalie Lamarche-Vane[2] & Richard C Trembath[1,3]

Prepared as a Brief Communication format

1. King’s College London, Department of Medical and Molecular Genetics, School of Medicine, Guy’s Hospital, London, United Kingdom.
2. McGill University, Department of Anatomy and Cell Biology, 3640 University Street, Montreal, Quebec, Canada.
3. Department of Clinical Genetics, Guy’s Hospital, London, United Kingdom.
4. MRC Human Genetics Unit, Western General Hospital, Crewe Road, Edinburgh, United Kingdom.
5. Department of Medical Genetics, University and University Hospital of Antwerp, Prins Boudewijnlaan 43, 2650 Edegem, Belgium.
6. Nelson R Mandela School of Medicine, Faculty of Health Sciences, Department of Paediatrics and Child Health, University of KwaZulu-Natal, Durban 4041, South Africa.
7. Our Lady's Hospital for Sick Children, Crumlin, Dublin 12, Ireland.
8. Medical and Molecular Genetics, School of Clinical and Experimental Medicine, College of Medical and Dental Sciences, University of Birmingham, Institute of Biomedical Research, Birmingham, United Kingdom.
9. West Midlands Regional Genetics Service, Birmingham Women's Hospital, Birmingham, United Kingdom.
10. Institute of Human Genetics, University Hospital Erlangen, University of Erlangen-Nuremberg, Schwabachanlage 10, 91054, Erlangen, Germany.
11. Institute of Human Genetics, University Hospital Magdeburg, Leipziger Str. 44, 39120 Magdeburg, Germany.
12. These authors contributed equally to this work.

Abstract

Regulation of cell proliferation and motility is essential for normal development. The Rho GTPases play a critical role in the control of cell polarity and movement through effects upon the cytoskeleton, membrane trafficking and cell adhesion. We investigated a recognized developmental disorder, characterized by the combination of aplasia cutis congenita (ACC) and terminal transverse limb defects (TTLD), the molecular etiology of which is unknown. Using genome-wide linkage analysis, we identified a locus for autosomal dominant ACC-TTLD on a region of chromosome 3q. We detected two independent premature truncating mutations in the terminal exon of the Rho GTPase activating protein 31 (*ARHGAP31*) gene, which encodes a Cdc42/Rac1 regulatory protein. Mutant transcripts are stable and increase ARHGAP31 activity *in vitro* through a gain-of-function mechanism. Constitutively active ARHGAP31 mutants result in a considerable loss of available active Cdc42, and consequently disrupt actin cytoskeletal assembly. *Arhgap31* expression in early development is substantially restricted to the terminal limb buds and craniofacial processes, closely mirroring the sites of impaired development that characterize this syndrome. These data identify the requirement for regulated Cdc42/Rac1 signaling processes during early human development.

Results and Discussion

We genotyped two unrelated multi-generational kindreds segregating the apparent autosomal dominant syndrome of ACC-TTLD (Figure 4.1a), also termed Adams-Oliver syndrome (AOS) [377]. Using a set of ~6,000 SNP markers (Illumina Human Linkage V panel) followed by genotyping of selected microsatellites, linkage analysis identified a locus for ACC-TTLD on chromosome 3q13.31-q13.33 (Supplementary Figure 4.1a). The critical interval was defined by the flanking markers rs714697 and D3S4523 at approximately 115.36 Mb and 120.89 Mb, respectively (Figure 4.1b). Scrutiny of public databases was performed to identify known genes within this 5.53 Mb region. We sequenced four genes in affected members of the linked AOS-5 and AOS-12 families. In each kindred we identified a distinct sequence variant (c.2047C>T and c.3260delA) within the terminal coding exon of the *ARHGAP31* gene (previously known as Cdc42 GTPase-activating protein, *CdGAP*), that segregate with the syndrome phenotype and predict the formation of premature truncating mutations (p.Q683X and p.K1087SfsX4) (Figure 4.1c and Supplementary Figure 4.1b,c). We did not detect any likely disease causing sequence variants in this or the other genes analyzed.

We screened *ARHGAP31* by DNA sequencing in affected members of a further three multiplex kindreds, unlinked to the chromosome 3 locus, and a cohort of 43 sporadic individuals with either ACC or TTLD alone, or these features in combination. A non-synonymous polymorphism (c.2180C>T; p.T727I) was detected in two sporadic cases, but no pathogenic sequence variants were identified in this extended cohort. To exclude the possibility that the truncating variants were also polymorphisms or that *ARHGAP31* harbors frequent but functionally insignificant variation, we re-sequenced all 12 exons in 72 unrelated control individuals. None of these individuals carried either the

likely disease-causing *ARHGAP31* mutations or any other missense or splice-site variants. We sequenced exon 12, the site of the putative disease-causing mutations, in an additional 1,138 Caucasian controls. The c.2180C>T polymorphism was detected in two control subjects. Neither the nonsense mutation predicting p.Q683X nor the frameshift p.K1087SfsX4 was detected in the combined total of over 2,000 chromosomes assayed.

The clinical phenotypes in the two kindreds with *ARHGAP31* mutations share a number of features. Both mutations are associated with scalp aplasia and upper/lower limb transverse bilateral termination defects but with significant variability (Supplementary Figure 4.1b,c). However, and in contrast to other families tested for mutation in *ARHGAP31* in this study, no affected subjects displayed evidence of structural cardiac abnormality of congenital origin.

We determined the expression of *ARHGAP31* in human fetal tissues and found evidence of abundant and ubiquitous expression in all tissues examined (Figure 4.1d). This was consistent with a previous report describing *ARHGAP31* with widespread expression and showing a major transcript of 7.5 kb by Northern blot [343], together with additional expression studies collated in the University of California at Santa Cruz (UCSC) genome browser. We next examined regional expression of *Arhgap31* during early development in mouse by whole-mount *in situ* hybridization (WISH) and optical projection tomography (OPT). At 9.5 days post-coitum (dpc), the strongest expression is in the developing heart, with regional localization to the ventral walls of primitive ventricle and primitive atrium (Figure 4.2a,b). By 10.5 dpc, *Arhgap31* expression becomes largely restricted to the lateral walls of the developing ventricle, with expression in the primitive atrium becoming localized to its outer wall (Figure 4.2c,d). At 11.5 dpc, *Arhgap31* expression is largely restricted to the surface ectoderm with strong expression overlying the entire heart field, symmetrical

regions of the head and flank and the apical regions of the hand and foot plates (Figure 4.2e,f and Supplementary Video 1). By 12.5 dpc, the expression in the surface ectoderm is not detectable by WISH (data not shown).

ARHGAP31 is a member of the RhoGAP family of proteins known to inactivate the Rho GTPases Cdc42 and Rac1 [343], which regulate signaling cascades that serve cellular functions including proliferation and cytoskeletal dynamics [59]. We first determined the impact of the exon 12 premature termination codon mutants upon transcript stability by quantitative reverse-transcription of RNA extracted from lymphoblasts, comparing control with two related subjects heterozygous for the c.2047C>T mutation. These data showed no significant difference in *ARHGAP31* transcript levels (Figure 4.3a), suggesting that the p.Q683X mutation does not activate the nonsense-mediated decay pathway, in keeping with premature termination codons downstream of the final splice junction [378]. Since the antibody to ARHGAP31 was unsuitable for protein detection by Western blot analysis, we used immunofluorescence and found ARHGAP31 predominantly localized to the intracellular Golgi organelles. Notably, previous observations have found Cdc42 expressed mainly in the Golgi in live cells [67]. We found no indication of protein degradation, typically implied by a loss of staining intensity or aggregate formation, and ARHGAP31 localization was normal in fibroblasts harboring the p.Q683X mutant gene (Figure 4.3b).

The Rho family members Rac1 and Cdc42 are active when GTP bound. The hydrolysis of GTP, for example stimulated by ARHGAP31, leads to inactivation of Cdc42 and, as such, intracellular Cdc42-GTP levels are inversely proportional to the activity of ARHGAP31. To assess the activity of the mutant proteins p.Q683X and p.K1087SfsX4, we engineered wild-type and mutagenized cDNA constructs. Following transient transfection into human

embryonic kidney (HEK 293) cells, lysates were used in a Cdc42 G-LISA assay to measure the levels of GTP-bound Cdc42. Relative to the full-length protein, both mutants displayed a marked augmentation of GAP function towards Cdc42, resulting in a significant down-regulation of the levels of active GTPase (Figure 4.3c). We conclude that both disease mutations in ARHGAP31 behave as dominant gain-of-function alleles.

Both the ARHGAP31 mutations associated with the ACC-TTLD phenotype are predicted to truncate the C-terminal tail. We hypothesized that the C-terminus of ARHGAP31 was capable of conformational hairpin folding so as to shield the RhoGAP domain located at the amino terminus, consistent with comparable auto-regulatory mechanisms reported for other members of GTPase pathways, for example p50RhoGAP and the downstream signaling intermediaries WASP and PAK1 [267, 379, 380]. In such a model, truncation of the C-terminal domain of the ARHGAP31 mutant proteins would result in the exposure of a constitutively active RhoGAP catalytic site. To determine whether ARHGAP31 is capable of intra-molecular interaction, we next generated a green fluorescent protein (GFP) tagged construct encoding the C-terminus (amino acids 1160-1425), to perform immunoprecipitation studies with a series of myc-tagged ARHGAP31 deletion constructs. These experiments demonstrated that the C-terminus of ARHGAP31 is indeed able to bind the N-terminus region comprising the GAP domain (amino acids 1-221), indicating the likelihood of auto-regulation (Figure 4.3d).

Perturbation of Cdc42 and/or Rac1 signaling impacts upon proliferation and directed migration in a cell-specific manner [381]. To determine the impact of ACC-TTLD mutation on these processes, we initially performed wound healing assays. We observed significant differences in the degree of cell migration by comparison to wild-type, suggestive of disorganized cell motility

(Figure 4.4a, Supplementary Figure 4.4 and Supplementary Video 2). In addition, mutant fibroblasts over a 10-day period showed a significant reduction in the ability to proliferate (Figure 4.4b).

Constitutive inactivation of Cdc42 by GTPase inhibitors, for example VopS, leads to cell rounding due to disruption of actin polymerization [382]. Transient transfection of disease-causing *ARHGAP31* mutant constructs revealed an atypical rounded phenotype in a significant proportion of HeLa cells (Figure 4.4c). However, cytoskeletal organization as assessed by actin staining of human fibroblasts heterozygous for the p.Q683X mutation was not quantitatively distinct from controls, presumably due to dosage compensation by the wild-type allele (data not shown).

Taken together, the evidence we have presented demonstrates that heterozygous gain-of-function mutations in *ARHGAP31* cause an autosomal dominant form of ACC-TTLD. The identified mutations introduce premature termination codons in the terminal exon of the gene. These mutations support the generation of a stable transcript and analysis of mutant cell lines reveals protein localization within the Golgi, the site of active Cdc42. These data indicate a novel regulatory mechanism for ARHGAP31, namely intramolecular C-terminal inhibition of the upstream RhoGAP domain, which when disabled by premature truncation leads to reduced activity of Cdc42. Tissue expression of *Arhgap31* during mouse development appears confined to the limb buds and cranium, but also early cardiac structures, providing a remarkable correlation between the restricted sites of gene expression and the specific developmental defects that define ACC-TTLD. These studies demonstrate the critical importance of Cdc42/Rac1 regulation during early human development.

Acknowledgments

The authors would like to express their gratitude to the families for participating in this study. We thank all clinicians who have recruited patients to the European AOS Consortium (see full list in Supplementary Information). This work was supported by grants from the British Heart Foundation (BHF) to R.C.T. (RG/08/006/25302), Wellcome Trust to E.R.M. and R.C.T. (078751/Z/05/Z), EU Framework 6 award for PULMOTENSION (LSHM-CT-2005-018725), Canadian Institute of Health Research grant to N.L-V. (MOP-84449) and German Research Foundation to M.Z. (ZE 524/2-2).

The authors acknowledge support from the Department of Health via the National Institute for Health Research (NIHR) comprehensive Biomedical Research Centre award to Guy's & St Thomas' NHS Foundation Trust in partnership with King's College London and King's College Hospital NHS Foundation Trust. R.C.T. is a senior investigator at the NIHR. R.D.M. is a BHF Intermediate Research Fellow (FS/07/036). P.B. and M.F. are Medical Research Council (MRC) career development fellows funded by the NIDCR (NIH) Craniofacial Center Grant (P50 DE-16215-05). D.R.F. is a MRC senior clinician scientist. N.L-V. is a Fonds de la Recherche en Santé du Quebec (FRSQ) chercheur-boursier senior.

Methods

Clinical ascertainment

Subjects were enrolled in these studies following informed consent in accordance with the protocol approved by the Guy's & St Thomas' NHS Foundation Trust local research ethics committee. Both AOS-5 and AOS-12 are kindreds previously reported in the medical literature [383] and were updated in 2009 [377]. Index subjects were recruited through regional genetics centers and via the Adams-Oliver syndrome support group. Additional family members (including unaffected individuals and spouses) were then invited to participate in the study. All family members underwent a detailed physical examination undertaken by experienced clinical geneticists. Diagnosis of the ACC-TTLD phenotype was based on suggested clinical guidelines [377] and further supported by radiological investigations in selected patients.

Gene expression analysis

Fetal expression of *ARHGAP31* was assessed using a human fetal multiple tissue cDNA (MTC) panel (Clontech). PCR was performed using standard protocols with primers ARHGAP31_3Fw (5′ AGCTCATGTGACCTCACCAA 3′) and ARHGAP31_3Rv (5′ AGACTGGAGCAGGGAAGGAG 3′) to generate a 976 bp fragment. *GAPDH* primers (Clontech) were used as an internal control.

For quantitative PCR, cDNA was generated by reverse transcription of 1 µg RNA extracted from patient and wild-type EBV-transformed lymphoblasts, using the Verso cDNA kit (ABgene) according to the manufacturer's instructions. Real time quantitative PCR was performed using *ARHGAP31* Taqman gene expression probes according to the standard protocol on a Real-time PCR 7900HT (Applied Biosystems). The *GAPDH* gene (Applied Biosystems) was

used as an endogenous control. Relative levels of gene expression were calculated by SDS v2.2 software (Applied Biosystems) using the Comparative CT method of data analysis using the equation Relative Quantity = 2 –ΔΔCt.

Optical projection tomography

In situ hybridization was performed as described in the Supplementary Methods. Embryos were mounted in 1% agarose, dehydrated in methanol and then cleared overnight in BABB (1 part Benzyl Alcohol: 2 parts Benzyl Benzoate). Samples were then imaged using a Bioptonics OPT Scanner 3001 (Bioptonics) using brightfield to detect the LacZ staining and for tissue autofluorescence (excitation 425nm, emission 475nm) to capture the anatomy [384]. The resulting images were reconstructed using Bioptonics proprietary software, automatically thresholded and merged to a single 3D image output using Bioptonics Viewer software. The downstream digital dissection and sectioning was performed using Amira (Visage Imaging) software.

Cloning and mutagenesis

Full-length myc-tagged ARHGAP31 was generated as previously described [343]. Mutant constructs were engineered by performing site-directed mutagenesis with the QuickChange kit (Stratagene) on the wild-type template. Primers are available on request.

Cell culture

Cells were maintained at 37 °C in a humidified incubator with 5% CO_2. HeLa cells (ATCC, Manassas, VA) were cultured in Dulbecco's Modified Eagle's Medium (DMEM) supplemented with 4.5 g/mL GlutaMax and 10% heat inactivated fetal bovine serum (FBS). EBV-transformed lymphoblasts (ECACC) were cultured in RPMI-1640 supplemented with 10% heat inactivated FBS.

Human dermal fibroblast primary cells were established from tissue biopsies from a normal control individual (WT) and an AOS patient carrying the p.Q683X mutation. Cells were grown in basal medium 106 supplemented with 2% (v/v) FBS, 1 µg/ml hydrocortisone, 10 ng/ml human epidermal growth factor, 3 ng/ml basic fibroblast growth factor, and 10 µg/ml heparin. All cell culture reagents were obtained from Invitrogen. Transient transfections of HeLa cells were performed using FuGENE (Roche) in accordance with manufacturer's instructions.

Immunofluorescence

HeLa cells were plated in 6-well plates (Corning) on acid-treated glass coverslips (Laboratory Sales Limited) and allowed to grow until 80% confluent. Cells were fixed in ice-cold methanol, rehydrated with 1 × PBS, and blocked with a 0.5% BSA (Sigma-Aldrich) in 1 × PBS solution. Following blocking, cells were incubated with a polyclonal rabbit antibody raised against a peptide corresponding to amino acids 541-562 of mouse Arhgap31 (PRD1) and purified on a Protein A-Sepharose column (1:500 dilution). After washing with blocking solution, a secondary rabbit-specific fluorophore-tagged antibody (Abcam Inc.) was added for 1 h. Coverslips were rinsed and mounted on slides with hard-set mounting medium containing a DAPI nuclear stain (Vector Labs). Golgi immunostaining was performed using a 58K Golgi protein antibody. A monoclonal tubulin antibody was used to visualize the cytoskeleton. Antibodies were diluted according to manufacturer's instructions (Abcam Inc.). As negative controls, preimmune serum from the antibody host rabbit replaced the Arhgap31 antibody and was labeled as described above. A second experiment utilized a blocking peptide specific to the PRD1 antibody epitope used at a 10:1 concentration (peptide to antibody). An additional blocking peptide specific to a random region of Arhgap31 was used as a negative control. Both blocking

peptides were synthesized by Sigma-Aldrich. All images were acquired on a Zeiss LSM 510 confocal microscope and processed with Adobe Photoshop. Statistical comparisons for cell rounding experiments were conducted using a χ^2 2×2 contingency table.

G-LISA CDC42 activation assay

HEK 293 cells grown to 70% confluency on 100 mm dishes were transiently transfected using polyethyleneimine (Polysciences Inc.) with 100 ng of empty vector or vector encoding myc-tagged wild-type ARHGAP31, p.K1087SfsX4 or p.Q683X. Cells were lysed 16 h post-transfection according to manufacturer's instructions (Cytoskeleton Inc.) and snap-frozen in liquid nitrogen. Samples used in the G-LISA assays were selected after determining similar levels of myc-tagged proteins and Cdc42 by western blotting using myc-specific (Cell Signaling Technology) and Cdc42-specific (Santa Cruz Biotechnology) polyclonal antibodies, respectively (Supplementary Figure 3). The relative amounts of GTP-bound Cdc42 in each condition were determined in duplicate according to the manufacturer's instructions. For each Cdc42-GTP measurement, 100 µg of protein lysate was used. To compare WT and patient Cdc42 activity, a student's *t*-test was used with a two-tail distribution.

Immunoprecipitation

HEK 293 cells were co-transfected with pRK5myc-Arhgap31 (1083-1425) and pEGFP-Arhgap31 (1-221 or 1-820). After 16 h, cells were lysed on ice in 25 mM HEPES pH 7.4, 100 mM NaCl, 10 mM $MgCl_2$, 5% glycerol, 1% NP-40, 1 mM Na_3VO_4, 10 mM NaF, 1 mM PMSF and protease cocktail inhibitors (Roche Applied Science). Protein lysates were centrifuged for 10 min at 14,000*g* and pre-cleared for 1 h at 4 °C with Protein G-Sepharose (GE Healthcare). Supernatants were incubated for 3 h at 4 °C with 2 µg of monoclonal myc-

specific antibody (9E10) and Protein G-Sepharose. Immune complexes were washed three times in lysis buffer and resuspended in SDS sample buffer. Proteins were resolved by SDS-PAGE and detected by western blotting using antibodies to GFP (A6455, Molecular probes) and myc.

Wound healing assay

Wound healing assay was performed in 35 mm tissue culture dishes using an IBIDI chamber at a density of 8500 cells/well in a volume of 70 µl. WT and p.Q683X primary dermal fibroblast cells were seeded to confluence onto fibronectin-coated 35 mm culture plates. Cells were serum and growth supplement starved for 12 h and then half of each well was denuded of cells using a sterile rubber policeman. The cultures were washed twice with 1 × PBS and wound margins were photographed (t=0 h). Cells were incubated overnight (37 °C, 5% CO_2) and wounding was performed 12 h later, and the same fields of the wound margin were photographed at different time points. Pictures were superimposed and areas were measured using Image J software.

Proliferation assay

A cell dilution series ranging from 100 to 50 × 10^4 cells was created in a 96-well cell culture microplate (Corning) with CyQUANT GR dye/lysis buffer, in final volumes of 200 µl per well. Cells were lysed at room temperature with 1 ml of CyQUANT GR dye/lysis buffer. Samples were incubated in darkness for 2–5 min at room temperature. The fluorescence of each sample was measured with a CytoFluor 2350 fluorescence microplate reader, with 485 nm (±10 nm) excitation and 530 nm (±12.5 nm) emission filters. For each experiment, a standard calibration curve was generated by plotting measured fluorescence values in these samples versus cell number, as determined previously from cell suspensions using a hemocytometer. 6-well culture plates of cells were

harvested on days 0 and 1–10. All microplates were lysed with 200 µl of the CyQUANT GR dye/lysis buffer. The samples were incubated in darkness for 2–5 min. Sample fluorescence was measured as above, and growth curves were plotted as fluorescence versus time. End-point values were compared by means of an unpaired *t*-test.

Supplementary Methods:

Genotyping, linkage analysis and mutation detection

Genomic DNA was extracted from either peripheral venous blood by standard techniques or from saliva using the Oragene-DNA self-collection kit (DNA Genotek Inc.), according to the manufacturer's instructions. A genome-wide screen was performed for 22 individuals from two multigenerational families, using the GoldenGate HumanLinkage V Panel on an iScan System (Illumina Inc.), following manufacturer's guidelines. Linkage analysis was performed using Merlin v1.1.2 software. Pedigree data were analyzed under an autosomal dominant disease model with a disease allele frequency of 0.0001 and a penetrance value of 85%. Additional polymorphic markers for refinement mapping were selected with an average heterozygosity of 74%. Fluorescently-tagged PCR fragments were analyzed on an ABI3730xl DNA Analyzer and genotypes were assigned using GeneMapper v3.7 software (Applied Biosystems). All coding exons and intron-exon boundaries of the candidate genes *LSAMP*, *ARHGAP31*, *POPDC2* and *GSK3B* were screened by direct DNA sequencing. Primers were designed using Primer3 software1. PCR products were purified with ExoSAP-IT (GE Healthcare), and sequenced using BigDye Terminator v3.1 chemistry (Applied Biosystems). Sequence traces were aligned to reference using Sequencher v4.9 software (Gene Codes Corporation).

Whole-mount *in situ* hybridization

The genomic sequence of *Arhgap31* was obtained from Ensembl. Primers were designed using Primer3 software1 to produce a PCR product of 543 bp from the 3' UTR of *Arhgap31* (genomic location: chr16:38,599,795-38,600,337). T3 and T7 RNA polymerase sites were added to the 5' end of the forward and reverse primers respectively (forward: *AATTAACCCTCACTAAAGG*CTGCTGGAGGAA-GGTTTCTG; reverse: *TAATACGACTCACTATAGG*CGCCTCTCCACAC-CATATTT). A template from riboprobe synthesis was generated by PCR of mouse genomic DNA, purified using the QIAquick gel extraction kit (Qiagen), and digoxigenin (DIG) labeled (Roche Applied Science) antisense riboprobes were generated by *in vitro* transcription of purified riboprobe DNA template using T7 RNA polymerase.

CD1 mouse embryos at developmental stages 9.5, 10.5, 11.5 and 12.5 days post-coitum (dpc) were obtained from the Mary Lyon Centre, MRC Harwell. Embryos were fixed overnight in 4% paraformaldehyde at 4 °C. Embryos were stored in methanol and were rehydrated in a series of graded methanol washes in PBST (PBS + 0.1% Tween 20). Proteinase K (10 µg/ml) (Roche Applied Science) permeabilization was performed for 15-35 min, depending on the stage of development. Embryos were washed twice in 0.1 M triethanolamine, with the addition of acetic anhydride to the second wash. Samples were then washed in PBST and re-fixed in 4% PFA/0.2% gluteraldehyde for 20 min. Following washing in PBST, embryos were prehybridized at 60 °C for 2 h and hybridization was for 2 nights at 60 °C in hybridization buffer containing the DIG-labeled probe. Samples were washed 3 times in 2 × SSC + Tween 20 for 20 min per wash and then 3 times in 0.2 × SSC + 0.1% Tween 20 for 30 min per wash at 60 °C. Samples were then washed twice in maleic acid buffer (MAB) for 15 min per wash at room temperature. A 2 h wash in MAB + 2% Boehringer-Mannheim

blocking reagent (BMB) + 20% heattreated lamb serum solution at room temperature preceeded an overnight incubation in the same solution containing a 1/2000 dilution of anti-DIG antibody coupled to alkaline phosphatase (Roche Applied Science). Embryos were then washed 3 times in MAB for 1 h per wash and color detected with 2 ml of BM purple precipitating solution (Roche Applied Science).

Migration assay

We determined the ability of fetal calf serum (FCS) to induce migration of human dermal fibroblasts *in vitro* by Transwell assays (Corning Labware and Equipment). 2×10^5 cells were plated in the upper chamber of 8-m-pore filter Transwell and cultured with basal medium supplemented with 2% BSA (Sigma-Aldrich). Following 12 h culturing, growth media was replaced in the bottom layer with basal medium supplemented with 20% FCS. Cells were allowed to migrate for 24 h. Media was then replaced with 450 µl of serum free media with 8 □M Calcein-AM and incubated for 1 h. Culture media and the chambers and 500 µl warm dissociation solution was added and cells were incubated for 2 h at 37 °C. The chambers were then discarded and fluorescence of each sample was measured with a CytoFluor 2350 fluorescence microplate reader at 520 nm. The average number of cells that migrated across the filter was quantified. Cells carrying the mutation were compared to control cells using an unpaired *t*-test of the means.

Figure 4.1 – Positional cloning of ACC-TTLD. (**a**) Characteristic phenotype of ACC-TTLD showing severe ACC (left panel) and a range of TTLD defects of the hands (top right panel) and feet (bottom right panel). (**b**) Physical map of the 5.53 Mb critical linkage interval on chromosome 3q13.31-q13.33, showing the genes in the region and the relative location of *ARHGAP31*. The *ARHGAP31* gene structure is expanded beneath. (**c**) Schematic of the ARHGAP31 protein structure, depicting the locations of the known RhoGAP and proline-rich domains. Amino acid positions are shown above and the positions of the identified ACC-TTLD mutations are below the protein structure. (**d**) PCR amplification of *ARHGAP31* in a human fetal cDNA tissue panel demonstrates global expression of the gene. A 983 bp fragment was amplified from all tissues using *GAPDH* primers. Neg = no DNA control.

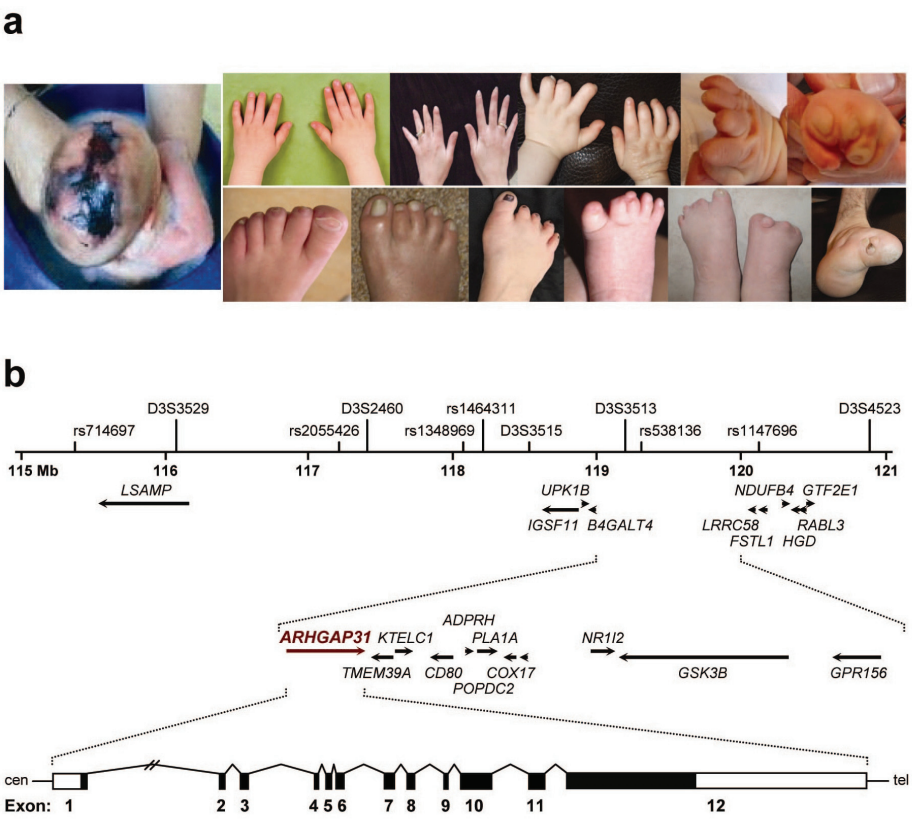
a
b
D3S3529
rs714697
D3S2460
rs2055426
rs1464311
rs1348969
D3S3515
D3S3513
rs538136
rs1147696
D3S4523
115 Mb
116
117
118
119
120
121
LSAMP
UPK1B
IGSF11 B4GALT4
NDUFB4 GTF2E1
LRRC58 RABL3
FSTL1 HGD
ADPRH
ARHGAP31 KTELC1 PLA1A
NR1I2
TMEM39A CD80 COX17
POPDC2
GSK3B
GPR156
cen
tel
Exon: 1 2 3 4 5 6 7 8 9 10 11 12
c
35 aa
213
779 790
986 994
1,444
RhoGAP
Proline-rich domains
p.Q683X
p.K1087SfsX4
d
Brain
Lung
Liver
Heart
Spleen
Thymus
Skeletal muscle
Neg
ARHGAP31
GAPDH

Figure 4.2 – Expression of Arhgap31 during mouse embryogenesis. (**a**) Right lateral view of volume rendered OPT 3-dimensional representation of a 9.5 dpc mouse embryo showing *Arhgap31* expression (red) in developing heart (he). (**b**) Digital section of same embryo as **a**, showing expression in ventral wall of the primitive ventricle and atrium of the heart and the first pharyngeal arch (pa). (**c**) Frontal view of rendered, and (**d**) digital coronal section through, OPT image of 10.5 dpc mouse embryo showing expression in the lateral walls of the primitive ventricles of the heart (he) and the first pharyngeal arch derived facial mesenchyme (fm). By 11.5 dpc (**e**, **f**) the expression is restricted to distinct regions of the surface ectoderm (se) including the surface ectoderm of the upper and lower limb bud (lbe).

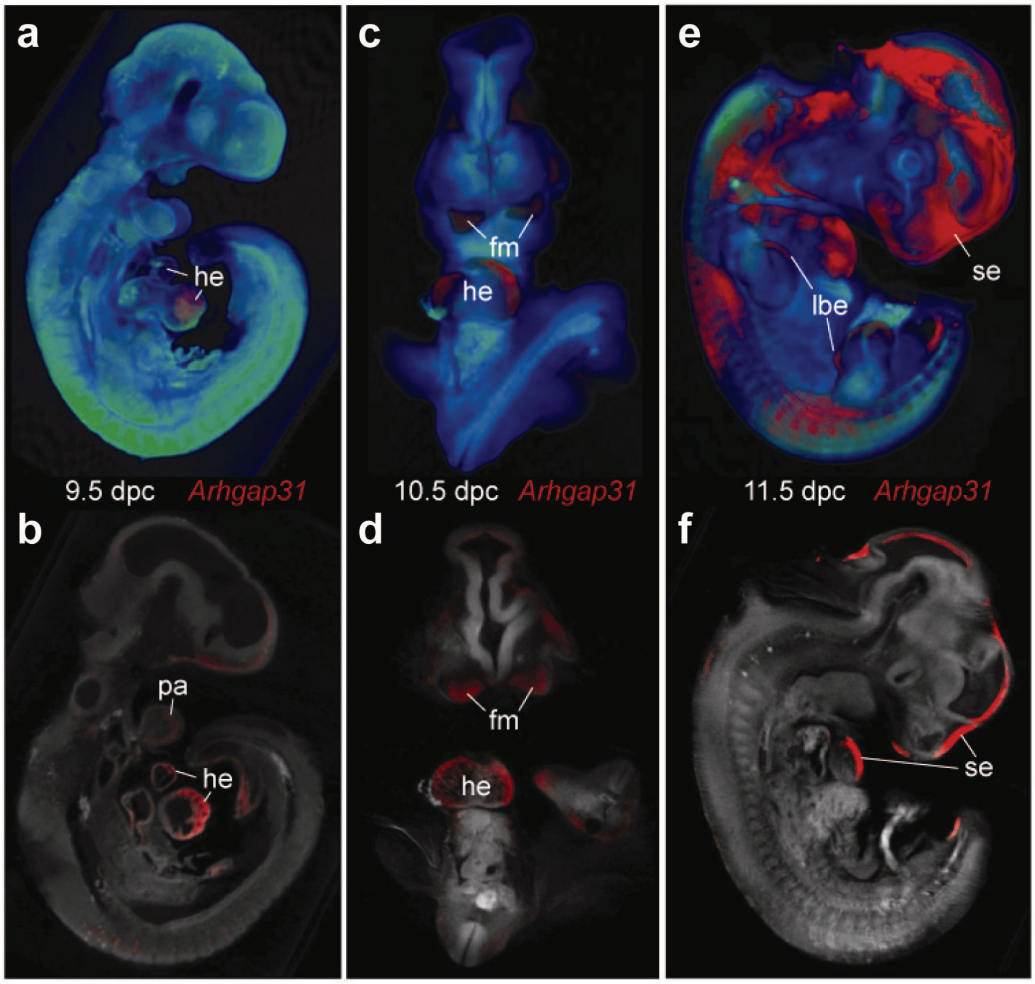
a
he
9.5 dpc Arhgap31
b
pa
he
c
fm
he
10.5 dpc Arhgap31
d
fm
he
e
lbe
se
11.5 dpc Arhgap31
f
se

Figure 4.3 – Functional characterization of ARHGAP31 mutations. (**a**) Quantitative RT-PCR examining *ARHGAP31* transcript levels in lymphoblasts from two related patients heterozygous for the c.2047C>T mutation, compared to a genotypically normal control (WT). Patient and control samples show no appreciable difference in transcript expression. (**b**) Immunostaining of (i) endogenous ARHGAP31 (red) and (ii) Golgi (green) shows marked levels of co-localization to the Golgi apparatus in HeLa cells (iii). (iv) The high specificity of the ARHGAP31 antibody is indicated by the absence of staining in the presence of blocking peptide to the binding epitope. ARHGAP31 distribution in (v) WT and (vi) mutant fibroblasts (p.Q683X) is identical and of equivalent intensity. (**c**) G-LISA assays were used to measure the relative amounts of Cdc42-GTP levels in HEK 293 cells expressing myc-tagged wild-type ARHGAP31 (full-length), p.K1087SfsX4 or p.Q683X. Relative Cdc42-GTP values are expressed as a ratio of Cdc42-GTP levels found in full-length ARHGAP31. Truncated proteins show higher GAP activity towards Cdc42 (**P<0.0002, ***P<0.00001). E.V. = empty vector. (**d**). Immunoprecipitation of deletion constructs using the C-terminus of ARHGAP31 map the intramolecular interaction between amino acids 1083-1425 and the proximal 221 residues harbouring the RhoGAP domain. Full-length protein products are marked by the arrows (smaller bands represent degradation products; *IgG light chain). Levels of transfected proteins, assessed by Western blotting of the lysates with antibody against the myc-tag, are displayed in the lower panel. Data in **a** and **c** are means from 3–4 independent experiments; error bars show s.d. and s.e.m. respectively.

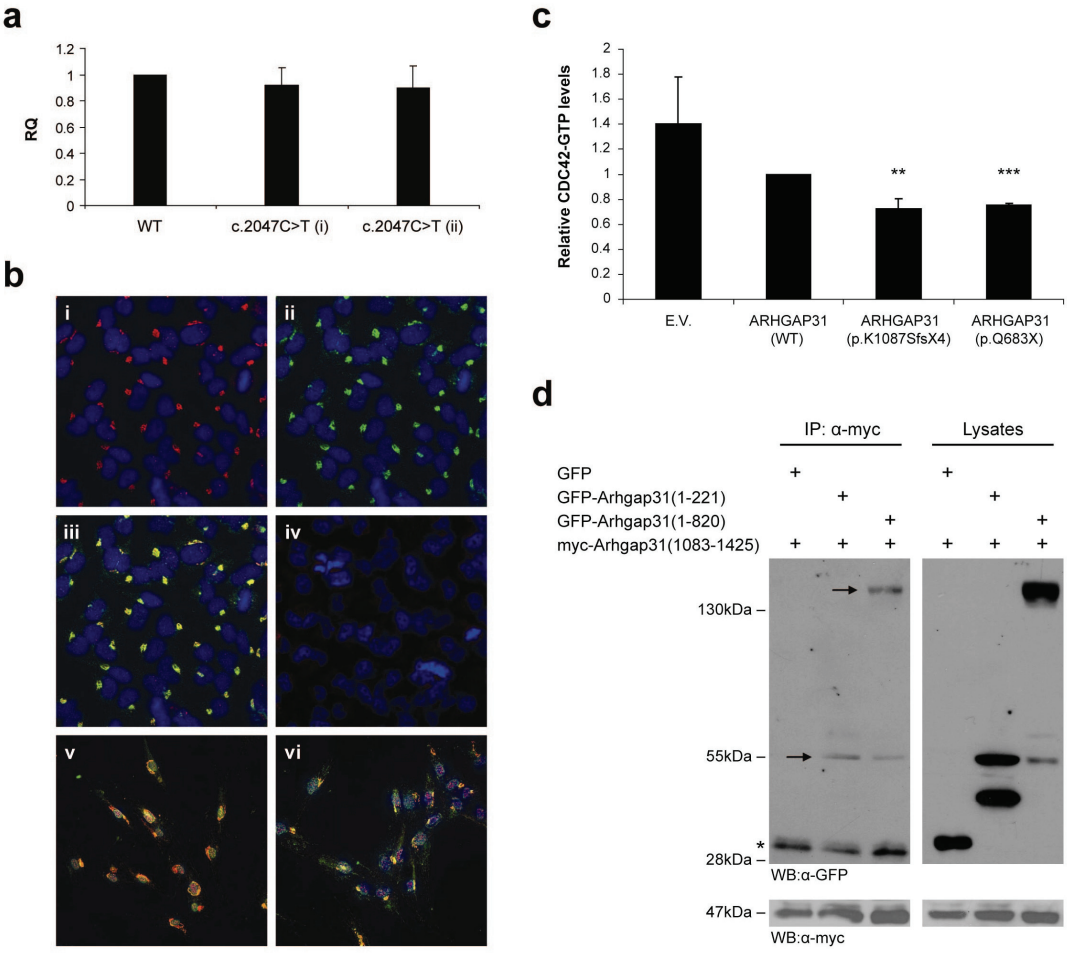
a
RQ
1.2
1
0.8
0.6
0.4
0.2
0
WT
c.2047C>T (i)
c.2047C>T (ii)
b
i
ii
iii
iv
v
vi
c
Relative CDC42-GTP levels
2
1.8
1.6
1.4
1.2
1
0.8
0.6
0.4
0.2
0
**
***
E.V.
ARHGAP31 (WT)
ARHGAP31 (p.K1087SfsX4)
ARHGAP31 (p.Q683X)
d
IP: α-myc
Lysates
GFP
GFP-Arhgap31(1-221)
GFP-Arhgap31(1-820)
myc-Arhgap31(1083-1425)
130kDa –
55kDa –
28kDa –
*
WB:α-GFP
47kDa –
WB:α-myc

Figure 4.4 – Cellular phenotype of ACC-TTLD disease alleles. (**a**) Coverage of cell-free gap by primary dermal fibroblasts heterozygous for the p.Q683X mutation and WT unaffected control cells at 24 hours post-wounding. Quantification of the percentage of wound healing is shown in Supplementary Figure 4a. (**b**) Comparison of proliferative activity measurements of p.Q683X primary dermal fibroblasts and WT unaffected control cells. Statistical analysis of the last time-point revealed a significant decrease in the proliferative ability of cells carrying the p.Q683X mutation compared to unaffected controls (***P*=0.0001). Data show means from three independent experiments with s.e.m. error bars. (**c**) HeLa cells were transiently transfected with myc-tagged WT ARHGAP31, p.Q683X and p.K1087SfsX4 constructs. Cell shape was visualized by confocal microscopy for tubulin and transfected cells indicated by co-staining with fluorescent conjugated antibody against the myc-tag. Levels of cell rounding were measured by examining three separate fields of vision in three independent transfection experiments. The bar-chart beneath shows the mean percentage of rounded cells observed for each construct (error bars indicate S.D.).

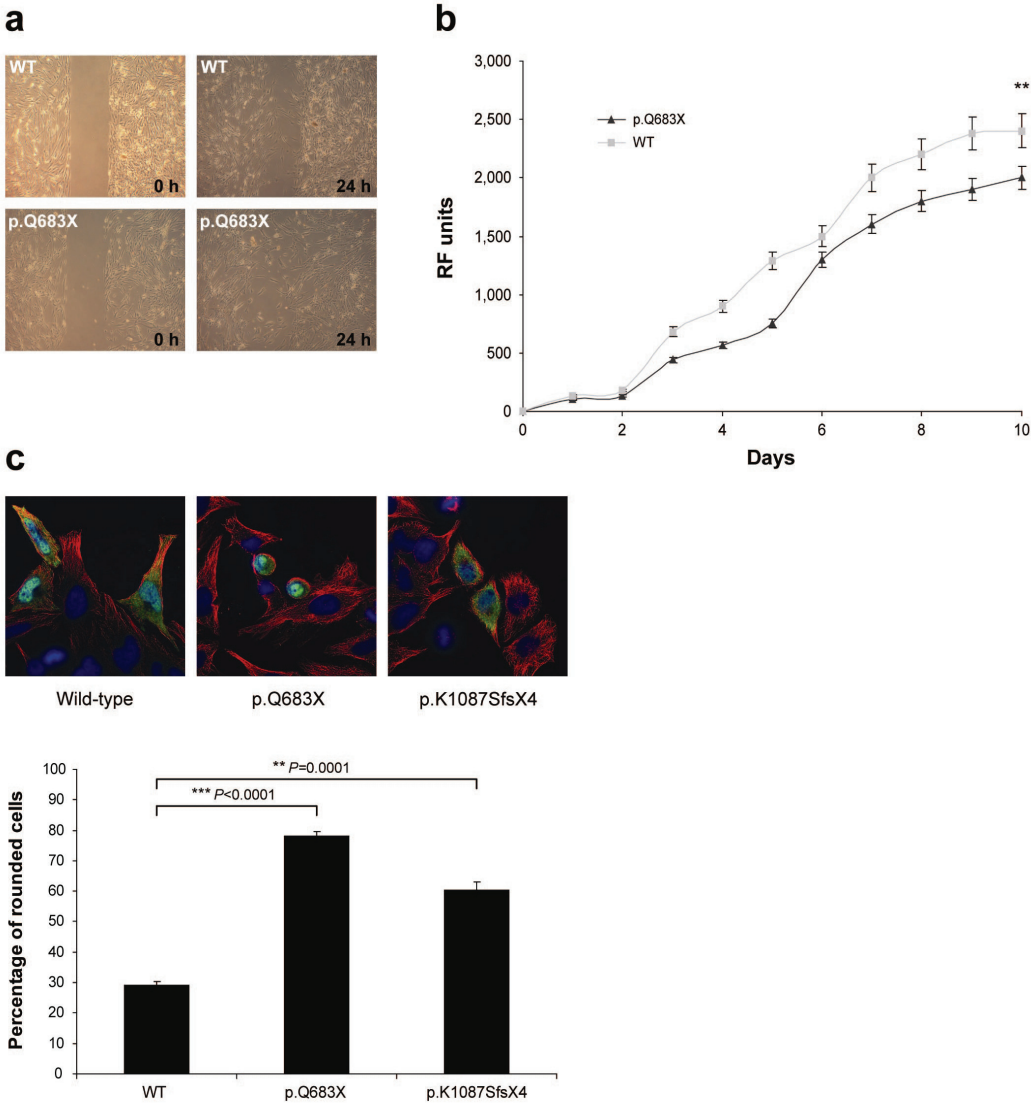
a
WT
0 h
WT
24 h
p.Q683X
0 h
p.Q683X
24 h
b
RF units
Days
p.Q683X
WT
**
c
Wild-type
p.Q683X
p.K1087SfsX4
Percentage of rounded cells
** P=0.0001
*** P<0.0001
WT
p.Q683X
p.K1087SfsX4

Supplementary Figure 4.1 – Linkage analysis and segregation of ARHGAP31 mutations with the ACC-TTLD phenotype (**a**) Segment of chromosome 3, showing the results of linkage analysis for families AOS-5 and AOS-12. A maximum multipoint LOD score of 4.93 was achieved at marker rs1464311. (**b**) Segregation of the disease haplotype and chromatogram of the c.2047C>T mutation in family AOS-12. (**c**) Segregation of the disease haplotype and chromatogram of the c.3260delA mutation in family AOS-5.

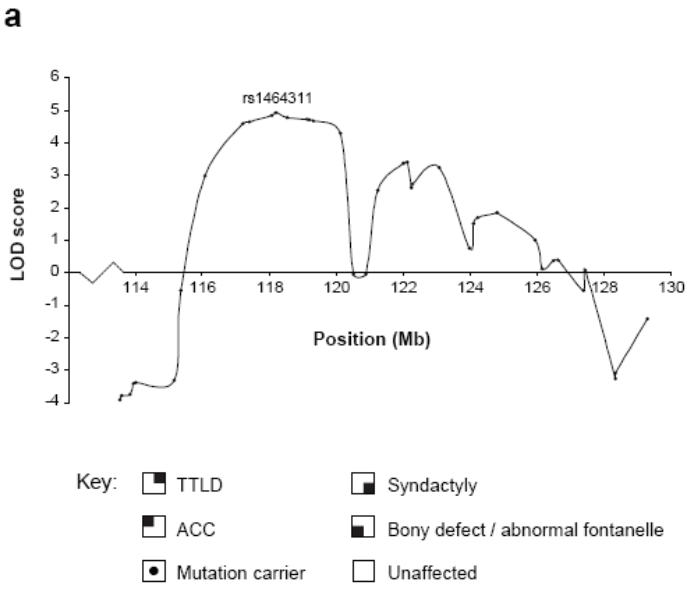
a
rs1464311
LOD score
Position (Mb)
Key:
TTLD
ACC
Mutation carrier
Syndactyly
Bony defect / abnormal fontanelle
Unaffected

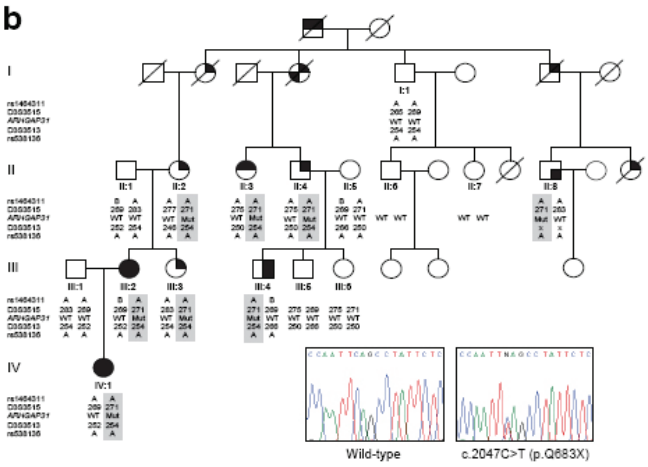
b
Wild-type
c.2047C>T (p.Q683X)

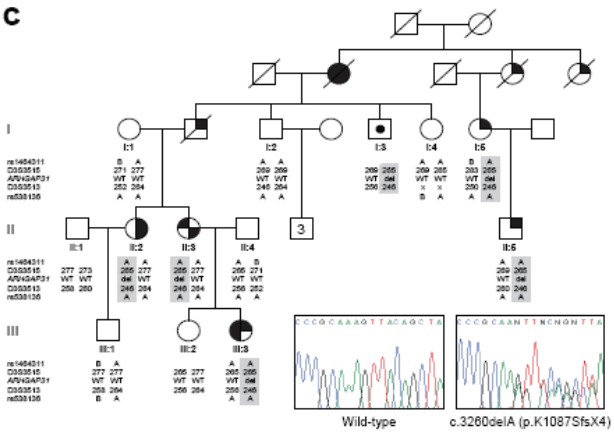
c
Wild-type
c.3260delA (p.K1087SfsX4)

Supplementary Figure 4.2 - (**A**) i) Volume rendering of *Arhgap31* expression in a 9.5 dpc embryo. Expression can be seen in the atrium and ventricle of the heart. ii) A transverse section through the 9.5 dpc embryo showing expression in the heart, craniofacial processes, tail and in intersomitic regions. iii) A sagittal section through the embryo shows expression in the 1st branchial arch and the tail. iv) A sagittal section showing *Arhgap31* expression in the developing hindlimb buds. (**B**) i) A volume rendering showing *Arhgap31* expression in a 10.5 dpc embryo. Expression can be seen in the craniofacial processes, the developing heart and in a periodic pattern between somites. ii) A transverse section through the 9.5 dpc embryo showing expression in the heart, craniofacial processes and in intersomitic regions. iii) A transverse section through the 9.5 dpc embryo showing expression in the heart and craniofacial processes. iv) A frontal view of the volume rendering showing *Arhgap31* expression in a 10.5 dpc embryo. Expression can be seen in the heart, hind limb buds and the nasal processes. v) A coronal section through a the 10.5 dpc embryo showing expression in the heart, hind limb bud and nasal processes. vi) A coronal section through a the 10.5 dpc embryo showing expression in the heart, hind limb buds, craniofacial processes and in the axial mesoderm adjacent to the neural tube. (**C**) i) Volume rendering of *Arhgap31* expression in a 11.5 dpc embryo. This shows expression in the limbs, tail, facial processes and heart. ii) A transverse section through the 11.5 dpc embryo showing expression in the heart, craniofacial processes and tail.

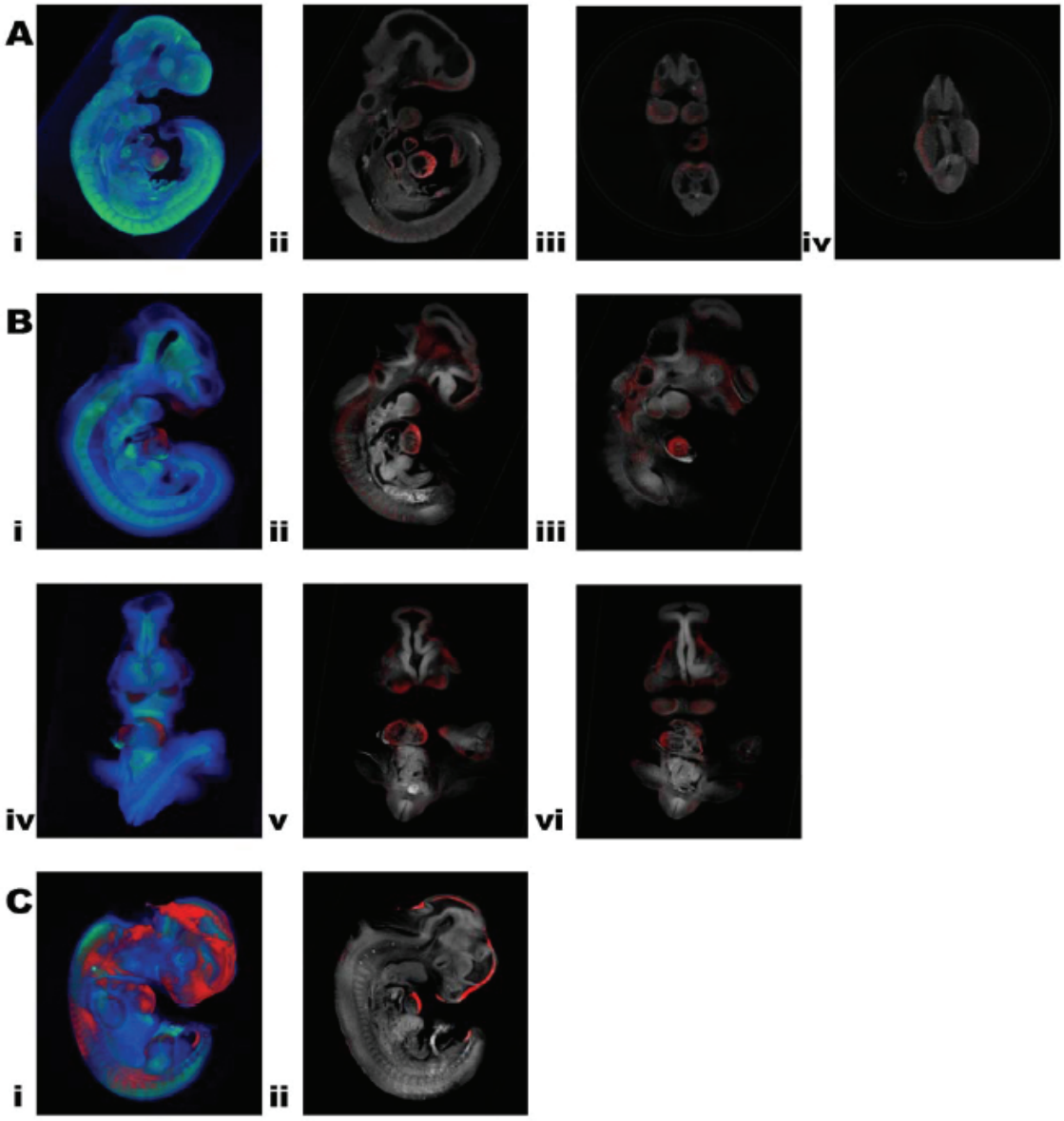
A
i
ii
iii
iv
B
i
ii
iii
iv
v
vi
C
i
ii

Supplementary Figure 4.3 – Western blot of G-LISA assay lysates. Equivalent levels of transfected wild-type and mutant ARHGAP31 were confirmed by immunostaining with antibody against the myc-tag and total endogenous Cdc42 measured by polyclonal Cdc42-specific antibody.

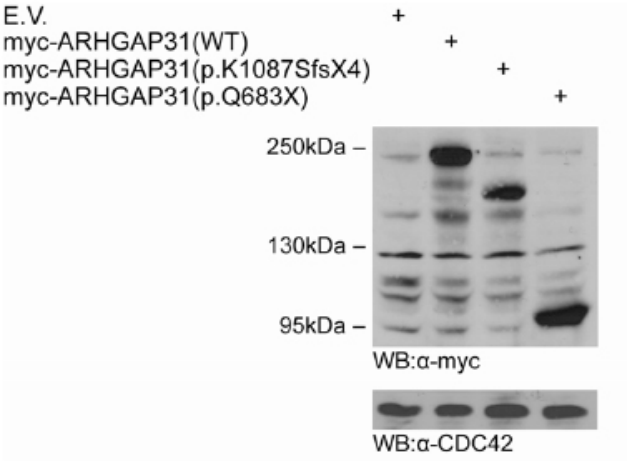
E.V.
myc-ARHGAP31(WT)
myc-ARHGAP31(p.K1087SfsX4)
myc-ARHGAP31(p.Q683X)
+
+
+
+
250kDa –
130kDa –
95kDa –
WB:α-myc
WB:α-CDC42

Supplementary Figure 4.4 – Wound healing and Transwell migration assays. (**a**) Wound healing migration assay. Plot showing percentage of wound restoration at 18, 24 and 30 hours post-wounding. Primary dermal fibroblasts from an AOS patient migrate at a significantly faster rate compared to similar unaffected control cells. (**b**) Transwell chemotaxis migration assay. Migration of cells towards varying concentrations of chemoattractant (15% FCS, 20% FCS). Primary dermal fibroblasts from an AOS patient migrate at a significantly faster rate at the highest concentration of chemoattractant compared to similar unaffected control cells. A highly invasive human endometrial tumour cell line (HeLa) was used as a positive control. Data for **a** and **b** show means from three independent experiments with s.e.m. error bars. Key: AOS = patient heterozygous for the p.Q683X mutation; WT = unaffected control

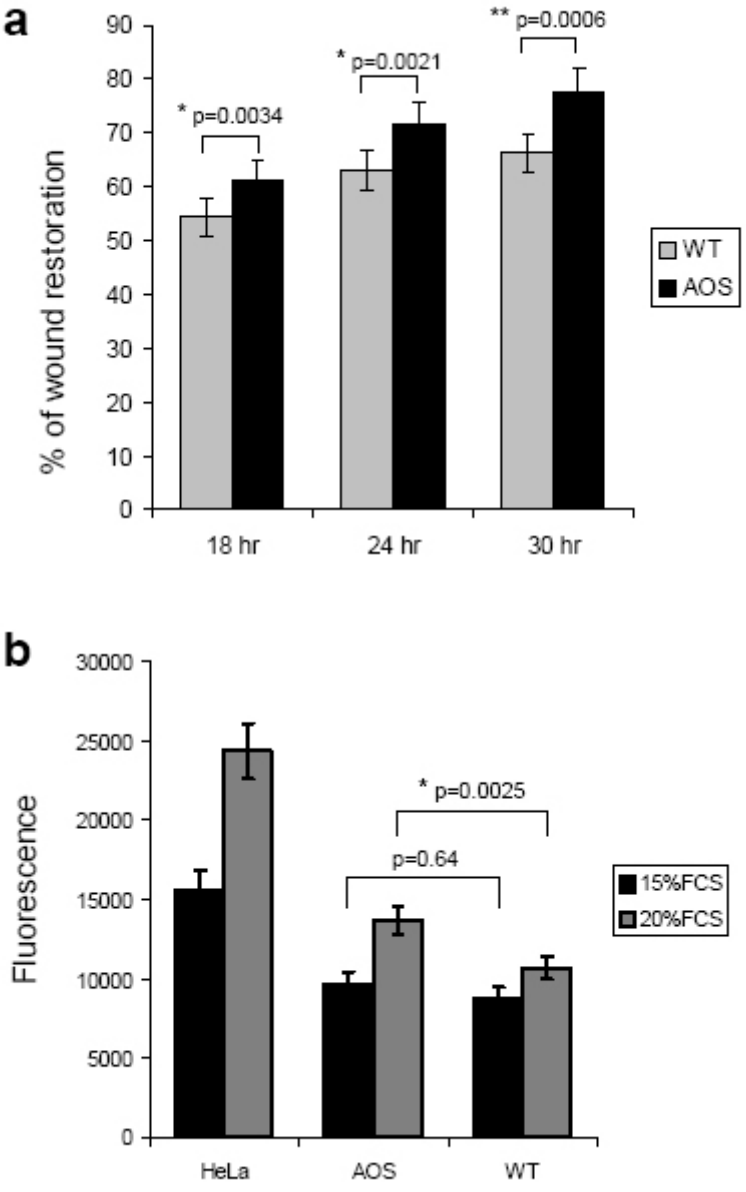
a
% of wound restoration
90
80
70
60
50
40
30
20
10
0
* p=0.0034
* p=0.0021
** p=0.0006
18 hr
24 hr
30 hr
WT
AOS
b
Fluorescence
30000
25000
20000
15000
10000
5000
0
* p=0.0025
p=0.64
HeLa
AOS
WT
15%FCS
20%FCS

Chapter 5 - General Discussion and Conclusions

5.1 Major Findings

5.1.1 Association of CdGAP with PI(3,4,5)P_3 through a polybasic cluster of amino acids.

Prior to studies in this thesis, very little was known about the functions of discrete regions in CdGAP/ARHGAP31, besides its GAP domain. In the second chapter, we describe how a small cluster of positively charged residues located at the N-terminus of CdGAP is required for the specific association of this protein with the phosphatidylinositol lipid PI(3,4,5)P_3. To demonstrate this interaction, we have reconstituted physiological membranes with a defined lipid composition in order to assess the capacity of specific lipids to recruit CdGAP proteins. We have also confirmed that recruitment of the GAP protein to lipid membranes is compulsory for prenylated Rac1 activation by CdGAP. Using cell biology experiments, we revealed that the residues implicated in PI(3,4,5)P_3 binding are also required for the normal GAP-associated functions of CdGAP inside the cell, without changing their intrinsic GAP activity. Although we have not performed experiments to demonstrate the association of CdGAP with PI(3,4,5)P_3 directly inside the cell, we propose that CdGAP associates with lipid membranes *in vivo* through a group of positively charged residues located directly at the N-terminus of the GAP domain of CdGAP. We further argue that this association is necessary for CdGAP to inactivate Rho GTPases. Interestingly, a close analysis of the amino acid composition of over 70 human RhoGAPs suggests the interesting idea that a large number of GAP proteins may use a similar mechanism to localize their GAP domain directly at the membrane. This investigation will be discussed in the section 5.3 of this thesis.

5.1.2 Selective association of Intersectin SH3D domain to a SKSK motif found in the BR domain of CdGAP

In the third chapter of this thesis, we endeavored to identify the minimal amino acid sequence required for the fourth SH3D domain of Intersectin to associate with CdGAP. We first confirmed that the binding between this SH3 domain and CdGAP is direct. Then, we found that the interaction site is confined to a region of CdGAP which is evolutionarily conserved in its closest homologs and revealed that one of these, ARHGAP30, could also associate with this SH3 domain through the same region. Using synthetic peptides, we revealed the selectivity of this SH3 domain for binding to peptides bearing a SKSK motif. After substituting evolutionarily conserved amino acids in the BR region of CdGAP proteins, we localized a site containing this SKSK motif that lost affinity for SH3D when the lysine residues were substituted to alanines. The same motif is found conserved in a region of Numb which also binds Intersectin through its SH3D domain.

5.1.3 Association of CdGAP gene mutations with a human development disorder

In the fourth chapter of this thesis, mutations in the human CdGAP gene have been identified and associated with a human development disorder characterized by aplasia cutis congenita (ACC) and terminal transverse limb defects (TTLD). Autosomal dominant transmission of this syndrome in two different families was associated with point mutations localized in the last exon of CdGAP, which lead to the production of truncated mutant proteins. We provided evidence suggesting that these truncated mutants display aberrant elevated GAP activity towards Cdc42 when expressed in mammalian cells. This

result correlates with the observation that cell rounding was also higher for the cells transiently expressing CdGAP truncated proteins. We also provided results suggesting that the C-terminal amino acids of CdGAP associate with its GAP domain and therefore we propose a regulatory mechanism in which the C-terminal region of CdGAP would fold on the GAP domain to prevent its aberrant activation. Overall, we contributed to show that CdGAP gain-of-function mutations are directly linked to this human developmental disorder.

5.2 Selective binding of CdGAP to PI(3,4,5)P_3

Selective binding of a Cdc42 and Rac1 specific RhoGAP to PI(3,4,5)P_3 has somewhat been surprising. This phosphatidylinositol PI(3,4,5)P_3 is mostly known for being transiently generated by PI3K enzymes at the plasma membrane following growth factor or hormone activation and to recruit proteins such as PKB/AKT or Cdc42/Rac GEFs to induce cell growth and directed cell migration, respectively [359, 385, 386]. Therefore, it is hard to reconcile how CdGAP could be activated by the same lipid to reduce Cdc42 and Rac1 signaling in that context. However, a recent large scale investigation of the PI(3,4,5)P_3 interactome using proteins extracted from LIM1215 colon cancer cell line revealed that the Cdc42 specific GAP, Cdc42GAP/ARHGAP1, also associates with PI(3,4,5)P_3, suggesting that CdGAP is not the only GAP capable of working in combination with this lipid [387]. These GAPs could be influenced by PI(3,4,5)P_3 in a different context than directed cell migration. Indeed, this lipid is also involved in polarization of endothelial cells, endocytosis, phagocytosis or even spindle orientation during mitosis [388, 389]. As we have not provided evidence of a direct association between PI(3,4,5)P_3 and CdGAP *in vivo*, future studies will not only need to focus on identifying the context of this interaction, but will also have to validate its occurence inside the cell. This could be partly

achieved by a FRET (fluorescence resonance energy transfer)-based approach using fluorescent proteins attached to a PI(3,4,5)P_3–binding probe and CdGAP, which would confirm intracellular proximity of these proteins in a PI(3,4,5)P_3 induceable manner. It would be of particular interest to examine cell polarization as our laboratory has previouly shown that GSK3 kinases, which are implicated with Cdc42 and PI(3,4,5)P_3 in the positioning of the microtubule organizing center (MTOC) in the cell, phosphorylate CdGAP [176, 349]. Although the precise function of these phosphorylation events are not fully understood, it is hypothesized that targetting of at least one site, located at position T776, negatively regulates the GAP activity of CdGAP [349]. Considering that AKT/PKB inactivates GSK3, one could propose a model where PI(3,4,5)P_3 production activates CdGAP by direct association with its PBR and by concomitantly inhibiting indirectly GSK3.

While we found strong specificity binding of CdGAP for PI(3,4,5)P_3, we have not assessed if the lipids PI(3,4)P_2 and PI(3,5)P_2 could also interact with this protein. Although their role is often hidden by PI(3,4,5)P_3 and PI(4,5)P_2, these lipids also contribute to biological functions. Indeed, as for PI(3,4,5)P_3, PI(3,4)P_2 mediates PI3K-dependant signaling effects in the cell, whereas PI(3,5)P_2 participates to endosomal trafficking [390]. Moreover, we have not assessed if other regions of CdGAP could directly associate with phosphatidylinositols. It would be of particular interest to test if the BR domain, which is enriched in positively-charged amino acids found conserved within CdGAP homologs, could also have a biological-relevant function associated with lipid interaction.

5.3 Presence of polybasic clusters in a large number of Rho GAPs

Our findings regarding the presence of a PBR involved in lipid binding at the N-terminus of CdGAP, in addition to the publication of similar mechanisms in DLC1 and p190RhoGAP, prompted us to analyse the primary amino acid sequence of human RhoGAPs (Table 5.1). We were impressed by the number of these proteins having PBR-like regions. At least 23 mammalian RhoGAP proteins contain a sequence enriched in positively charged amino acids at the N-terminus of their GAP domain. In several cases, as for Chimaerins, Myo9, ARHGAP8 and ARHGAP10, a lipid binding domain is located at this position and probably accounts for the absence of a PBR. Therefore, there is a probability that additional RhoGAPs associate with lipids in a similar fashion than CdGAP, DLC1 and p190RhoGAP. Since a small discrepancy between polybasic clusters can potentially change the specificity of the lipid binding, as observed for CdGAP and DLC1 [324], PBRs could add an additional level of specificity *in vivo* between Rho GAP and GTPases, bearing their association for the same type of lipid. Indeed, Rho GTPases also have a PBR at their C-terminus that was shown in some cases to be directly involved with their localization and function [127-129], although their capacity to discriminate $PI(3,4,5)P_3$ from $PI(4,5)P_2$ remains ambiguous [65].

To date, most *in vitro* experiments addressing the specificity of GAPs towards RhoGTPases have been performed in an environment that did not account for the membrane context of their interaction. Although their composition does not reflect precisely the *in vivo* nature of cellular membranes, the use of multilamellar vesicles (MLVs) or small- and large-unilamellar vesicules (SUVs, LUVs) with prenylated GTPases provides a framework to study GTPase regulators in a more physiological context.

Table 5.1. Occurrence in RhoGAP proteins of sequences enriched in positively charged amino acids at the N-terminus of the GAP domain

M.m. Rho GAP	Amino acids located at the N-terminus of the GAP domain
CdGAP/ARHGAP31	1-M**K**N**K**GA**K**Q**K**L**KRK**GAASAFGCDLTEYLESSG-31
ARHGAP30	1-M**K**S**R**Q**K**G**KKK**GSA**K**E**R**VFGCDL**R**EHLQHSG-30
RICS-S/ARHGAP32-S	1-M**K**S**R**PT**K**Q**K**L**K**Q**R**GIL**K**E**R**VFGCDLGEHLLNSG-32
RICS-Ls/ARHGAP32-L	351-M**K**S**R**PT**K**Q**K**L**K**Q**R**GIL**K**E**R**VFGCDLGEHLLNSG-382
NOMAGAP/ARHGAP33	318-**R**S**R**PS**R**Q**R**L**R**Q**R**GIL**R**Q**R**VFGCDLGEHLSNSG-349
DLC1	632-P**K**FM**KR**I**K**VPDY**K**D**R**SVFGVPLTVNVQ**R**SG-652
DLC2	644-P**K**FM**KR**I**K**APDY**R**D**K**AVFGVPLIVHVQ**R**TG-673
DLC3	548-P**K**FM**KR**N**K**TPDY**R**GHHVFGVPPLIHVQ**R**TG-578
p190RhoB/ARHGAP05	1224-DD**KK**I**KKK**TH**K**V**K**ED**KK**Q**KKK**T**K**TFNPPT**RR**NWESN-YFGMPLQDLVTAE-1272
p190RhoGAP/GRLF1	1214-**RRR**NIL**R**SL**RR**NT**KK**P**K**P**K**P**R**PSIT**K**ATWESNYFGV-PLTTVVTPE-1258
BCR	1017-TVIDMNGIEV**K**LSV**K**FTS**R**EFSL**KR**MPS**RK**QTGVFGV**K**I-AVVT**KR**E**R**-1063
ABR	613-IEMNGI**K**VEFSM**K**FTS**R**DMSL**KR**TPS**KK**QTGVFGV**K**ISV-VT**KR**E**R**-657
ARHGAP4	461-G**R**SILS**K**LQA**K**HE**K**LQEAIQQGN**K**E**K**QETS**R**TQCTE**RK**F-H**K**SH-PPHP**R**FQYNQ**R**LFGGDLE**K**FIQSSG-528
ARhGAP6/ARHGAPX-1	377-S**R**LLEALQLSLPAEAQS**KK**E**K**A**R**D**KK**LSLNPIY-409
ARHGAP9	210-S**K**SLM**R**LGS**RR**TSS**R**CAEGTDQ**K**N**R**V**R**N**K**L**KR**LIA**KR**P-TLQSLQ-E**R**GLF**R**DQVFGCQLESLCQ**R**EG-275
ARHGAP12	588-E**K**HD**K**E**K**DQ**K**EL**KKLR**SM**K**GSSMDSSEQ**KK**T**KK**NL-**KK**FLT**RR**PTLQAV**R**E**K**GYI**K**DQVFGSNLANLCQ**R**EN-658
ARHGAP15	228-**RK**EQ**K**PEH**RK**SFMF**R**LHHSASDTSD**K**N**R**V**K**S**R**L**KK**FIS-**RR**PSL**K**TLQE**K**GLI**K**DQIFGSHLHTVCE**R**EH-297
ARHGAP18	307-F**K**QQ**K**AV**K**I**K**T**R**DSGLFGIPLTILLEQDQ**RK**VPG
ARHGAP19	97-FF**R**SLMSL**KRK**E**K**GVVFGSPLT-118
ARHGAP23	807-GEDPGCANQALIS**KK**LNDY**RK**VSHSSGP**K**ADSSP**K**GS**R**-GLGGL**K**SEFL**K**QTAV**R**GL**R**TQEQPPGS**K**EDSVAAP**K**TPWGIN II**KK**N**KK**AAP**R**AFGI**R**LEECQPATEN-912
ARHGAP27/CAMGAP1	444-LS**R**V**R**H**K**L**RK**FLQ**RR**PTLQSL**R**D**K**GYI**K**DQVFGCALA-QLCE**R**E**R**-488
ARHGAP36	145-**R**MLG**R**M**RR**FFS**RRR**NEPTLP**R**EFT**RR**G**RR**GAVSADSA-DELENGALLLQILQLSQLSSPIGQ**R**LLGS**KRK**MSLNPIA-220
Ralbp1 / RBP1	65-**K**DHG**KKK**G**K**F**KKK**E**KR**TEGYAAFQEDSSGDEAESPS**K**V-**KR**S**K**GIHVF**KK**PSFS**KKK**E**K**DF**K**I**K**E**K**P**K**EE**K**H**K**EE**K**H**K**EE**K**H**K**E**KK**S**K**DLTAADVV**K**QW**K**E**KKKKKK**PIQEPEVPQMDAPSV **K**PIFGVPLVDAVE**R**TMMYDG-206

5.4 Possible function of the Intersectin-CdGAP association

Recognition by a SH3 domain of specific positively charged amino acids is not uncommon. Conventional class I ([R/K]xXPxXP) or class II (XPxXPx[R/K]) and atypical motifs including PxxxPR, PxxDY, RKxxY, Px(V/I)(D/N)RxxKP (RxxK) are all caracterized by the presence of at least one basic redidue [74, 339, 369-372]. However, the xKx(K/R) motif in CdGAP is unique since it seems to require the conservation of only two amino acids for its association with SH3D. Indeed, our analysis revealed the need for at least one of three lysine residues in the interaction, with two of these forming an SKSK sequence. Considering the conservation of the x(K)x(R/K) motif in CdGAP, ARHGAP30 and Numb, we believe that the two positively charged amino acids are essential for the interaction. Nevertheless, precise understanding of the minimal amino acid requirement for this binding will require additional experiments, as mutation of these basic residues could reduce, but not abolish the interaction. It will be interesting to determine if the BR domain adopts a three-dimensional structure by itself, or upon binding to the SH3D domain, to bring additional specificity to the interaction, especially due to the nature of this SH3 domain. Indeed, as revealed by analysis of its primary amino acid sequence, the SH3D domain of Intersectin is distinct from other SH3 domains that bind to canonical SH3-binding motifs in that it lacks a negatively charged amino acid (Q1085 in *M.m.*Intersectin-1). This renders the canonical interface for SH3-binding motifs incompetent in recognizing positively charged amino acids (Figure 5.1). Therefore, association of CdGAP to SH3D could be mediated by another interface of this domain, as is the case with Asef and PINCH-1, which both require structural folds to bind their respective SH3 domain [375, 391]. Thus, we suspect the BR domain residues of CdGAP do adopt a three-dimensional structure that would account for the evolutionary conservation of BR domain residues in CdGAP homologs.

The precise function of the interaction between CdGAP and Intersectin short or long isoforms remains to be established. However, it is not surprising to see a Cdc42/Rac1 regulator binding to endocytic proteins as Rho GTPases have not only been associated with endocytosis or exocytosis events, but also endosome trafficking [152, 154, 155]. Indeed, Rac1 and Cdc42 are both required for phagocytosis and exocytosis [392-394]. Of the two, Cdc42 is the only one that is known to be implicated in vesicular trafficking because of its role as a polarity maintenance protein [180]. Cdc42 affects vesicle transport by activating the N-WASP-Arp2/3 complex to promote actin-filament formation. By this action, it facilitates membrane deformation to drive vesicle formation, scission and fusion, it generates force for vesicle movement and provides microfilament tracks for motor protein-based vesicle transport [376]. Moreover, the subfamily members Cdc42, TC10 and TCL, could turn out to be the main targets of CdGAP *in vivo* as they also activate N-WASP. These GTPases were previously shown to localize to intracellular vesicles where they are involved in membrane receptor recycling and exocytosis [152-156]. Indeed, NOMA-GAP, a close homolog of CdGAP, is a known regulator of TC10 [320]. Alternatively, CdGAP interaction with Intersectin could be linked to the local regulation of small pools of Rho GTPases on intracellular membranes. Indeed, Cdc42 localizes to the Golgi apparatus in mammalian cells where it promotes vesicle formation through its activation of N-WASP [395-398]. Moreover, a pool of Rac1 GTPases associated with endosomes was shown to be locally activated by Tiam1 on these structures to allow its export back to the plasma membrane [399]. Therefore, localized activation and inactivation of Rho GTPases on internal membranes is primordial for the distribution of these proteins and for endosomal trafficking.

Conservation of the BR domain in CdGAP homolog proteins raises the possibility that they could all interact with Intersectin through the SH3D domain.

Indeed, we have presented data demonstrating that suggest that ARHGAP30 also binds to Intersectin. This gene has not yet been the focus of any publication and its specificity towards Rac1 and Cdc42 remains to be demonstrated. However, NOMA-GAP and RICS have both been linked with intracellular trafficking of vesicles. In adipocytes, NOMA-GAP is recruited to the plasma membrane following insulin stimulation and promotes exocytosis of GLUT4 containing endosomes [340]. RICS colocalizes with ER proteins in resting cells and is implicated the transport of the N-cadherin/β-catenin complex to the secretory pathway [298]. It would therefore be interesting to see if these events also involve Intersectin.

Nonetheless, the most interesting hypothesis regarding the CdGAP-Intersectin interaction is the possibility that, in a neuronal context, binding of the long isoform of Intersectin to CdGAP would create a “double switch” mechanism leading to Cdc42 activation through simultaneous inhibition of CdGAP by its interaction with the SH3D domain, and relief of the autoinhibited state of Intersectin-1L. Future experiments will need to address this question, which could reveal a new cellular role for CdGAP.

5.5 Gain-of-function CdGAP mutations associated with aplasia cutis congenita (ACC) and terminal transverse limb defects (TTLD)

A number of RhoGAP proteins are linked to different human diseases. For instance, DLC1/ARHGAP7 (Deleted in Liver Cancer protein) protein levels are downregulated in hepatocellular carcinoma and in other cancers [321][304, 305]. However, most human GAP-related health problems occur because of point mutations within their gene coding sequence which lead to either amino

Figure 5.1 – Comparison of SH3 domain canonical binding sites

SH3 domains commonly associate with a peptide through the same interface. Here, SH3 domain of Src complexed with peptide class II peptide motif APPLPPRN (PDB code:1QWE) (A) and Gads SH3 domain binding to a peptide from SLP-76 containing the RxxK motif (PDB code: 1H3H) (B) bind to their respective motif using the same region of the SH3 domain and recognize basic residues within the same site. (C) Three-dimensional structure of *M.m.*Intersectin-1 SH3D domain as predicted by Swiss-model [400]. This SH3 domain lacks a key negatively-charged pocket on this interface to potentially stabilize a xKx(K/R) motif. The SH3 domain (white) and associated peptide (green), contain key amino acids: acidic residus (red), basic residues (blue), proline amino acid (yellow) and tryptophan (grey). Black ellipses show the four sites where amino acids of the peptide and SH3 domain interact. Images were created using PyMOL (The PyMOL Molecular Graphics System, Schrödinger, LLC.).

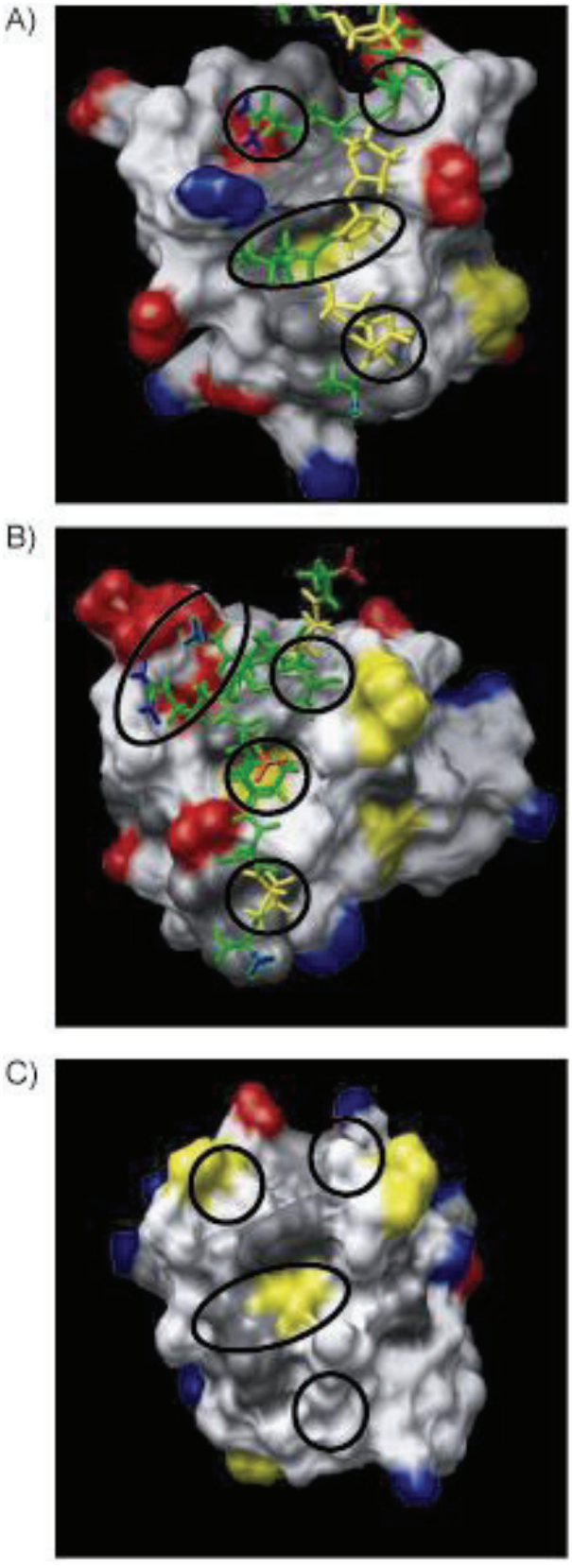
A)
B)
C)

acid substitution or truncation of the RhoGAP protein. Mutations in Oligophrenin were associated with X-linked mental retardation [306-309] and were shown, or predicted, to result in GAP loss-of-function [310]. Conversely, α2-chimaerin mutations were related to a congenital eye movement disorder named Duane's Retraction Syndrome (DRS) and produce hyperactive GAP proteins that escape from their autoinhibited state [297].

CdGAP mutations associated with ACC and TTLD also appear to be gain-of-function mutations. Indeed, transient expression of CdGAP deletion mutants in HEK 293 cells resulted in a marked decrease in the levels of Cdc42-GTP compared to wild-type CdGAP, suggesting an increase in GAP activity. This observation correlates with increased cell rounding observed in Hela cells expressing the same proteins. Higher levels of GAP activity could originate from aberrant localization of CdGAP in the cell owing to missing protein-protein interactions involved in its regulation. Alternatively, it could be a consequence of the alteration or absence of an intramolecular regulation as in the case of α2-chimaerin. Therefore, we assessed if the C-terminal amino-acids (1083 to 1425) of CdGAP could interact with its N-terminus (1 to 221) and found that both regions could associate. Thus, the C-terminal region absent in both ACC-TTLD-related CdGAP mutant proteins can bind to a region of CdGAP containing its GAP domain and the PBR. Consequently, the C-terminal region of CdGAP could have one of two functions. As for the C1 domain of α2-chimaerin, it could either prevent direct binding of the GTPases to the GAP domain, or thwart the GAP domain from gaining access to the membrane by masking the charges of the polybasic cluster of residues.

Although gain-of-function CdGAP mutations have been associated with the ACC-TTLD syndrome, we can only put forward a hypothetical physiological model to explain how they contribute to these phenotypes. As we have shown,

the tissue expression of CdGAP mRNA during mouse development is partially limited to the limb buds and cranium. Therefore, the sites of CdGAP gene expression correlate with the specific developmental defects that define ACC-TTLD. However, it is yet difficult to determine if the protein expression profile of CdGAP follows the same trend and how the local overexpression of an abberant GAP activity towards Cdc42 and Rac1 would both affect the normal development of scalp and digit tissues. Abberant regulation of Cdc42 and Rac1 could affect directed cell migration [401]. Indeed, cell migration experiments performed with isolated adult primary dermal fibroblasts from an ACC-TTLD patient showed an increase in the migration rate of these cells compared to the ones of a non-ACC-TTLD individual. However, given that the cells used in these experiments came from two individuals with different genetic backgrounds, it is hard to confirm that the observations made are strictly linked to the CdGAP mutations. Moreover, it is impossible to judge the expression levels of CdGAP proteins in these cells compared to the embryonic cells which were shown to express high levels of CdGAP at some point during development.

Therefore, future studies on this syndrome will need to address with more precision how the abberant activity of CdGAP directly affects normal development of the scalp and the limbs, but also refine the mechanism by which the C-terminus domain of CdGAP prevents activation of the GAP domain.

5.6 CdGAP knockout mouse generation

Considering the early mRNA expression of CdGAP at embryonic day 9.5 in mice, generation of a CdGAP knockout mouse should provide valuable information regarding its role during development and eventually to a better understanding of its cellular functions. During the preparation of this thesis, we

designed and built a targeting vector in order to produce a conditional knock-out mouse. We expect the birth of the first null-CdGAP mouse for Fall 2010 / Winter 2011. This approach should provide insightful information regarding the implication of CdGAP during development and offer an explanation as to why this gene has been conserved in so many species.

5.7 Conclusion

This thesis has provided a concrete understanding of how different domains of CdGAP are involved in its function and regulation. By using a combination of biochemistry, cell biology and molecular biology techniques, we have demonstrated how specific lipids can influence CdGAP and refined our understanding of the molecular interactions involved in its association with its regulator Intersectin. Moreover, we contributed to understand how point mutations in the human CdGAP gene are associated with the occurrence of a rare autosomal dominant syndrome in humans.

Ultimately, the knowledge provided by this thesis will increase our understanding of how the activity of RhoGAPs can be modulated. These negative regulators of Rho GTPases cooperate with GEFs to fine-tune these molecular switches and control the activity of multiple GTPase pools with distinct functions in time and space. By performing this task, they control different cellular functions ranging from cell migration, neurite outgrowth and cell adhesion. Therefore, they represent premium medical targets for researchers looking to limit cancer progression or to regenerate axon growth of neurons. This is precisely true when considering that the number of GEFs and GAPs greatly exceeds that of RhoGTPases, potentially providing more specific pharmacological targets. To reach this goal, scientists will need to expand the knowledge on GEFs and GAPs, learn how they are regulated in time and space and even more importantly, address the question of specificity between Rho GTPases and their regulators.

References

1. Mojzsis, S.J., et al., *Evidence for life on Earth before 3,800 million years ago.* Nature, 1996. **384**(6604): p. 55-9.

2. Schrödinger, E., *What is life and other scientific essays*. 1956, Garden City, N.Y.: Doubleday. 263 pages.

3. Nishimura, T., et al., *Role of numb in dendritic spine development with a Cdc42 GEF intersectin and EphB2.* Mol Biol Cell, 2006. **17**(3): p. 1273-85.

4. Harvey, J.J., *An Unidentified Virus Which Causes the Rapid Production of Tumours in Mice.* Nature, 1964. **204**: p. 1104-5.

5. Kirsten, W.H., K.D. Somers, and L.A. Mayer, *Multiplicity of cell response to a murine erythroblastosis virus.* Bibl Haematol, 1968. **30**: p. 64-5.

6. Kirsten, W.H. and L.A. Mayer, *Malignant lymphomas of extrathymic origin induced in rats by murine erythroblastosis virus.* J Natl Cancer Inst, 1969. **43**(3): p. 735-46.

7. Scolnick, E.M. and W.P. Parks, *Harvey sarcoma virus: a second murine type C sarcoma virus with rat genetic information.* J Virol, 1974. **13**(6): p. 1211-9.

8. Chien, U.H., et al., *Heteroduplex analysis of the sequence relationships between the genomes of Kirsten and Harvey sarcoma viruses, their respective parental murine leukemia viruses, and the rat endogenous 30S RNA.* J Virol, 1979. **31**(3): p. 752-60.

9. Shih, T.Y., et al., *Comparison of the genomic organization of Kirsten and Harvey sarcoma viruses.* J Virol, 1978. **27**(1): p. 45-55.

10. Shih, T.Y., et al., *Physical map of the Kirsten sarcoma virus genome as determined by fingerprinting RNase T1-resistant oligonucleotides.* J Virol, 1978. **25**(1): p. 238-52.

11. Coffin, J.M., et al., *Proposal for naming host cell-derived inserts in retrovirus genomes.* J Virol, 1981. **40**(3): p. 953-7.

12. Barbacid, M., *ras genes.* Annu Rev Biochem, 1987. **56**: p. 779-827.

13. Perucho, M., et al., *Human-tumor-derived cell lines contain common and different transforming genes.* Cell, 1981. **27**(3 Pt 2): p. 467-76.

14. Krontiris, T.G. and G.M. Cooper, *Transforming activity of human tumor DNAs.* Proc Natl Acad Sci U S A, 1981. **78**(2): p. 1181-4.

15. Shih, C., et al., *Transforming genes of carcinomas and neuroblastomas introduced into mouse fibroblasts.* Nature, 1981. **290**(5803): p. 261-4.

16. Willingham, M.C., et al., *Localization of the src gene product of the Harvey strain of MSV to plasma membrane of transformed cells by electron microscopic immunocytochemistry.* Cell, 1980. **19**(4): p. 1005-14.

17. Shih, T.Y., et al., *Guanine nucleotide-binding and autophosphorylating activities associated with the p21src protein of Harvey murine sarcoma virus.* Nature, 1980. **287**(5784): p. 686-91.

18. Scolnick, E.M., A.G. Papageorge, and T.Y. Shih, *Guanine nucleotide-binding activity as an assay for src protein of rat-derived murine sarcoma viruses.* Proc Natl Acad Sci U S A, 1979. **76**(10): p. 5355-9.

19. Temeles, G.L., et al., *Yeast and mammalian ras proteins have conserved biochemical properties.* Nature, 1985. **313**(6004): p. 700-3.

20. Sweet, R.W., et al., *The product of ras is a GTPase and the T24 oncogenic mutant is deficient in this activity.* Nature, 1984. **311**(5983): p. 273-5.

21. Hurley, J.B., et al., *Homologies between signal transducing G proteins and ras gene products.* Science, 1984. **226**(4676): p. 860-2.

22. West, M., H.F. Kung, and T. Kamata, *A novel membrane factor stimulates guanine nucleotide exchange reaction of ras proteins.* FEBS Lett, 1990. **259**(2): p. 245-8.

23. Trahey, M. and F. McCormick, *A cytoplasmic protein stimulates normal N-ras p21 GTPase, but does not affect oncogenic mutants.* Science, 1987. **238**(4826): p. 542-5.

24. Crechet, J.B., et al., *Enhancement of the GDP-GTP exchange of RAS proteins by the carboxyl-terminal domain of SCD25.* Science, 1990. **248**(4957): p. 866-8.

25. Wolfman, A. and I.G. Macara, *A cytosolic protein catalyzes the release of GDP from p21ras.* Science, 1990. **248**(4951): p. 67-9.

26. Lander, E.S., et al., *Initial sequencing and analysis of the human genome.* Nature, 2001. **409**(6822): p. 860-921.

27. Venter, J.C., et al., *The sequence of the human genome.* Science, 2001. **291**(5507): p. 1304-51.

28. Colicelli, J., *Human RAS superfamily proteins and related GTPases.* Sci STKE, 2004. **2004**(250): p. RE13.

29. Milburn, M.V., et al., *Molecular switch for signal transduction: structural differences between active and inactive forms of protooncogenic ras proteins.* Science, 1990. **247**(4945): p. 939-45.

30. Dvorsky, R. and M.R. Ahmadian, *Always look on the bright site of Rho: structural implications for a conserved intermolecular interface.* EMBO Rep, 2004. **5**(12): p. 1130-6.

31. Fivaz, M. and T. Meyer, *Specific localization and timing in neuronal signal transduction mediated by protein-lipid interactions.* Neuron, 2003. **40**(2): p. 319-30.

32. Hoffman, G.R., N. Nassar, and R.A. Cerione, *Structure of the Rho family GTP-binding protein Cdc42 in complex with the multifunctional regulator RhoGDI.* Cell, 2000. **100**(3): p. 345-56.

33. Moores, S.L., et al., *Sequence dependence of protein isoprenylation.* J Biol Chem, 1991. **266**(22): p. 14603-10.

34. Shimizu, K., et al., *Three human transforming genes are related to the viral ras oncogenes.* Proc Natl Acad Sci U S A, 1983. **80**(8): p. 2112-6.

35. Reedquist, K.A., et al., *The small GTPase, Rap1, mediates CD31-induced integrin adhesion.* J Cell Biol, 2000. **148**(6): p. 1151-8.

36. Raaijmakers, J.H. and J.L. Bos, *Specificity in Ras and Rap signaling.* J Biol Chem, 2009. **284**(17): p. 10995-9.

37. Jin, R., J. R. Junutula, et al., Exo84 and Sec5 are competitive regulatory Sec6/8 effectors to the RalA GTPase. Embo J, 2005. **24**(12): p. 2064-74.

38. Moskalenko, S., et al., *Ral GTPases regulate exocyst assembly through dual subunit interactions.* J Biol Chem, 2003. **278**(51): p. 51743-8.

39. Moskalenko, S., et al., *The exocyst is a Ral effector complex.* Nat Cell Biol, 2002. **4**(1): p. 66-72.

40. Zhang, Y., et al., *Rheb is a direct target of the tuberous sclerosis tumour suppressor proteins.* Nat Cell Biol, 2003. **5**(6): p. 578-81.

41. Inoki, K., et al., *TSC2 is phosphorylated and inhibited by Akt and suppresses mTOR signalling.* Nat Cell Biol, 2002. **4**(9): p. 648-57.

42. Martin, D.E. and M.N. Hall, *The expanding TOR signaling network.* Curr Opin Cell Biol, 2005. **17**(2): p. 158-66.

43. Touchot, N., P. Chardin, and A. Tavitian, *Four additional members of the ras gene superfamily isolated by an oligonucleotide strategy: molecular cloning of YPT-related cDNAs from a rat brain library.* Proc Natl Acad Sci U S A, 1987. **84**(23): p. 8210-4.

44. Stenmark, H., *Rab GTPases as coordinators of vesicle traffic.* Nat Rev Mol Cell Biol, 2009. **10**(8): p. 513-25.

45. Bernards, A. and J. Settleman, *GAP control: regulating the regulators of small GTPases.* Trends Cell Biol, 2004. **14**(7): p. 377-85.

46. Wennerberg, K., K.L. Rossman, and C.J. Der, *The Ras superfamily at a glance.* J Cell Sci, 2005. **118**(Pt 5): p. 843-6.

47. Moore, M.S. and G. Blobel, *The GTP-binding protein Ran/TC4 is required for protein import into the nucleus.* Nature, 1993. **365**(6447): p. 661-3.

48. Clarke, P.R. and C. Zhang, *Spatial and temporal coordination of mitosis by Ran GTPase.* Nat Rev Mol Cell Biol, 2008. **9**(6): p. 464-77.

49. Kahn, R.A. and A.G. Gilman, *Purification of a protein cofactor required for ADP-ribosylation of the stimulatory regulatory component of adenylate cyclase by cholera toxin.* J Biol Chem, 1984. **259**(10): p. 6228-34.

50. Sewell, J.L. and R.A. Kahn, *Sequences of the bovine and yeast ADP-ribosylation factor and comparison to other GTP-binding proteins.* Proc Natl Acad Sci U S A, 1988. **85**(13): p. 4620-4.

51. Antonny, B., et al., *N-terminal hydrophobic residues of the G-protein ADP-ribosylation factor-1 insert into membrane phospholipids upon GDP to GTP exchange.* Biochemistry, 1997. **36**(15): p. 4675-84.

52. Lee, M.C., et al., *Sar1p N-terminal helix initiates membrane curvature and completes the fission of a COPII vesicle.* Cell, 2005. **122**(4): p. 605-17.

53. Beck, R., et al., *Membrane curvature induced by Arf1-GTP is essential for vesicle formation.* Proc Natl Acad Sci U S A, 2008. **105**(33): p. 11731-6.

54. Gillingham, A.K. and S. Munro, *The small G proteins of the Arf family and their regulators.* Annu Rev Cell Dev Biol, 2007. **23**: p. 579-611.

55. D'Souza-Schorey, C. and P. Chavrier, *ARF proteins: roles in membrane traffic and beyond.* Nat Rev Mol Cell Biol, 2006. **7**(5): p. 347-58.

56. Matsuoka, K., et al., *COPII-coated vesicle formation reconstituted with purified coat proteins and chemically defined liposomes.* Cell, 1998. **93**(2): p. 263-75.

57. Klassen, M.P., et al., *An Arf-like small G protein, ARL-8, promotes the axonal transport of presynaptic cargoes by suppressing vesicle aggregation.* Neuron, 2010. **66**(5): p. 710-23.

58. Vega, F.M. and A.J. Ridley, *Rho GTPases in cancer cell biology.* FEBS Lett, 2008. **582**(14): p. 2093-101.

59. Heasman, S.J. and A.J. Ridley, *Mammalian Rho GTPases: new insights into their functions from in vivo studies.* Nat Rev Mol Cell Biol, 2008. **9**(9): p. 690-701.

60. Freeman, J.L., A. Abo, and J.D. Lambeth, *Rac "insert region" is a novel effector region that is implicated in the activation of NADPH oxidase, but not PAK65.* J Biol Chem, 1996. **271**(33): p. 19794-801.

61. Wu, W.J., et al., *Interaction between Cdc42Hs and RhoGDI is mediated through the Rho insert region.* J Biol Chem, 1997. **272**(42): p. 26153-8.

62. Low, B.C., K.T. Seow, and G.R. Guy, *Evidence for a novel Cdc42GAP domain at the carboxyl terminus of BNIP-2.* J Biol Chem, 2000. **275**(19): p. 14415-22.

63. Valencia, A., et al., *The ras protein family: evolutionary tree and role of conserved amino acids.* Biochemistry, 1991. **30**(19): p. 4637-48.

64. Nobes, C.D. and A. Hall, *Rho, rac, and cdc42 GTPases regulate the assembly of multimolecular focal complexes associated with actin stress fibers, lamellipodia, and filopodia.* Cell, 1995. **81**(1): p. 53-62.

65. Heo, W.D., et al., *PI(3,4,5)P3 and PI(4,5)P2 lipids target proteins with polybasic clusters to the plasma membrane.* Science, 2006. **314**(5804): p. 1458-61.

66. Michaelson, D., et al., *Postprenylation CAAX processing is required for proper localization of Ras but not Rho GTPases.* Mol Biol Cell, 2005. **16**(4): p. 1606-16.

67. Michaelson, D., et al., *Differential localization of Rho GTPases in live cells: regulation by hypervariable regions and RhoGDI binding.* J Cell Biol, 2001. **152**(1): p. 111-26.

68. Williams, C.L., *The polybasic region of Ras and Rho family small GTPases: a regulator of protein interactions and membrane association and a site of nuclear localization signal sequences.* Cell Signal, 2003. **15**(12): p. 1071-80.

69. Chardin, P., et al., *The mammalian G protein rhoC is ADP-ribosylated by Clostridium botulinum exoenzyme C3 and affects actin microfilaments in Vero cells.* Embo J, 1989. **8**(4): p. 1087-92.

70. Ridley, A.J., et al., *The small GTP-binding protein rac regulates growth factor-induced membrane ruffling.* Cell, 1992. **70**(3): p. 401-10.

71. Ridley, A.J. and A. Hall, *The small GTP-binding protein rho regulates the assembly of focal adhesions and actin stress fibers in response to growth factors.* Cell, 1992. **70**(3): p. 389-99.

72. Madaule, P. and R. Axel, *A novel ras-related gene family.* Cell, 1985. **41**(1): p. 31-40.

73. Madaule, P., R. Axel, and A.M. Myers, *Characterization of two members of the rho gene family from the yeast Saccharomyces cerevisiae.* Proc Natl Acad Sci U S A, 1987. **84**(3): p. 779-83.

74. Mayer, B.J., *SH3 domains: complexity in moderation.* J Cell Sci, 2001. **114**(Pt 7): p. 1253-63.

75. Primeau, M. and N. Lamarche-Vane, *[A brief overview of the small Rho GTPases].* Med Sci (Paris), 2008. **24**(2): p. 157-62.

76. Yeramian, P., et al., *Nucleotide sequence of human rho cDNA clone 12.* Nucleic Acids Res, 1987. **15**(4): p. 1869.

77. Chardin, P., P. Madaule, and A. Tavitian, *Coding sequence of human rho cDNAs clone 6 and clone 9.* Nucleic Acids Res, 1988. **16**(6): p. 2717.

78. Aktories, K., et al., *The rho gene product expressed in E. coli is a substrate of botulinum ADP-ribosyltransferase C3.* Biochem Biophys Res Commun, 1989. **158**(1): p. 209-13.

79. Sekine, A., M. Fujiwara, and S. Narumiya, *Asparagine residue in the rho gene product is the modification site for botulinum ADP-ribosyltransferase.* J Biol Chem, 1989. **264**(15): p. 8602-5.

80. Paterson, H.F., et al., *Microinjection of recombinant p21rho induces rapid changes in cell morphology.* J Cell Biol, 1990. **111**(3): p. 1001-7.

81. Wheeler, A.P. and A.J. Ridley, *Why three Rho proteins? RhoA, RhoB, RhoC, and cell motility.* Exp Cell Res, 2004. **301**(1): p. 43-9.

82. Armstrong, S.A., et al., *CAAX geranylgeranyl transferase transfers farnesyl as efficiently as geranylgeranyl to RhoB.* J Biol Chem, 1995. **270**(14): p. 7864-8.

83. Adamson, P., et al., *Post-translational modifications of p21rho proteins.* J Biol Chem, 1992. **267**(28): p. 20033-8.

84. Adamson, P., H.F. Paterson, and A. Hall, *Intracellular localization of the P21rho proteins.* J Cell Biol, 1992. **119**(3): p. 617-27.

85. Abraham, M.T., et al., *Motility-related proteins as markers for head and neck squamous cell cancer.* Laryngoscope, 2001. **111**(7): p. 1285-9.

86. Gomez del Pulgar, T., et al., *Rho GTPase expression in tumourigenesis: evidence for a significant link.* Bioessays, 2005. **27**(6): p. 602-13.

87. Adnane, J., et al., *Suppression of rho B expression in invasive carcinoma from head and neck cancer patients.* Clin Cancer Res, 2002. **8**(7): p. 2225-32.

88. Liu, A.X., et al., *RhoB is dispensable for mouse development, but it modifies susceptibility to tumor formation as well as cell adhesion and growth factor signaling in transformed cells.* Mol Cell Biol, 2001. **21**(20): p. 6906-12.

89. Sandilands, E., et al., *RhoB and actin polymerization coordinate Src activation with endosome-mediated delivery to the membrane.* Dev Cell, 2004. **7**(6): p. 855-69.

90. Wallar, B.J., et al., *RhoB and the mammalian Diaphanous-related formin mDia2 in endosome trafficking.* Exp Cell Res, 2007. **313**(3): p. 560-71.

91. Friedl, P. and K. Wolf, *Tumour-cell invasion and migration: diversity and escape mechanisms.* Nat Rev Cancer, 2003. **3**(5): p. 362-74.

92. Kardash, E., et al., *A role for Rho GTPases and cell-cell adhesion in single-cell motility in vivo.* Nat Cell Biol, 2010. **12**(1): p. 47-53; sup pp 1-11.

93. Maekawa, M., et al., *Signaling from Rho to the actin cytoskeleton through protein kinases ROCK and LIM-kinase.* Science, 1999. **285**(5429): p. 895-8.

94. Alberts, A.S., et al., *Analysis of RhoA-binding proteins reveals an interaction domain conserved in heterotrimeric G protein beta subunits and the yeast response regulator protein Skn7.* J Biol Chem, 1998. **273**(15): p. 8616-22.

95. Nakano, K., et al., *Distinct actions and cooperative roles of ROCK and mDia in Rho small G protein-induced reorganization of the actin cytoskeleton in Madin-Darby canine kidney cells.* Mol Biol Cell, 1999. **10**(8): p. 2481-91.

96. Coleman, M.L., et al., *Membrane blebbing during apoptosis results from caspase-mediated activation of ROCK I.* Nat Cell Biol, 2001. **3**(4): p. 339-45.

97. Li, F. and H.N. Higgs, *The mouse Formin mDia1 is a potent actin nucleation factor regulated by autoinhibition.* Curr Biol, 2003. **13**(15): p. 1335-40.

98. Chrzanowska-Wodnicka, M. and K. Burridge, *Rho-stimulated contractility drives the formation of stress fibers and focal adhesions.* J Cell Biol, 1996. **133**(6): p. 1403-15.

99. Hotchin, N.A. and A. Hall, *The assembly of integrin adhesion complexes requires both extracellular matrix and intracellular rho/rac GTPases.* J Cell Biol, 1995. **131**(6 Pt 2): p. 1857-65.

100. Aijaz, S., et al., *Binding of GEF-H1 to the tight junction-associated adaptor cingulin results in inhibition of Rho signaling and G1/S phase transition.* Dev Cell, 2005. **8**(5): p. 777-86.

101. Terry, S., et al., *Rho signaling and tight junction functions.* Physiology (Bethesda), 2010. **25**(1): p. 16-26.

102. Olson, M.F., H.F. Paterson, and C.J. Marshall, *Signals from Ras and Rho GTPases interact to regulate expression of p21Waf1/Cip1.* Nature, 1998. **394**(6690): p. 295-9.

103. Croft, D.R. and M.F. Olson, *The Rho GTPase effector ROCK regulates cyclin A, cyclin D1, and p27Kip1 levels by distinct mechanisms.* Mol Cell Biol, 2006. **26**(12): p. 4612-27.

104. Sugihara, K., et al., *Rac1 is required for the formation of three germ layers during gastrulation.* Oncogene, 1998. **17**(26): p. 3427-33.

105. Jordan, P., et al., *Cloning of a novel human Rac1b splice variant with increased expression in colorectal tumors.* Oncogene, 1999. **18**(48): p. 6835-9.

106. Singh, A., et al., *Rac1b, a tumor associated, constitutively active Rac1 splice variant, promotes cellular transformation.* Oncogene, 2004. **23**(58): p. 9369-80.

107. Matos, P., J.G. Collard, and P. Jordan, *Tumor-related alternatively spliced Rac1b is not regulated by Rho-GDP dissociation inhibitors and exhibits selective downstream signaling.* J Biol Chem, 2003. **278**(50): p. 50442-8.

108. Hwang, S.L., et al., *Rac1 gene mutations in human brain tumours.* Eur J Surg Oncol, 2004. **30**(1): p. 68-72.

109. Mira, J.P., et al., *Endogenous, hyperactive Rac3 controls proliferation of breast cancer cells by a p21-activated kinase-dependent pathway.* Proc Natl Acad Sci U S A, 2000. **97**(1): p. 185-9.

110. Roberts, A.W., et al., *Deficiency of the hematopoietic cell-specific Rho family GTPase Rac2 is characterized by abnormalities in neutrophil function and host defense.* Immunity, 1999. **10**(2): p. 183-96.

111. Miki, H., S. Suetsugu, and T. Takenawa, *WAVE, a novel WASP-family protein involved in actin reorganization induced by Rac.* Embo J, 1998. **17**(23): p. 6932-41.

112. Steffen, A., et al., *Sra-1 and Nap1 link Rac to actin assembly driving lamellipodia formation.* Embo J, 2004. **23**(4): p. 749-59.

113. Lebensohn, A.M. and M.W. Kirschner, *Activation of the WAVE complex by coincident signals controls actin assembly.* Mol Cell, 2009. **36**(3): p. 512-24.

114. Arcaro, A., *The small GTP-binding protein Rac promotes the dissociation of gelsolin from actin filaments in neutrophils.* J Biol Chem, 1998. **273**(2): p. 805-13.

115. Wennerberg, K. and C.J. Der, *Rho-family GTPases: it's not only Rac and Rho (and I like it).* J Cell Sci, 2004. **117**(Pt 8): p. 1301-12.

116. Kumar, R., A.E. Gururaj, and C.J. Barnes, *p21-activated kinases in cancer.* Nat Rev Cancer, 2006. **6**(6): p. 459-71.

117. Bagrodia, S., et al., *Identification of a mouse p21Cdc42/Rac activated kinase.* J Biol Chem, 1995. **270**(39): p. 22731-7.

118. Yang, N., et al., *Cofilin phosphorylation by LIM-kinase 1 and its role in Rac-mediated actin reorganization.* Nature, 1998. **393**(6687): p. 809-12.

119. Lamarche, N., et al., *Rac and Cdc42 induce actin polymerization and G1 cell cycle progression independently of p65PAK and the JNK/SAPK MAP kinase cascade.* Cell, 1996. **87**(3): p. 519-29.

120. Westwick, J.K., et al., *Rac regulation of transformation, gene expression, and actin organization by multiple, PAK-independent pathways.* Mol Cell Biol, 1997. **17**(3): p. 1324-35.

121. Joneson, T., et al., *RAC regulation of actin polymerization and proliferation by a pathway distinct from Jun kinase.* Science, 1996. **274**(5291): p. 1374-6.

122. Sanders, L.C., et al., *Inhibition of myosin light chain kinase by p21-activated kinase.* Science, 1999. **283**(5410): p. 2083-5.

123. Vadlamudi, R.K., et al., *Filamin is essential in actin cytoskeletal assembly mediated by p21-activated kinase 1.* Nat Cell Biol, 2002. **4**(9): p. 681-90.

124. Vadlamudi, R.K., et al., *p41-Arc subunit of human Arp2/3 complex is a p21-activated kinase-1-interacting substrate.* EMBO Rep, 2004. **5**(2): p. 154-60.

125. Knaus, U.G., et al., *Structural requirements for PAK activation by Rac GTPases.* J Biol Chem, 1998. **273**(34): p. 21512-8.

126. Haataja, L., J. Groffen, and N. Heisterkamp, *Characterization of RAC3, a novel member of the Rho family.* J Biol Chem, 1997. **272**(33): p. 20384-8.

127. Hajdo-Milasinovic, A., et al., *Rac1 and Rac3 have opposing functions in cell adhesion and differentiation of neuronal cells.* J Cell Sci, 2007. **120**(Pt 4): p. 555-66.

128. Kreck, M.L., et al., *Membrane association of Rac is required for high activity of the respiratory burst oxidase.* Biochemistry, 1996. **35**(49): p. 15683-92.

129. Del Pozo, M.A., et al., *Integrins regulate GTP-Rac localized effector interactions through dissociation of Rho-GDI.* Nat Cell Biol, 2002. **4**(3): p. 232-9.

130. Katoh, H., et al., *Small GTPase RhoG is a key regulator for neurite outgrowth in PC12 cells.* Mol Cell Biol, 2000. **20**(19): p. 7378-87.

131. Fujimoto, S., M. Negishi, and H. Katoh, *RhoG promotes neural progenitor cell proliferation in mouse cerebral cortex.* Mol Biol Cell, 2009. **20**(23): p. 4941-50.

132. Ellerbroek, S.M., et al., *SGEF, a RhoG guanine nucleotide exchange factor that stimulates macropinocytosis.* Mol Biol Cell, 2004. **15**(7): p. 3309-19.

133. Nakaya, M., et al., *Opposite effects of rho family GTPases on engulfment of apoptotic cells by macrophages.* J Biol Chem, 2006. **281**(13): p. 8836-42.

134. Katoh, H. and M. Negishi, *RhoG activates Rac1 by direct interaction with the Dock180-binding protein Elmo.* Nature, 2003. **424**(6947): p. 461-4.

135. Roppenser, B., et al., *Yersinia enterocolitica differentially modulates RhoG activity in host cells.* J Cell Sci, 2009. **122**(Pt 5): p. 696-705.

136. Patel, J.C. and J.E. Galan, *Differential activation and function of Rho GTPases during Salmonella-host cell interactions.* J Cell Biol, 2006. **175**(3): p. 453-63.

137. Hartwell, L.H., et al., *Genetic Control of the Cell Division Cycle in Yeast: V. Genetic Analysis of cdc Mutants.* Genetics, 1973. **74**(2): p. 267-86.

138. Johnson, D.I. and J.R. Pringle, *Molecular characterization of CDC42, a Saccharomyces cerevisiae gene involved in the development of cell polarity.* J Cell Biol, 1990. **111**(1): p. 143-52.

139. Drubin, D.G., *Development of cell polarity in budding yeast.* Cell, 1991. **65**(7): p. 1093-6.

140. Shinjo, K., et al., *Molecular cloning of the gene for the human placental GTP-binding protein Gp (G25K): identification of this GTP-binding protein as the human homolog of the yeast cell-division-cycle protein CDC42.* Proc Natl Acad Sci U S A, 1990. **87**(24): p. 9853-7.

141. Munemitsu, S., et al., *Molecular cloning and expression of a G25K cDNA, the human homolog of the yeast cell cycle gene CDC42.* Mol Cell Biol, 1990. **10**(11): p. 5977-82.

142. Hart, M.J., et al., *Catalysis of guanine nucleotide exchange on the CDC42Hs protein by the dbl oncogene product.* Nature, 1991. **354**(6351): p. 311-4.

143. Eva, A. and S.A. Aaronson, *Isolation of a new human oncogene from a diffuse B-cell lymphoma.* Nature, 1985. **316**(6025): p. 273-5.

144. Eva, A., et al., *The predicted DBL oncogene product defines a distinct class of transforming proteins.* Proc Natl Acad Sci U S A, 1988. **85**(7): p. 2061-5.

145. Ron, D., et al., *Molecular cloning and characterization of the human dbl proto-oncogene: evidence that its overexpression is sufficient to transform NIH/3T3 cells.* Embo J, 1988. **7**(8): p. 2465-73.

146. Lin, R., et al., *A novel Cdc42Hs mutant induces cellular transformation.* Curr Biol, 1997. **7**(10): p. 794-7.

147. Marks, P.W. and D.J. Kwiatkowski, *Genomic organization and chromosomal location of murine Cdc42.* Genomics, 1996. **38**(1): p. 13-8.

148. Kang, R., et al., *Neural palmitoyl-proteomics reveals dynamic synaptic palmitoylation.* Nature, 2008. **456**(7224): p. 904-9.

149. Wilson, A.L., et al., *Prenylation of Rab8 GTPase by type I and type II geranylgeranyl transferases.* Biochem J, 1998. **333 (Pt 3)**: p. 497-504.

150. Fu, H.W. and P.J. Casey, *Enzymology and biology of CaaX protein prenylation.* Recent Prog Horm Res, 1999. **54**: p. 315-42; discussion 342-3.

151. Vignal, E., et al., *Characterization of TCL, a new GTPase of the rho family related to TC10 andCcdc42.* J Biol Chem, 2000. **275**(46): p. 36457-64.

152. de Toledo, M., et al., *The GTP/GDP cycling of rho GTPase TCL is an essential regulator of the early endocytic pathway.* Mol Biol Cell, 2003. **14**(12): p. 4846-56.

153. Dupraz, S., et al., *The TC10-Exo70 complex is essential for membrane expansion and axonal specification in developing neurons.* J Neurosci, 2009. **29**(42): p. 13292-301.

154. Chiang, S.H., et al., *Insulin-stimulated GLUT4 translocation requires the CAP-dependent activation of TC10.* Nature, 2001. **410**(6831): p. 944-8.

155. Inoue, M., et al., *The exocyst complex is required for targeting of Glut4 to the plasma membrane by insulin.* Nature, 2003. **422**(6932): p. 629-33.

156. Okada, S., et al., *CDK5-dependent phosphorylation of the Rho family GTPase TC10(alpha) regulates insulin-stimulated GLUT4 translocation.* J Biol Chem, 2008. **283**(51): p. 35455-63.

157. Tanabe, K., et al., *The small GTP-binding protein TC10 promotes nerve elongation in neuronal cells, and its expression is induced during nerve regeneration in rats.* J Neurosci, 2000. **20**(11): p. 4138-44.

158. Erschbamer, M.K., C.P. Hofstetter, and L. Olson, *RhoA, RhoB, RhoC, Rac1, Cdc42, and Tc10 mRNA levels in spinal cord, sensory ganglia, and corticospinal tract neurons and long-lasting specific changes following spinal cord injury.* J Comp Neurol, 2005. **484**(2): p. 224-33.

159. Aspenstrom, P., U. Lindberg, and A. Hall, *Two GTPases, Cdc42 and Rac, bind directly to a protein implicated in the immunodeficiency disorder Wiskott-Aldrich syndrome.* Curr Biol, 1996. **6**(1): p. 70-5.

160. Symons, M., et al., *Wiskott-Aldrich syndrome protein, a novel effector for the GTPase CDC42Hs, is implicated in actin polymerization.* Cell, 1996. **84**(5): p. 723-34.

161. Kolluri, R., et al., *Direct interaction of the Wiskott-Aldrich syndrome protein with the GTPase Cdc42.* Proc Natl Acad Sci U S A, 1996. **93**(11): p. 5615-8.

162. Derry, J.M., H.D. Ochs, and U. Francke, *Isolation of a novel gene mutated in Wiskott-Aldrich syndrome.* Cell, 1994. **78**(4): p. 635-44.

163. Blaese, R.M., et al., *The Wiskott-Aldrich syndrome. A disorder with a possible defect in antigen processing or recognition.* Lancet, 1968. **1**(7551): p. 1056-61.

164. Kenney, D., et al., *Morphological abnormalities in the lymphocytes of patients with the Wiskott-Aldrich syndrome.* Blood, 1986. **68**(6): p. 1329-32.

165. Miki, H., K. Miura, and T. Takenawa, *N-WASP, a novel actin-depolymerizing protein, regulates the cortical cytoskeletal rearrangement*

in a PIP2-dependent manner downstream of tyrosine kinases. Embo J, 1996. **15**(19): p. 5326-35.

166. Miki, H., et al., *Induction of filopodium formation by a WASP-related actin-depolymerizing protein N-WASP.* Nature, 1998. **391**(6662): p. 93-6.

167. Prehoda, K.E., et al., *Integration of multiple signals through cooperative regulation of the N-WASP-Arp2/3 complex.* Science, 2000. **290**(5492): p. 801-6.

168. Hemsath, L., et al., *An electrostatic steering mechanism of Cdc42 recognition by Wiskott-Aldrich syndrome proteins.* Mol Cell, 2005. **20**(2): p. 313-24.

169. Peng, J., et al., *Disruption of the Diaphanous-related formin Drf1 gene encoding mDia1 reveals a role for Drf3 as an effector for Cdc42.* Curr Biol, 2003. **13**(7): p. 534-45.

170. Xu, Y., et al., *Crystal structures of a Formin Homology-2 domain reveal a tethered dimer architecture.* Cell, 2004. **116**(5): p. 711-23.

171. Otomo, T., et al., *Structural basis of actin filament nucleation and processive capping by a formin homology 2 domain.* Nature, 2005. **433**(7025): p. 488-94.

172. Bagrodia, S., et al., *Cdc42 and PAK-mediated signaling leads to Jun kinase and p38 mitogen-activated protein kinase activation.* J Biol Chem, 1995. **270**(47): p. 27995-8.

173. Sachdev, P., L. Zeng, and L.H. Wang, *Distinct role of phosphatidylinositol 3-kinase and Rho family GTPases in Vav3-induced cell transformation, cell motility, and morphological changes.* J Biol Chem, 2002. **277**(20): p. 17638-48.

174. Lin, D., et al., *A mammalian PAR-3-PAR-6 complex implicated in Cdc42/Rac1 and aPKC signalling and cell polarity.* Nat Cell Biol, 2000. **2**(8): p. 540-7.

175. Joberty, G., et al., *The cell-polarity protein Par6 links Par3 and atypical protein kinase C to Cdc42.* Nat Cell Biol, 2000. **2**(8): p. 531-9.

176. Etienne-Manneville, S. and A. Hall, *Cdc42 regulates GSK-3beta and adenomatous polyposis coli to control cell polarity.* Nature, 2003. **421**(6924): p. 753-6.

177. Pegtel, D.M., et al., *The Par-Tiam1 complex controls persistent migration by stabilizing microtubule-dependent front-rear polarity.* Curr Biol, 2007. **17**(19): p. 1623-34.

178. Martin-Belmonte, F., et al., *PTEN-mediated apical segregation of phosphoinositides controls epithelial morphogenesis through Cdc42.* Cell, 2007. **128**(2): p. 383-97.

179. Gao, L., G. Joberty, and I.G. Macara, *Assembly of epithelial tight junctions is negatively regulated by Par6.* Curr Biol, 2002. **12**(3): p. 221-5.

180. Balklava, Z., et al., *Genome-wide analysis identifies a general requirement for polarity proteins in endocytic traffic.* Nat Cell Biol, 2007. **9**(9): p. 1066-73.

181. Kanzaki, M., et al., *Atypical protein kinase C (PKCzeta/lambda) is a convergent downstream target of the insulin-stimulated phosphatidylinositol 3-kinase and TC10 signaling pathways.* J Cell Biol, 2004. **164**(2): p. 279-90.

182. Tao, W., et al., *Wrch-1, a novel member of the Rho gene family that is regulated by Wnt-1.* Genes Dev, 2001. **15**(14): p. 1796-807.

183. Chenette, E.J., A. Abo, and C.J. Der, *Critical and distinct roles of amino- and carboxyl-terminal sequences in regulation of the biological activity of the Chp atypical Rho GTPase.* J Biol Chem, 2005. **280**(14): p. 13784-92.

184. Shutes, A., et al., *Atypical mechanism of regulation of the Wrch-1 Rho family small GTPase.* Curr Biol, 2004. **14**(22): p. 2052-6.

185. Berzat, A.C., et al., *Transforming activity of the Rho family GTPase, Wrch-1, a Wnt-regulated Cdc42 homolog, is dependent on a novel carboxyl-terminal palmitoylation motif.* J Biol Chem, 2005. **280**(38): p. 33055-65.

186. Ory, S., H. Brazier, and A. Blangy, *Identification of a bipartite focal adhesion localization signal in RhoU/Wrch-1, a Rho family GTPase that regulates cell adhesion and migration.* Biol Cell, 2007. **99**(12): p. 701-16.

187. Brady, D.C., et al., *The transforming Rho family GTPase Wrch-1 disrupts epithelial cell tight junctions and epithelial morphogenesis.* Mol Cell Biol, 2009. **29**(4): p. 1035-49.

188. Alan, J.K., et al., *Regulation of the Rho family small GTPase Wrch-1 by Src-mediated tyrosine phosphorylation of its C-terminal membrane targeting domain.* Mol Cell Biol, 2010.

189. Foster, R., et al., *Identification of a novel human Rho protein with unusual properties: GTPase deficiency and in vivo farnesylation.* Mol Cell Biol, 1996. **16**(6): p. 2689-99.

190. Nobes, C.D., et al., *A new member of the Rho family, Rnd1, promotes disassembly of actin filament structures and loss of cell adhesion.* J Cell Biol, 1998. **141**(1): p. 187-97.

191. Riento, K., et al., *RhoE binds to ROCK I and inhibits downstream signaling.* Mol Cell Biol, 2003. **23**(12): p. 4219-29.

192. Wennerberg, K., et al., *Rnd proteins function as RhoA antagonists by activating p190 RhoGAP.* Curr Biol, 2003. **13**(13): p. 1106-15.

193. Oinuma, I., et al., *The Semaphorin 4D receptor Plexin-B1 is a GTPase activating protein for R-Ras.* Science, 2004. **305**(5685): p. 862-5.

194. Boureux, A., et al., *Evolution of the Rho family of ras-like GTPases in eukaryotes.* Mol Biol Evol, 2007. **24**(1): p. 203-16.

195. Aspenstrom, P., A. Fransson, and J. Saras, *Rho GTPases have diverse effects on the organization of the actin filament system.* Biochem J, 2004. **377**(Pt 2): p. 327-37.

196. Ellis, S. and H. Mellor, *The novel Rho-family GTPase rif regulates coordinated actin-based membrane rearrangements.* Curr Biol, 2000. **10**(21): p. 1387-90.

197. Murphy, C., et al., *Endosome dynamics regulated by a Rho protein.* Nature, 1996. **384**(6608): p. 427-32.

198. Gasman, S., Y. Kalaidzidis, and M. Zerial, *RhoD regulates endosome dynamics through Diaphanous-related Formin and Src tyrosine kinase.* Nat Cell Biol, 2003. **5**(3): p. 195-204.

199. Pellegrin, S. and H. Mellor, *The Rho family GTPase Rif induces filopodia through mDia2.* Curr Biol, 2005. **15**(2): p. 129-33.

200. Rivero, F., et al., *The Dictyostelium discoideum family of Rho-related proteins.* Nucleic Acids Res, 2001. **29**(5): p. 1068-79.

201. Aspenstrom, P., A. Ruusala, and D. Pacholsky, *Taking Rho GTPases to the next level: the cellular functions of atypical Rho GTPases.* Exp Cell Res, 2007. **313**(17): p. 3673-9.

202. Wilkins, A., Q. Ping, and C.L. Carpenter, *RhoBTB2 is a substrate of the mammalian Cul3 ubiquitin ligase complex.* Genes Dev, 2004. **18**(8): p. 856-61.

203. Hamaguchi, M., et al., *DBC2, a candidate for a tumor suppressor gene involved in breast cancer.* Proc Natl Acad Sci U S A, 2002. **99**(21): p. 13647-52.

204. Beder, L.B., et al., *Identification of a candidate tumor suppressor gene RHOBTB1 located at a novel allelic loss region 10q21 in head and neck cancer.* J Cancer Res Clin Oncol, 2006. **132**(1): p. 19-27.

205. Espinosa, E.J., et al., *RhoBTB3: a Rho GTPase-family ATPase required for endosome to Golgi transport.* Cell, 2009. **137**(5): p. 938-48.

206. Li, X., et al., *The hematopoiesis-specific GTP-binding protein RhoH is GTPase deficient and modulates activities of other Rho GTPases by an inhibitory function.* Mol Cell Biol, 2002. **22**(4): p. 1158-71.

207. Dorn, T., et al., *RhoH is important for positive thymocyte selection and T-cell receptor signaling.* Blood, 2007. **109**(6): p. 2346-55.

208. Gu, Y., et al., *RhoH GTPase recruits and activates Zap70 required for T cell receptor signaling and thymocyte development.* Nat Immunol, 2006. **7**(11): p. 1182-90.

209. Bourne, H.R., D.A. Sanders, and F. McCormick, *The GTPase superfamily: a conserved switch for diverse cell functions.* Nature, 1990. **348**(6297): p. 125-32.

210. Hart, M.J., et al., *Cellular transformation and guanine nucleotide exchange activity are catalyzed by a common domain on the dbl oncogene product.* J Biol Chem, 1994. **269**(1): p. 62-5.

211. Ron, D., et al., *The N-terminal region of proto-dbl down regulates its transforming activity.* Oncogene, 1989. **4**(9): p. 1067-72.

212. Katzav, S., et al., *Loss of the amino-terminal helix-loop-helix domain of the vav proto-oncogene activates its transforming potential.* Mol Cell Biol, 1991. **11**(4): p. 1912-20.

213. van Leeuwen, F.N., et al., *Oncogenic activity of Tiam1 and Rac1 in NIH3T3 cells.* Oncogene, 1995. **11**(11): p. 2215-21.

214. Miki, T., et al., *Oncogene ect2 is related to regulators of small GTP-binding proteins.* Nature, 1993. **362**(6419): p. 462-5.

215. Chan, A.M., et al., *Isolation of a novel oncogene, NET1, from neuroepithelioma cells by expression cDNA cloning.* Oncogene, 1996. **12**(6): p. 1259-66.

216. Wells, C.D., et al., *Identification of potential mechanisms for regulation of p115 RhoGEF through analysis of endogenous and mutant forms of the exchange factor.* J Biol Chem, 2001. **276**(31): p. 28897-905.

217. Sterpetti, P., et al., *Activation of the Lbc Rho exchange factor proto-oncogene by truncation of an extended C terminus that regulates transformation and targeting.* Mol Cell Biol, 1999. **19**(2): p. 1334-45.

218. Snyder, J.T., et al., *Quantitative analysis of the effect of phosphoinositide interactions on the function of Dbl family proteins.* J Biol Chem, 2001. **276**(49): p. 45868-75.

219. Rossman, K.L., et al., *A crystallographic view of interactions between Dbs and Cdc42: PH domain-assisted guanine nucleotide exchange.* Embo J, 2002. **21**(6): p. 1315-26.

220. Ron, D., et al., *A region of proto-dbl essential for its transforming activity shows sequence similarity to a yeast cell cycle gene, CDC24, and the human breakpoint cluster gene, bcr.* New Biol, 1991. **3**(4): p. 372-9.

221. Whitehead, I., et al., *Expression cloning of lfc, a novel oncogene with structural similarities to guanine nucleotide exchange factors and to the regulatory region of protein kinase C.* J Biol Chem, 1995. **270**(31): p. 18388-95.

222. Rossman, K.L., C.J. Der, and J. Sondek, *GEF means go: turning on RHO GTPases with guanine nucleotide-exchange factors.* Nat Rev Mol Cell Biol, 2005. **6**(2): p. 167-80.

223. Pucharcos, C., et al., *The human intersectin genes and their spliced variants are differentially expressed.* Biochim Biophys Acta, 2001. **1521**(1-3): p. 1-11.

224. Portales-Casamar, E., et al., *Identification of novel neuronal isoforms of the Rho-GEF Trio.* Biol Cell, 2006. **98**(3): p. 183-93.

225. McPherson, C.E., B.A. Eipper, and R.E. Mains, *Multiple novel isoforms of Trio are expressed in the developing rat brain.* Gene, 2005. **347**(1): p. 125-35.

226. McPherson, C.E., B.A. Eipper, and R.E. Mains, *Genomic organization and differential expression of Kalirin isoforms.* Gene, 2002. **284**(1-2): p. 41-51.

227. Schmidt, A. and A. Hall, *Guanine nucleotide exchange factors for Rho GTPases: turning on the switch.* Genes Dev, 2002. **16**(13): p. 1587-609.

228. Hussain, N.K., et al., *Endocytic protein intersectin-l regulates actin assembly via Cdc42 and N-WASP.* Nat Cell Biol, 2001. **3**(10): p. 927-32.

229. Gulbins, E., et al., *Tyrosine kinase-stimulated guanine nucleotide exchange activity of Vav in T cell activation.* Science, 1993. **260**(5109): p. 822-5.

230. Katzav, S., et al., *The protein tyrosine kinase ZAP-70 can associate with the SH2 domain of proto-Vav.* J Biol Chem, 1994. **269**(51): p. 32579-85.

231. Li, P., et al., *Internal dynamics control activation and activity of the autoinhibited Vav DH domain.* Nat Struct Mol Biol, 2008. **15**(6): p. 613-8.

232. Aghazadeh, B., et al., *Structural basis for relief of autoinhibition of the Dbl homology domain of proto-oncogene Vav by tyrosine phosphorylation.* Cell, 2000. **102**(5): p. 625-33.

233. Advani, A.S. and A.M. Pendergast, *Bcr-Abl variants: biological and clinical aspects.* Leuk Res, 2002. **26**(8): p. 713-20.

234. Hadano, S., et al., *A gene encoding a putative GTPase regulator is mutated in familial amyotrophic lateral sclerosis 2.* Nat Genet, 2001. **29**(2): p. 166-73.

235. Eymard-Pierre, E., et al., *Infantile-onset ascending hereditary spastic paralysis is associated with mutations in the alsin gene.* Am J Hum Genet, 2002. **71**(3): p. 518-27.

236. Pasteris, N.G., et al., *Isolation and characterization of the faciogenital dysplasia (Aarskog-Scott syndrome) gene: a putative Rho/Rac guanine nucleotide exchange factor.* Cell, 1994. **79**(4): p. 669-78.

237. Orrico, A., et al., *Phenotypic and molecular characterisation of the Aarskog-Scott syndrome: a survey of the clinical variability in light of FGD1 mutation analysis in 46 patients.* Eur J Hum Genet, 2004. **12**(1): p. 16-23.

238. Engers, R., et al., *Tiam1 mutations in human renal-cell carcinomas.* Int J Cancer, 2000. **88**(3): p. 369-76.

239. Minard, M.E., et al., *The role of the guanine nucleotide exchange factor Tiam1 in cellular migration, invasion, adhesion and tumor progression.* Breast Cancer Res Treat, 2004. **84**(1): p. 21-32.

240. Minard, M.E., et al., *The guanine nucleotide exchange factor Tiam1 increases colon carcinoma growth at metastatic sites in an orthotopic nude mouse model.* Oncogene, 2005. **24**(15): p. 2568-73.

241. Yang, W., et al., *Up-regulation of Tiam1 and Rac1 Correlates with Poor Prognosis in Hepatocellular Carcinoma.* Jpn J Clin Oncol, 2010.

242. Engers, R., et al., *Prognostic relevance of Tiam1 protein expression in prostate carcinomas.* Br J Cancer, 2006. **95**(8): p. 1081-6.

243. Debily, M.A., et al., *Expression and molecular characterization of alternative transcripts of the ARHGEF5/TIM oncogene specific for human breast cancer.* Hum Mol Genet, 2004. **13**(3): p. 323-34.

244. Kourlas, P.J., et al., *Identification of a gene at 11q23 encoding a guanine nucleotide exchange factor: evidence for its fusion with MLL in acute myeloid leukemia.* Proc Natl Acad Sci U S A, 2000. **97**(5): p. 2145-50.

245. Gumienny, T.L., et al., *CED-12/ELMO, a novel member of the CrkII/Dock180/Rac pathway, is required for phagocytosis and cell migration.* Cell, 2001. **107**(1): p. 27-41.

246. Wu, Y.C., et al., *C. elegans CED-12 acts in the conserved crkII/DOCK180/Rac pathway to control cell migration and cell corpse engulfment.* Dev Cell, 2001. **1**(4): p. 491-502.

247. Cote, J.F. and K. Vuori, *Identification of an evolutionarily conserved superfamily of DOCK180-related proteins with guanine nucleotide exchange activity.* J Cell Sci, 2002. **115**(Pt 24): p. 4901-13.

248. Miyamoto, Y., et al., *Dock6, a Dock-C subfamily guanine nucleotide exchanger, has the dual specificity for Rac1 and Cdc42 and regulates neurite outgrowth.* Exp Cell Res, 2007. **313**(4): p. 791-804.

249. Cote, J.F., et al., *A novel and evolutionarily conserved PtdIns(3,4,5)P3-binding domain is necessary for DOCK180 signalling.* Nat Cell Biol, 2005. **7**(8): p. 797-807.

250. Fukui, Y., et al., *Haematopoietic cell-specific CDM family protein DOCK2 is essential for lymphocyte migration.* Nature, 2001. **412**(6849): p. 826-31.

251. Watabe-Uchida, M., et al., *The Rac activator DOCK7 regulates neuronal polarity through local phosphorylation of stathmin/Op18.* Neuron, 2006. **51**(6): p. 727-39.

252. Pinheiro, E.M. and F.B. Gertler, *Nervous Rac: DOCK7 regulation of axon formation.* Neuron, 2006. **51**(6): p. 674-6.

253. Dovas, A. and J.R. Couchman, *RhoGDI: multiple functions in the regulation of Rho family GTPase activities.* Biochem J, 2005. **390**(Pt 1): p. 1-9.

254. DerMardirossian, C. and G.M. Bokoch, *GDIs: central regulatory molecules in Rho GTPase activation.* Trends Cell Biol, 2005. **15**(7): p. 356-63.

255. Zalcman, G., et al., *RhoGDI-3 is a new GDP dissociation inhibitor (GDI). Identification of a non-cytosolic GDI protein interacting with the small GTP-binding proteins RhoB and RhoG.* J Biol Chem, 1996. **271**(48): p. 30366-74.

256. Adra, C.N., et al., *RhoGDIgamma: a GDP-dissociation inhibitor for Rho proteins with preferential expression in brain and pancreas.* Proc Natl Acad Sci U S A, 1997. **94**(9): p. 4279-84.

257. Brunet, N., A. Morin, and B. Olofsson, *RhoGDI-3 regulates RhoG and targets this protein to the Golgi complex through its unique N-terminal domain.* Traffic, 2002. **3**(5): p. 342-57.

258. Bourmeyster, N. and P.V. Vignais, *Phosphorylation of Rho GDI stabilizes the Rho A-Rho GDI complex in neutrophil cytosol.* Biochem Biophys Res Commun, 1996. **218**(1): p. 54-60.

259. Takahashi, K., et al., *Direct interaction of the Rho GDP dissociation inhibitor with ezrin/radixin/moesin initiates the activation of the Rho small G protein.* J Biol Chem, 1997. **272**(37): p. 23371-5.

260. Kim, O., J. Yang, and Y. Qiu, *Selective activation of small GTPase RhoA by tyrosine kinase Etk through its pleckstrin homology domain.* J Biol Chem, 2002. **277**(33): p. 30066-71.

261. Yamashita, T. and M. Tohyama, *The p75 receptor acts as a displacement factor that releases Rho from Rho-GDI.* Nat Neurosci, 2003. **6**(5): p. 461-7.

262. Fidyk, N.J. and R.A. Cerione, *Understanding the catalytic mechanism of GTPase-activating proteins: demonstration of the importance of switch domain stabilization in the stimulation of GTP hydrolysis.* Biochemistry, 2002. **41**(52): p. 15644-53.

263. Bos, J.L., H. Rehmann, and A. Wittinghofer, *GEFs and GAPs: critical elements in the control of small G proteins.* Cell, 2007. **129**(5): p. 865-77.

264. Tcherkezian, J. and N. Lamarche-Vane, *Current knowledge of the large RhoGAP family of proteins.* Biol Cell, 2007. **99**(2): p. 67-86.

265. Kandpal, R.P., *Rho GTPase activating proteins in cancer phenotypes.* Curr Protein Pept Sci, 2006. **7**(4): p. 355-65.

266. Garrett, M.D., et al., *Identification of distinct cytoplasmic targets for ras/R-ras and rho regulatory proteins.* J Biol Chem, 1989. **264**(1): p. 10-3.

267. Moskwa, P., et al., *Autoinhibition of p50 Rho GTPase-activating protein (GAP) is released by prenylated small GTPases.* J Biol Chem, 2005. **280**(8): p. 6716-20.

268. Wang, L., et al., *Genetic deletion of Cdc42GAP reveals a role of Cdc42 in erythropoiesis and hematopoietic stem/progenitor cell survival, adhesion, and engraftment.* Blood, 2006. **107**(1): p. 98-105.

269. Wang, L., et al., *Cdc42 GTPase-activating protein deficiency promotes genomic instability and premature aging-like phenotypes.* Proc Natl Acad Sci U S A, 2007. **104**(4): p. 1248-53.

270. Rivadeneira, F., et al., *Twenty bone-mineral-density loci identified by large-scale meta-analysis of genome-wide association studies.* Nat Genet, 2009. **41**(11): p. 1199-206.

271. Heckman, B.M., et al., *Crosstalk between the p190-B RhoGAP and IGF signaling pathways is required for embryonic mammary bud development.* Dev Biol, 2007. **309**(1): p. 137-49.

272. Matheson, S.F., et al., *Distinct but overlapping functions for the closely related p190 RhoGAPs in neural development.* Dev Neurosci, 2006. **28**(6): p. 538-50.

273. Brouns, M.R., S.F. Matheson, and J. Settleman, *p190 RhoGAP is the principal Src substrate in brain and regulates axon outgrowth, guidance and fasciculation.* Nat Cell Biol, 2001. **3**(4): p. 361-7.

274. Bradley, W.D., et al., *Integrin signaling through Arg activates p190RhoGAP by promoting its binding to p120RasGAP and recruitment to the membrane.* Mol Biol Cell, 2006. **17**(11): p. 4827-36.

275. Liang, X., N.A. Draghi, and M.D. Resh, *Signaling from integrins to Fyn to Rho family GTPases regulates morphologic differentiation of oligodendrocytes.* J Neurosci, 2004. **24**(32): p. 7140-9.

276. Arthur, W.T., L.A. Petch, and K. Burridge, *Integrin engagement suppresses RhoA activity via a c-Src-dependent mechanism.* Curr Biol, 2000. **10**(12): p. 719-22.

277. Brouns, M.R., et al., *The adhesion signaling molecule p190 RhoGAP is required for morphogenetic processes in neural development.* Development, 2000. **127**(22): p. 4891-903.

278. Billuart, P., et al., *Regulating axon branch stability: the role of p190 RhoGAP in repressing a retraction signaling pathway.* Cell, 2001. **107**(2): p. 195-207.

279. Sordella, R., et al., *Modulation of Rho GTPase signaling regulates a switch between adipogenesis and myogenesis.* Cell, 2003. **113**(2): p. 147-58.

280. Sordella, R., et al., *Modulation of CREB activity by the Rho GTPase regulates cell and organism size during mouse embryonic development.* Dev Cell, 2002. **2**(5): p. 553-65.

281. Jiang, W., et al., *p190A RhoGAP is a glycogen synthase kinase-3-beta substrate required for polarized cell migration.* J Biol Chem, 2008. **283**(30): p. 20978-88.

282. Chang, J.H., et al., *c-Src regulates the simultaneous rearrangement of actin cytoskeleton, p190RhoGAP, and p120RasGAP following epidermal growth factor stimulation.* J Cell Biol, 1995. **130**(2): p. 355-68.

283. Ligeti, E., et al., *Phospholipids can switch the GTPase substrate preference of a GTPase-activating protein.* J Biol Chem, 2004. **279**(7): p. 5055-8.

284. Levay, M., J. Settleman, and E. Ligeti, *Regulation of the substrate preference of p190RhoGAP by protein kinase C-mediated phosphorylation of a phospholipid binding site.* Biochemistry, 2009. **48**(36): p. 8615-23.

285. Leung, T., et al., *Cerebellar beta 2-chimaerin, a GTPase-activating protein for p21 ras-related rac is specifically expressed in granule cells and has a unique N-terminal SH2 domain.* J Biol Chem, 1994. **269**(17): p. 12888-92.

286. Brown, M., et al., *Alpha2-chimaerin, cyclin-dependent Kinase 5/p35, and its target collapsin response mediator protein-2 are essential components in semaphorin 3A-induced growth-cone collapse.* J Neurosci, 2004. **24**(41): p. 8994-9004.

287. Mizuno, T., T. Yamashita, and M. Tohyama, *Chimaerins act downstream from neurotrophins in overcoming the inhibition of neurite outgrowth produced by myelin-associated glycoprotein.* J Neurochem, 2004. **91**(2): p. 395-403.

288. Iwasato, T., et al., *Rac-GAP alpha-chimerin regulates motor-circuit formation as a key mediator of EphrinB3/EphA4 forward signaling.* Cell, 2007. **130**(4): p. 742-53.

289. Wegmeyer, H., et al., *EphA4-dependent axon guidance is mediated by the RacGAP alpha2-chimaerin.* Neuron, 2007. **55**(5): p. 756-67.

290. Caloca, M.J., et al., *beta2-chimaerin is a novel target for diacylglycerol: binding properties and changes in subcellular localization mediated by ligand binding to its C1 domain.* Proc Natl Acad Sci U S A, 1999. **96**(21): p. 11854-9.

291. Canagarajah, B., et al., *Structural mechanism for lipid activation of the Rac-specific GAP, beta2-chimaerin.* Cell, 2004. **119**(3): p. 407-18.

292. Griner, E.M., et al., *A novel cross-talk in diacylglycerol signaling: the Rac-GAP beta2-chimaerin is negatively regulated by protein kinase Cdelta-mediated phosphorylation.* J Biol Chem, 2010. **285**(22): p. 16931-41.

293. Hall, C., et al., *Novel human brain cDNA encoding a 34,000 Mr protein n-chimaerin, related to both the regulatory domain of protein kinase C and BCR, the product of the breakpoint cluster region gene.* J Mol Biol, 1990. **211**(1): p. 11-6.

294. Leung, T., et al., *Germ cell beta-chimaerin, a new GTPase-activating protein for p21rac, is specifically expressed during the acrosomal assembly stage in rat testis.* J Biol Chem, 1993. **268**(6): p. 3813-6.

295. Lim, H.H., et al., *Developmental regulation and neuronal expression of the mRNA of rat n-chimaerin, a p21rac GAP:cDNA sequence.* Biochem J, 1992. **287 (Pt 2)**: p. 415-22.

296. Hall, C., et al., *alpha2-chimaerin, a Cdc42/Rac1 regulator, is selectively expressed in the rat embryonic nervous system and is involved in neuritogenesis in N1E-115 neuroblastoma cells.* J Neurosci, 2001. **21**(14): p. 5191-202.

297. Miyake, N., et al., *Human CHN1 mutations hyperactivate alpha2-chimaerin and cause Duane's retraction syndrome.* Science, 2008. **321**(5890): p. 839-43.

298. Wong, K., et al., *Signal transduction in neuronal migration: roles of GTPase activating proteins and the small GTPase Cdc42 in the Slit-Robo pathway.* Cell, 2001. **107**(2): p. 209-21.

299. Guerrier, S., et al., *The F-BAR domain of srGAP2 induces membrane protrusions required for neuronal migration and morphogenesis.* Cell, 2009. **138**(5): p. 990-1004.

300. Li, X., et al., *Structural basis of Robo proline-rich motif recognition by the srGAP1 Src homology 3 domain in the Slit-Robo signaling pathway.* J Biol Chem, 2006. **281**(38): p. 28430-7.

301. Christerson, L.B., et al., *p115 Rho GTPase activating protein interacts with MEKK1.* J Cell Physiol, 2002. **192**(2): p. 200-8.

302. Vogt, D.L., et al., *ARHGAP4 is a novel RhoGAP that mediates inhibition of cell motility and axon outgrowth.* Mol Cell Neurosci, 2007. **36**(3): p. 332-42.

303. Zimmerberg, J. and S. McLaughlin, *Membrane curvature: how BAR domains bend bilayers.* Curr Biol, 2004. **14**(6): p. R250-2.

304. Wells, C.D., et al., *A Rich1/Amot complex regulates the Cdc42 GTPase and apical-polarity proteins in epithelial cells.* Cell, 2006. **125**(3): p. 535-48.

305. Gallop, J.L., et al., *Mechanism of endophilin N-BAR domain-mediated membrane curvature.* Embo J, 2006. **25**(12): p. 2898-910.

306. Govek, E.E., et al., *The X-linked mental retardation protein oligophrenin-1 is required for dendritic spine morphogenesis.* Nat Neurosci, 2004. **7**(4): p. 364-72.

307. Billuart, P., et al., *Oligophrenin-1 encodes a rhoGAP protein involved in X-linked mental retardation.* Nature, 1998. **392**(6679): p. 923-6.

308. Philip, N., et al., *Mutations in the oligophrenin-1 gene (OPHN1) cause X linked congenital cerebellar hypoplasia.* J Med Genet, 2003. **40**(6): p. 441-6.

309. Bergmann, C., et al., *Oligophrenin 1 (OPHN1) gene mutation causes syndromic X-linked mental retardation with epilepsy, rostral ventricular enlargement and cerebellar hypoplasia.* Brain, 2003. **126**(Pt 7): p. 1537-44.

310. Zanni, G., et al., *Oligophrenin 1 mutations frequently cause X-linked mental retardation with cerebellar hypoplasia.* Neurology, 2005. **65**(9): p. 1364-9.

311. Khelfaoui, M., et al., *Loss of X-linked mental retardation gene oligophrenin1 in mice impairs spatial memory and leads to ventricular enlargement and dendritic spine immaturity.* J Neurosci, 2007. **27**(35): p. 9439-50.

312. Nadif Kasri, N., et al., *The Rho-linked mental retardation protein oligophrenin-1 controls synapse maturation and plasticity by stabilizing AMPA receptors.* Genes Dev, 2009. **23**(11): p. 1289-302.

313. Nakano-Kobayashi, A., et al., *The Rho-linked mental retardation protein OPHN1 controls synaptic vesicle endocytosis via endophilin A1.* Curr Biol, 2009. **19**(13): p. 1133-9.

314. Eberth, A., et al., *A BAR domain-mediated autoinhibitory mechanism for RhoGAPs of the GRAF family.* Biochem J, 2009. **417**(1): p. 371-7.

315. Fauchereau, F., et al., *The RhoGAP activity of OPHN1, a new F-actin-binding protein, is negatively controlled by its amino-terminal domain.* Mol Cell Neurosci, 2003. **23**(4): p. 574-86.

316. Lundmark, R., et al., *The GTPase-activating protein GRAF1 regulates the CLIC/GEEC endocytic pathway.* Curr Biol, 2008. **18**(22): p. 1802-8.

317. Dubois, T., et al., *Golgi-localized GAP for Cdc42 functions downstream of ARF1 to control Arp2/3 complex and F-actin dynamics.* Nat Cell Biol, 2005. **7**(4): p. 353-64.

318. Miura, K., et al., *ARAP1: a point of convergence for Arf and Rho signaling.* Mol Cell, 2002. **9**(1): p. 109-19.

319. Krugmann, S., et al., *Identification of ARAP3, a novel PI3K effector regulating both Arf and Rho GTPases, by selective capture on phosphoinositide affinity matrices.* Mol Cell, 2002. **9**(1): p. 95-108.

320. Yoon, H.Y., et al., *ARAP2 effects on the actin cytoskeleton are dependent on Arf6-specific GTPase-activating-protein activity and binding to RhoA-GTP.* J Cell Sci, 2006. **119**(Pt 22): p. 4650-66.

321. Yuan, B.Z., et al., *Cloning, characterization, and chromosomal localization of a gene frequently deleted in human liver cancer (DLC-1) homologous to rat RhoGAP.* Cancer Res, 1998. **58**(10): p. 2196-9.

322. Liao, Y.C. and S.H. Lo, *Deleted in liver cancer-1 (DLC-1): a tumor suppressor not just for liver.* Int J Biochem Cell Biol, 2008. **40**(5): p. 843-7.

323. Durkin, M.E., et al., *DLC-1, a Rho GTPase-activating protein with tumor suppressor function, is essential for embryonic development.* FEBS Lett, 2005. **579**(5): p. 1191-6.

324. Erlmann, P., et al., *DLC1 activation requires lipid interaction through a polybasic region preceding the RhoGAP domain.* Mol Biol Cell, 2009. **20**(20): p. 4400-11.

325. Homma, Y. and Y. Emori, *A dual functional signal mediator showing RhoGAP and phospholipase C-delta stimulating activities.* Embo J, 1995. **14**(2): p. 286-91.

326. Hirose, K., et al., *MgcRacGAP is involved in cytokinesis through associating with mitotic spindle and midbody.* J Biol Chem, 2001. **276**(8): p. 5821-8.

327. Minoshima, Y., et al., *Phosphorylation by aurora B converts MgcRacGAP to a RhoGAP during cytokinesis.* Dev Cell, 2003. **4**(4): p. 549-60.

328. Wolfe, B.A., et al., *Polo-like kinase 1 directs assembly of the HsCyk-4 RhoGAP/Ect2 RhoGEF complex to initiate cleavage furrow formation.* PLoS Biol, 2009. **7**(5): p. e1000110.

329. Seguin, L., et al., *CUX1 and E2F1 regulate coordinated expression of the mitotic complex genes Ect2, MgcRacGAP, and MKLP1 in S phase.* Mol Cell Biol, 2009. **29**(2): p. 570-81.

330. Miller, A.L. and W.M. Bement, *Regulation of cytokinesis by Rho GTPase flux.* Nat Cell Biol, 2009. **11**(1): p. 71-7.

331. O'Connell, C.B. and M.S. Mooseker, *Native Myosin-IXb is a plus-, not a minus-end-directed motor.* Nat Cell Biol, 2003. **5**(2): p. 171-2.

332. Abouhamed, M., et al., *Myosin IXa regulates epithelial differentiation and its deficiency results in hydrocephalus.* Mol Biol Cell, 2009. **20**(24): p. 5074-85.

333. Monsuur, A.J., et al., *Myosin IXB variant increases the risk of celiac disease and points toward a primary intestinal barrier defect.* Nat Genet, 2005. **37**(12): p. 1341-4.

334. Ohta, Y., J.H. Hartwig, and T.P. Stossel, *FilGAP, a Rho- and ROCK-regulated GAP for Rac binds filamin A to control actin remodelling.* Nat Cell Biol, 2006. **8**(8): p. 803-14.

335. Nakamura, F., et al., *Molecular basis of filamin A-FilGAP interaction and its impairment in congenital disorders associated with filamin A mutations.* PLoS One, 2009. **4**(3): p. e4928.

336. Sagnier, T., et al., *Dynamic expression of d-CdGAPr, a novel Drosophila melanogaster gene encoding a GTPase activating protein.* Mech Dev, 2000. **94**(1-2): p. 267-70.

337. Murakami, S., et al., *Focal adhesion kinase controls morphogenesis of the Drosophila optic stalk.* Development, 2007. **134**(8): p. 1539-48.

338. Lamarche-Vane, N. and A. Hall, *CdGAP, a novel proline-rich GTPase-activating protein for Cdc42 and Rac.* J Biol Chem, 1998. **273**(44): p. 29172-7.

339. Kaneko, T., L. Li, and S.S. Li, *The SH3 domain--a family of versatile peptide- and protein-recognition module.* Front Biosci, 2008. **13**: p. 4938-52.

340. Radivojac, P., et al., *Intrinsic disorder and functional proteomics.* Biophys J, 2007. **92**(5): p. 1439-56.

341. Schumacher, C., et al., *The SH3 domain of Crk binds specifically to a conserved proline-rich motif in Eps15 and Eps15R.* J Biol Chem, 1995. **270**(25): p. 15341-7.

342. Tcherkezian, J., et al., *Extracellular signal-regulated kinase 1 interacts with and phosphorylates CdGAP at an important regulatory site.* Mol Cell Biol, 2005. **25**(15): p. 6314-29.

343. Tcherkezian, J., et al., *The human orthologue of CdGAP is a phosphoprotein and a GTPase-activating protein for Cdc42 and Rac1 but not RhoA.* Biol Cell, 2006. **98**(8): p. 445-56.

344. Itoh, R.E., et al., *Activation of rac and cdc42 video imaged by fluorescent resonance energy transfer-based single-molecule probes in the membrane of living cells.* Mol Cell Biol, 2002. **22**(18): p. 6582-91.

345. Kurokawa, K., et al., *Coactivation of Rac1 and Cdc42 at lamellipodia and membrane ruffles induced by epidermal growth factor.* Mol Biol Cell, 2004. **15**(3): p. 1003-10.

346. LaLonde, D.P., et al., *CdGAP associates with actopaxin to regulate integrin-dependent changes in cell morphology and motility.* Curr Biol, 2006. **16**(14): p. 1375-85.

347. Jenna, S., et al., *The activity of the GTPase-activating protein CdGAP is regulated by the endocytic protein intersectin.* J Biol Chem, 2002. **277**(8): p. 6366-73.

348. He, Y., et al., *CdGAP is required for Transforming Growth Factor-β and Neu/Erb-2-induced breast cancer cell motility and invasion.* submitted, 2010.

349. Danek, E.I., et al., *Glycogen synthase kinase-3 phosphorylates CdGAP at a consensus ERK 1 regulatory site.* J Biol Chem, 2007. **282**(6): p. 3624-31.

350. Chiang, S.H., et al., *TCGAP, a multidomain Rho GTPase-activating protein involved in insulin-stimulated glucose transport.* Embo J, 2003. **22**(11): p. 2679-91.

351. Rosario, M., et al., *The neurite outgrowth multiadaptor RhoGAP, NOMA-GAP, regulates neurite extension through SHP2 and Cdc42.* J Cell Biol, 2007. **178**(3): p. 503-16.

352. Liu, H., et al., *Physical and functional interaction of Fyn tyrosine kinase with a brain-enriched Rho GTPase-activating protein TCGAP.* J Biol Chem, 2006. **281**(33): p. 23611-9.

353. Hayashi, T., et al., *PX-RICS, a novel splicing variant of RICS, is a main isoform expressed during neural development.* Genes Cells, 2007. **12**(8): p. 929-39.

354. Nakamura, T., et al., *PX-RICS mediates ER-to-Golgi transport of the N-cadherin/beta-catenin complex.* Genes Dev, 2008. **22**(9): p. 1244-56.

355. Pertz, O.C., et al., *Spatial mapping of the neurite and soma proteomes reveals a functional Cdc42/Rac regulatory network.* Proc Natl Acad Sci U S A, 2008. **105**(6): p. 1931-6.

356. Papayannopoulos, V., et al., *A polybasic motif allows N-WASP to act as a sensor of PIP(2) density.* Mol Cell, 2005. **17**(2): p. 181-91.

357. Bigay, J., et al., *ArfGAP1 responds to membrane curvature through the folding of a lipid packing sensor motif.* Embo J, 2005. **24**(13): p. 2244-53.

358. Kliouchnikov, L., et al., *Discrete determinants in ArfGAP2/3 conferring Golgi localization and regulation by the COPI coat.* Mol Biol Cell, 2009. **20**(3): p. 859-69.

359. Di Paolo, G. and P. De Camilli, *Phosphoinositides in cell regulation and membrane dynamics.* Nature, 2006. **443**(7112): p. 651-7.

360. Oikawa, T., et al., *PtdIns(3,4,5)P3 binding is necessary for WAVE2-induced formation of lamellipodia.* Nat Cell Biol, 2004. **6**(5): p. 420-6.

361. Yuce, O., A. Piekny, and M. Glotzer, *An ECT2-centralspindlin complex regulates the localization and function of RhoA.* J Cell Biol, 2005. **170**(4): p. 571-82.

362. Simon, G.C., et al., *Sequential Cyk-4 binding to ECT2 and FIP3 regulates cleavage furrow ingression and abscission during cytokinesis.* Embo J, 2008. **27**(13): p. 1791-803.

363. Guipponi, M., et al., *Two isoforms of a human intersectin (ITSN) protein are produced by brain-specific alternative splicing in a stop codon.* Genomics, 1998. **53**(3): p. 369-76.

364. Pechstein, A., O. Shupliakov, and V. Haucke, *Intersectin 1: a versatile actor in the synaptic vesicle cycle.* Biochem Soc Trans, 2010. **38**(Pt 1): p. 181-6.

365. Yamabhai, M., et al., *Intersectin, a novel adaptor protein with two Eps15 homology and five Src homology 3 domains.* J Biol Chem, 1998. **273**(47): p. 31401-7.

366. Simpson, F., et al., *SH3-domain-containing proteins function at distinct steps in clathrin-coated vesicle formation.* Nat Cell Biol, 1999. **1**(2): p. 119-24.

367. Zamanian, J.L. and R.B. Kelly, *Intersectin 1L guanine nucleotide exchange activity is regulated by adjacent src homology 3 domains that are also involved in endocytosis.* Mol Biol Cell, 2003. **14**(4): p. 1624-37.

368. Graham, F.L. and A.J. van der Eb, *A new technique for the assay of infectivity of human adenovirus 5 DNA.* Virology, 1973. **52**(2): p. 456-67.

369. Kowanetz, K., et al., *CIN85 associates with multiple effectors controlling intracellular trafficking of epidermal growth factor receptors.* Mol Biol Cell, 2004. **15**(7): p. 3155-66.

370. Mongiovi, A.M., et al., *A novel peptide-SH3 interaction.* Embo J, 1999. **18**(19): p. 5300-9.

371. Kang, H., et al., *SH3 domain recognition of a proline-independent tyrosine-based RKxxYxxY motif in immune cell adaptor SKAP55.* Embo J, 2000. **19**(12): p. 2889-99.

372. Liu, Q., et al., *Structural basis for specific binding of the Gads SH3 domain to an RxxK motif-containing SLP-76 peptide: a novel mode of peptide recognition.* Mol Cell, 2003. **11**(2): p. 471-81.

373. Stamenova, S.D., et al., *Ubiquitin binds to and regulates a subset of SH3 domains.* Mol Cell, 2007. **25**(2): p. 273-84.

374. Ahmad, K.F. and W.A. Lim, *The minimal autoinhibited unit of the guanine nucleotide exchange factor intersectin.* PLoS One, 2010. **5**(6): p. e11291.

375. Murayama, K., et al., *Crystal structure of the rac activator, Asef, reveals its autoinhibitory mechanism.* J Biol Chem, 2007. **282**(7): p. 4238-42.

376. Harris, K.P. and U. Tepass, *Cdc42 and Vesicle Trafficking in Polarized Cells.* Traffic, 2010.

377. Snape, K.M., et al., *The spectra of clinical phenotypes in aplasia cutis congenita and terminal transverse limb defects.* Am J Med Genet A, 2009. **149A**(8): p. 1860-81.

378. Hentze, M.W. and A.E. Kulozik, *A perfect message: RNA surveillance and nonsense-mediated decay.* Cell, 1999. **96**(3): p. 307-10.

379. Lei, M., et al., *Structure of PAK1 in an autoinhibited conformation reveals a multistage activation switch.* Cell, 2000. **102**(3): p. 387-97.

380. Devriendt, K., et al., *Constitutively activating mutation in WASP causes X-linked severe congenital neutropenia.* Nat Genet, 2001. **27**(3): p. 313-7.

381. Etienne-Manneville, S. and A. Hall, *Rho GTPases in cell biology.* Nature, 2002. **420**(6916): p. 629-35.

382. Yarbrough, M.L., et al., *AMPylation of Rho GTPases by Vibrio VopS disrupts effector binding and downstream signaling.* Science, 2009. **323**(5911): p. 269-72.

383. Verdyck, P., et al., *Adams-Oliver syndrome: clinical description of a four-generation family and exclusion of five candidate genes.* Clin Genet, 2006. **69**(1): p. 86-92.

384. Sharpe, J., et al., *Optical projection tomography as a tool for 3D microscopy and gene expression studies.* Science, 2002. **296**(5567): p. 541-5.

385. Vivanco, I. and C.L. Sawyers, *The phosphatidylinositol 3-Kinase AKT pathway in human cancer.* Nat Rev Cancer, 2002. **2**(7): p. 489-501.

386. Li, Z., et al., *Directional sensing requires G beta gamma-mediated PAK1 and PIX alpha-dependent activation of Cdc42.* Cell, 2003. **114**(2): p. 215-27.

387. Catimel, B., et al., *PI(3,4,5)P3 Interactome.* J Proteome Res, 2009. **8**(7): p. 3712-26.

388. Gassama-Diagne, A., et al., *Phosphatidylinositol-3,4,5-trisphosphate regulates the formation of the basolateral plasma membrane in epithelial cells.* Nat Cell Biol, 2006. **8**(9): p. 963-70.

389. Toyoshima, F., et al., *PtdIns(3,4,5)P3 regulates spindle orientation in adherent cells.* Dev Cell, 2007. **13**(6): p. 796-811.

390. Downes, C.P., A. Gray, and J.M. Lucocq, *Probing phosphoinositide functions in signaling and membrane trafficking.* Trends Cell Biol, 2005. **15**(5): p. 259-68.

391. Vaynberg, J., et al., *Structure of an ultraweak protein-protein complex and its crucial role in regulation of cell morphology and motility.* Mol Cell, 2005. **17**(4): p. 513-23.

392. Caron, E. and A. Hall, *Identification of two distinct mechanisms of phagocytosis controlled by different Rho GTPases.* Science, 1998. **282**(5394): p. 1717-21.

393. Trifaro, J.M., S. Gasman, and L.M. Gutierrez, *Cytoskeletal control of vesicle transport and exocytosis in chromaffin cells.* Acta Physiol (Oxf), 2008. **192**(2): p. 165-72.

394. Momboisse, F., et al., *betaPIX-activated Rac1 stimulates the activation of phospholipase D, which is associated with exocytosis in neuroendocrine cells.* J Cell Sci, 2009. **122**(Pt 6): p. 798-806.

395. Erickson, J.W., et al., *Mammalian Cdc42 is a brefeldin A-sensitive component of the Golgi apparatus.* J Biol Chem, 1996. **271**(43): p. 26850-4.

396. Musch, A., et al., *cdc42 regulates the exit of apical and basolateral proteins from the trans-Golgi network.* Embo J, 2001. **20**(9): p. 2171-9.

397. Luna, A., et al., *Regulation of protein transport from the Golgi complex to the endoplasmic reticulum by CDC42 and N-WASP.* Mol Biol Cell, 2002. **13**(3): p. 866-79.

398. Matas, O.B., J.A. Martinez-Menarguez, and G. Egea, *Association of Cdc42/N-WASP/Arp2/3 signaling pathway with Golgi membranes.* Traffic, 2004. **5**(11): p. 838-46.

399. Palamidessi, A., et al., *Endocytic trafficking of Rac is required for the spatial restriction of signaling in cell migration.* Cell, 2008. **134**(1): p. 135-47.

400. Arnold, K., et al., *The SWISS-MODEL workspace: a web-based environment for protein structure homology modelling.* Bioinformatics, 2006. **22**(2): p. 195-201.

401. Ridley, A.J., et al., *Cell migration: integrating signals from front to back.* Science, 2003. **302**(5651): p. 1704-9.